Design and Simulation of a Hybrid Optical Antenna on Engineered Silicon-on-Insulator

A Thesis

Submitted in fulfilment of the requirement for the award of the degree

of

Doctor of Philosophy

Submitted by

VARUN KUMAR

Regd. No. 951106004

Under the guidance of

Dr. Mukesh Kumar

Associate Professor, Indian Institute of Technology (IIT), Indore

THAPAR INSTITUTE
OF ENGINEERING & TECHNOLOGY
(Deemed to be University)

DEPARTMENT OF ELECTRONICS & COMMUNICATION ENGINEERING

THAPAR INSTITUTE OF ENGINEERING AND TECHNOLOGY

PATIALA-147004, PUNJAB, INDIA

2018

Certificate

I, Varun Kumar, hereby declare that the work which is being presented in the thesis entitled "Design and Simulation of a Hybrid Optical Antenna on Engineered Silicon-on-Insulator" is an authentic record of my own work carried out toward the partial fulfillment for the award of degree of Doctor of Philosophy in Electronics and Communication Engineering Department, Thapar Institute of Engineering and Technology, Patiala, under the guidance of Dr Mukesh Kumar.

The matter presented in this thesis is not submitted in any other university or institute for the award of any degree.

Varun Kumar

Dated: 13.08.2018 Signature of Student

This is certified that the above statement made by the candidate is correct to the best of my knowledge and belief.

Dr Mukesh Kumar

Dated: 13.08.2018 Associate Professor, IIT Indore

Abstract

Microwave photonics has emerged as a promising technology for smart and efficient microwave and photonic networks. Smart antennas together with their counterpart photonic devices are crucial for the realization of microwave photonic systems. In this work, novel design of a hybrid optical antenna containing coupling waveguide, photodetector and an engineered patch antenna is proposed to realize a microwave photonic system. The detailed analysis of the whole hybrid device is presented. An efficient coupling of optical modulated signal on this hybrid chip (antenna) with ultra-low transmission losses at narrow-core waveguide is achieved to obtain high performance photodetection and optimized radiation from an engineered antenna.

Firstly, an efficient broadband in-coupler on engineered Silicon-on-Insulator (SOI) for strong coupling of optical modulated signal and hybrid chip is designed and analyzed using grating based photonic coupler approach. High-index contrast grating (HCG) is one of the innovative form of grating which is used for this coupling scheme. The formation of high-index contrast grating (HCG) by the periodic layers of silicon and air on top layer of silicon of SOI allows a tight interaction between the guided mode and the grating thereby efficient coupling is achieved by optimizing the different grating parameters i.e. grating thickness (t_g), grating period (Λ) and duty cycle (C) over a broad range of wavelength (λ).

Further, a new plan for ultra low-loss transmission of this efficient coupled light through HCG assisted narrow-core optical waveguide structure is proposed. The analysis of transmission of guided modes within narrow-core waveguide is done by Finite-difference-time-domain (FDTD) numerical method. An ultra low transmission loss through proposed design is achieved in the narrow-core hollow waveguide due to unique polarization and angular dependence of the HCG reflection spectrum. Finally, HCG assisted hollow waveguide considerably reduces the dispersion and nonlinear effects in data transmission, and it is insensitive to temperature variations. With all these attractive characteristics, the grating based hollow waveguide can be a perfect applicant for on-chip optical communication, compact low loss optical delay lines, and interferometric sensors.

Now, an innovative design for hybrid integration of HCG embedded narrow-core waveguide in engineered SOI for efficient photodetection is proposed. A high performance photodetection is realized by integrating of PIN photodetection layer within HCG-assisted

narrow-core hollow waveguide. The proposed design demonstrates a good performance device for generating relatively large power at terahertz (THz) frequencies with sufficiently high responsivity and quantum efficiency which is possible because of the presence of surface modes within HCG which get coupled in the photodetection layer leading to a strong optical confinement in that layer. High reflectivity, small penetration length and coupling of lateral surface modes in HCG make it possible to offer improved waveguiding thereby increases the transmitted power.

Further, a direct integration of compact terahertz patch antenna with high performance photodetector on engineered SOI is proposed. It is revealed that the multi-resonance of terahertz rays in a copper patch on SOI can be successfully controlled with HCG on the patch. The proposed antenna is shown to work for thirteen frequency bands with suitably low return losses in THz region. The HCG enabled guiding of terahertz rays make it feasible to offer a compact design with an improvement in the antenna characteristics in the form of antenna-gain (G), antenna-directivity (D) and radiation efficiency (η) on a compact platform which is feasible since the improved interaction of electromagnetic (EM) fields with the copper patch.

All integrated high performance compact optoelectronic devices demonstrate the effectiveness and usefulness of the concept of the photonic feeding antenna and its potential applications to the real radio-over-fiber system. This hybrid chip provides a good solution for the future photonic and microwave wireless communication system. This on-chip integration of these compact devices may also find applications in sensing and in future microwave/millimetre wave wireless communication system based on photonic networks.

Acknowledgement

Firstly, I would like to offer my heartiest salutation to the Almighty for giving me the strength and patience to work through all these years so that today I can stand proudly with my head held high.

At this moment of accomplishment I am greatly indebted to my respected supervisor ***Dr. Mukesh Kumar***, Associate Professor, Department of Electrical Engineering, Indian Institute of Technology (IIT) Indore, whose exemplary guidance, constant encouragement, insight and most of all patience, has made a wonderful experience. Without his guidance, inspiration, and his knack for explaining things clearly and unequivocally, this would have been a more arduous process. He has helped me more than I can say. I sincerely thank him from bottom of my heart and will be truly indebted to him throughout my life time.

I would like to express my sincere gratitude to ***Dr. O.P. Pandey***, Dean (RSP), ***Dr. Alpana Aggarwal***, Head ECED and members of **doctorate committee** for their continuous support during my Ph.D programme.

Many thanks go to my colleagues-cum-friends of the research group, ***Dr. Tarun Sharma, Er Harpinder Kaur***, ***Er. Ajay Kumar*** and ***Mr Sulabh Vohra*** for their constant encouragement and help throughout the years of research.

My deep sense of appreciation to my parents ***Sh Mohinder Pal Mehta*** and ***Smt Sushma*** for showing faith in me and giving me liberty to choose what I desired.

Finally, I owe thanks to a very special person, my dearest life partner ***Anisha*** for continued and unfailing love, support and understanding during my pursuit of Ph.D degree. Last but not the least, my beloved son ***Kiyansh*** who always remained the source of energy for me and making my work stress free. Also, I express my thanks to my younger brother ***Yogesh Mehta***, for his support and prayers.

My heart-felt regard goes to my father-in-law and mother-in-law for their love and moral support. I also place on record, my sense of gratitude to one and all, who directly or indirectly, have lent their hand in this venture.

Varun Mehta

Table of Contents

List of Figures

List of symbols

dB	Decibals
λ	Wavelength
Si	Silicon
SiO_2	Silica
E	Electric field
n	Refractive Index
ε	Permittivity
ε_{si}	Permittivity of Silicon
ε_{SiO2}	Permittivity of Silica
I	Laser Intensity
f_h	Higher Frequency
f_l	Lower Frequency
f_r	Resonant Frequency
G	Antenna Gain
ε_{rad}	Radiation Efficiency
D	Directivity
$P(\theta,\psi)$	Angular Power Density
P_{loss}	Power Loss
Prad	Power Radiated
BW	Bandwidth

μ	Permeability
n_{eff}	Effective Refractive Index
Λ	Grating Period
C	Duty Cycle
β	Propagation constant
A_{eff}	effective mode area
Ψ	wave function
t_g	Grating thickness
t_{si}	Silicon thickness
m	Diffraction mode

List of Acronyms and Abbreviation

EM	Electromagnetic
UV	Ultraviolet
nm	nanometer
mm	millimeter
μm	micrometer
THz	Terahertz
GHz	Gigahertz
PhCs	Photonics crystals
IR	Infrared
ICs	Integrated Circuits
LED	Light Emitting Diode
TE	Transverse Electric
TM	Transverse Magnetic
TEM	Transverse Electromagnetic
1D	One dimensional
2D	Two dimensional
3D	Three dimensional
TIR	Total Internal Reflection
HOA	Hybrid Optical Antenna
MWP	Microwave Photonics
RoF	Radio-over-Fiber

HCG	High Contrast Grating
HCW	Hollow core waveguide
SOI	Silicon-on-Insulator
c-Si	Crystalline Silicon
CMOS	Complementary metal oxide Semiconductor
PCW	Photonic Crystal Waveguide
FDTD	Finite-Difference-Time-Domain
CS	Central Station
BS	Base Station
RF	Radio Frequency
IF	Intermediate Frequency
BB	Baseband
VCSEL	Vertical Cavity Surface Emitting Lasers
PD	Photodetector
WDM	Wavelength Division Multiplexing
PIC	Photonic Integrated Circuits
SOA	Semiconductor Optical Amplifiers
A	Absorption
R	Reflection
S	Scattering

PML	Perfectly Matched Layers
VNA	Vector Network Analyzer
TDS	Time domain Spectroscopy
VSWR	Voltage standing wave Ratio
FEM	Finite Element Method
FBG	Fiber Bragg Grating
DBR	Distributed Bragg Reflector
PICs	Photonic Integrated Circuits
QE	Quantum Efficiency
PLCs	Planar Light wave Circuits
ICT	Information and Communications Technology
SNR	Signal-to-Noise Ratio

CHAPTER – 1

Introduction to Terahertz Photonics

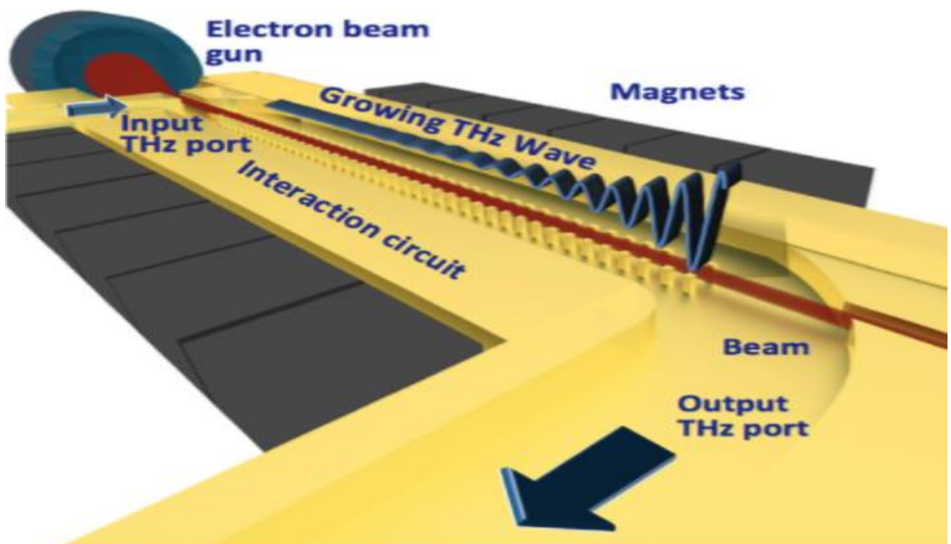

Chapter 1
Introduction to Terahertz Photonics

1.1 Introduction

In the present time, optical technology has been flourished and expanded for semiconductor industry. Now-a-days, the growth of semiconductor industry is moving full stream in context of ‘compact size, better device integration and less complexity’ to concentrate on highly efficient data processing. As the physical limitations of metallic interconnect begin to threaten the semiconductor industry's future. Therefore, research scholars and multi-national companies rely on “growth in photonics” that will lead to combine the existing semiconductor infrastructure with optical technology, and a merger of electronics and photonics into one integrated dual-functional device. Photonics is the technology of signal processing, transmission and detection where the signal is carried by photons (light) and it is already heavily used in photonic devices such as lasers, waveguides or optical fibers [1]. Further, challenges in power delivery for integrated network are very daunting and required innovative solutions and technology now and also in the future. The primary objective of the power delivery network is to distribute power efficiency to all devices on a chip while maintaining an acceptable level of power supply noise. Advances in interconnection technology in form of silicon photonics have played a key role in the continued improvements in integrated circuit density, performance, and cost per function [2].

The fiber-optic communication is a well–established technology for data transmission; however, the fundamental test is to make low-loss data transmission for silicon photonics. This goal can be achieved by creating silicon photonic devices fabricated from standard CMOS systems as opposed to building altogether new modern industrial infrastructure from scratch [3]. In this way, the principle objective of silicon photonics is to develop a technology for controlling and manipulating the high frequency light signals as similar to the computer chips that control and manipulate the electrical signal for the development of Terahertz (THz) technology.

Terahertz (THz) Technology has drawn a considerable amount of interest; it has proven to be one of the most elusive parts of the electromagnetic spectrum. THz regime is also referred to as the “THz gap” as neither optical nor microwave devices could fully conquer this shadowy domain with its many hidden scientific treasures. This THZ gap has multiple GHz channel bandwidth which provides high data rates with less power consumption and higher channel capacity. High imaging resolution is also provided at THz frequencies than at microwave frequency. Communication at THz frequencies are highly directional than at microwave frequency as THz waves diffracts less than the microwave. Thus systems at THz frequencies employ low power devices when compared to microwave frequency. The numerous potential THz applications, ranging from medical imaging, security scanning and process control to ultra-fast communications, lead to a rapid development of THz systems[4]. In the more recent time, THz amplifiers for example power amplifiers and pre-amplifiers which are utilized as transmitters and receivers respectively, have started to be developed even with Si technologies. With the utilization of such amplifiers, photonics based THz wireless technology can be more practice. Here, we review the latest trends in THz communications research, focusing on how photonics technologies have played a key role in the development of first-age THz communication systems. The integration of electronic devices and photonic devices by using contemporary manufacturing technologies, for example, silicon photonics make THz transceivers compact and cost–effective [5]. This research work investigates the realization of the fully integrated compact optoelectronic devices integrated on Silicon-on-Insulator to form a hybrid optical antenna chip for sensing and communication applications.

1.2 Radio-over-Fiber (RoF) Technology

To complete the demands of wireless technology, RoF technology is an obvious choice. A great deal of innovation has been developed to explore its limitations and grow novel and superior RoF innovations since this technology was utilized at the very beginning in 1990 for cordless telephones or mobiles [6]. In this technology, different base stations (BSs) are connected to Central station (CS) by means of an optical fiber. The base station converts optical modulated signal wirelessly to free space. However, all other manipulations such as coding, routing modulation and demodulation, etc are executed in central station (CS). That means, ROF network uses highly linear optical fiber links between CS and BSs to distribute the RF signals.

For the existing and upcoming generation, the purpose of RF over fiber links is to provide low noise, high dynamic range and great communication security that covered low frequency signals to extremely high frequency spectrum[7].The optical fiber systems can transmit RF signal over kilometers with loss-less medium and can be designed for unity gain RF links. Various low noise amplifiers to reduce the noise can be appeared for raising the RF signal over the noise caused by laser. However, to include signal gain at far and receiver site and to overcome any optical link loss, post RF amplifiers can be used. To achieve broadband access, RoF links can provide the flexibility and capability to wireless communication services to transmit and distribute RF signals from a CS to the number of remote locations; RoF also uses analogue fiber optic links. RoF is reliable and cost effective because of higher bandwidth, no interference to electromagnetic radiations, low power consumption.

The processing of RF signal functions, for example, carrier modulation, multiplexing and frequency up-conversion are executed at the BSs and instantly fed into the antenna system. Therefore, the antenna systems need to implement amplification functions and optoelectronic conversion. The transmission equipment near to the antennas has less complexity as analog optical links work on them. The other advantage of using these optical links is that the operational cost of the network is very low because of sharing infrastructure among various BSs. To increase the capacity and quality of service, optical fiber technology in wireless networks should be deployed. The mobility and flexibility of wireless access networks can be combined with the limit of optical network with the usage of RoF technology [8].

RoF incorporates processing of RF signal functions in one shared location of CS and therefore it is conceivable to utilize optical fiber system which provides minimum signal loss(0.3 dB/km at λ of 1550-nm, and 0.5 dB/km λ of 1310-nm) to distribute the radio frequency signals to the Base Station, as appeared in Fig. 1.1.

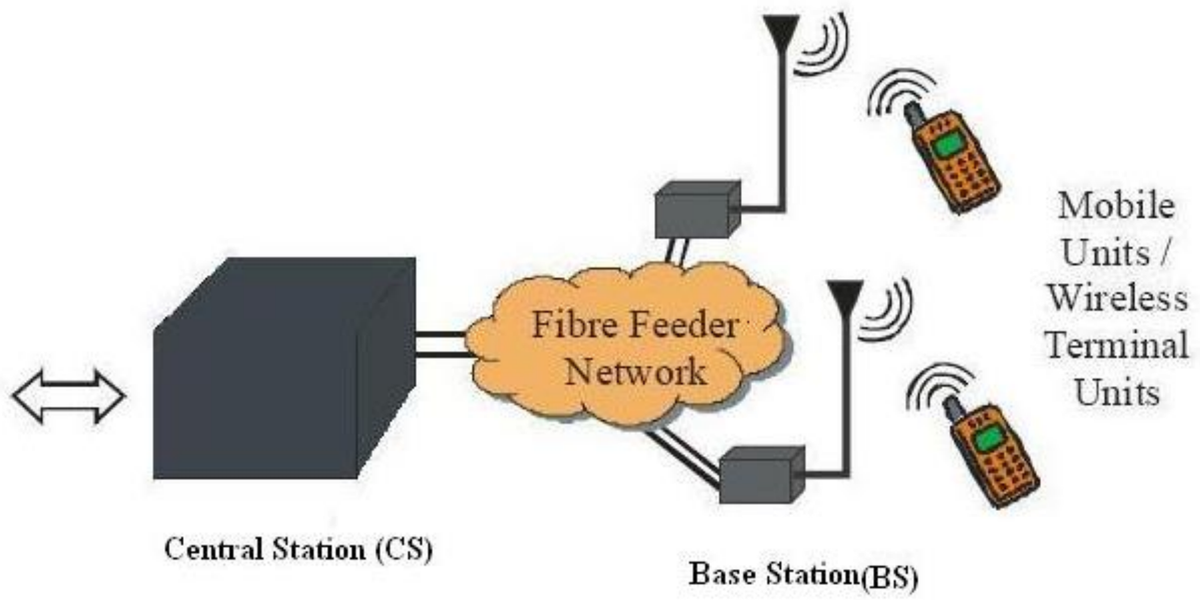

Fig.1.1Concept of Radio over Fiber System [9]

In the general sense, RoF works on the principal of analog based transmission system as it allocates the RF signal from a CS to a BS specifically at the radio carrier frequency. In fact, the analog signal that is modulated over fiber optic link and transmitted can either be IF,RF or baseband signals. The extra equipment which up-converts the analog signal to RF spectrum is needed at the base station for IF (Intermediate Frequency) and BB transmission case. The analog signal (RF/IF/BB) can be forced on the light carrier by utilizing direct or external modulation technique of the laser light at optical transmitter. However, in an ideal case the optical modulated output signal from fiber optic link will be a duplicate of input RF signal. In spite of the fact that, there are some limitations in the modulation device and laser as well as dispersion in the optical fiber due to non linearity and frequency response limits. The analog signals which are transmitted have some requirements with respect to the dynamic scope and linearity of the fiber optic link. These requirements are distinctive and more exact than demands on digital based transmission systems [10].

1.3 Microwave Photonics

Microwave photonics (MWP) [11-12] is a multidisciplinary field that includes optoelectronics as well as the world of radio frequency engineering. MWP imparts more incentive to the conventional microwave and RF systems as it permits the realization of key functionalities in these systems which are not feasible directly in the radio frequency domain or if it is feasible, that is very complex phenomenon. Additionally, MWP created new avenues and opportunities for ICT and network benefitting by coalition of radio frequency fields and optics. Therefore, these qualities of MWP are captivating research scholars and industrialists from the last two decades.

Williams and Seeds characterized MWP with couple of viewpoints [13]: (i) the investigation of photonic/optoelectronic devices which are fit for handling MW signals, and (ii) the utilization of photonic devices and methods to MW systems. According to the first definition, the researchers use devices, for example, modulators, lasers and photodetector which are fit for handling of signals up to 300 GHz. This kind of work is similar to the optical fiber communications field which work with rapid fiber-optic links. The second definition is aftereffect of fast optoelectronic/photonic devices that were initially produced for the telecommunications industry to access 'off-the shelf'. This has enabled the components to be utilized not just for the processing of MW signals in the optical domain but also to be utilized for the analog signaltransmission.MW signals over fiber optic link for instance analogue - to -

digital conversion and filtering are such tasks. The reason of utilizing photonics in a MW system is that it has immense bandwidth capability of optical fiber combined with low optical loss.

Both photonic region and microwave region of electromagnetic spectrum process electromagnetic waves of their regions respectively, however, after combining together in an appropriate sequence, a microwave photonic systems is created. This concept is illustrated by an example shown in Fig 1.2 which exhibits a scheme that highlights the principal idea of a straight forward MW based photonic link. Atleast one analog signal is transmitted through a fiber optic or photonic link at a microwave frequency with a conversion from electrical-to –optical and optical-to electrical at the transmitting and receiving end of the photonic link. Reduced weight, size and cost; constant and low attenuation over the whole MW; immunity to electromagnetic interference; millimeter-wave modulation frequency range; high data transfer capacity and dispersion are the significant benefits of MW based photonic links through traditional analog based transmission system, for example, waveguides or coaxial cables.

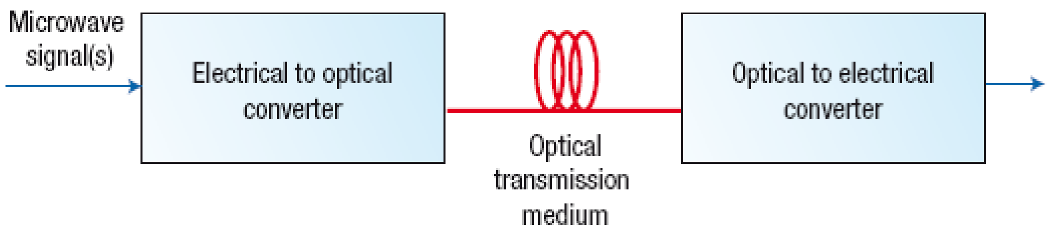

Fig. 1.2 Microwave Photonic Link [11]

The basic building blocks for a Microwave Photonic is illustrated in Fig. 1.3. It shows the major parts of the front end leading to the application-specific processing receiver: photonic preconditioning, encoding based upon electrical-optical(E-O) conversion, photonic conditioning and transport, conversion of optical-electrical (O-E) signal along with conditioning and an RF oscillator, for the execution of photonic link. The photonics RF front end can be connected with any input MW signal, for example, array element outputs or sub array outputs, a single antenna feed additionally some other MW system. The output which is desired from a photonic RF frontend is an analog based signal of reasonable width and frequency for the electronic implementations receiver with suitable SNR ratio and spurious-free characteristics for the coveted application [14].

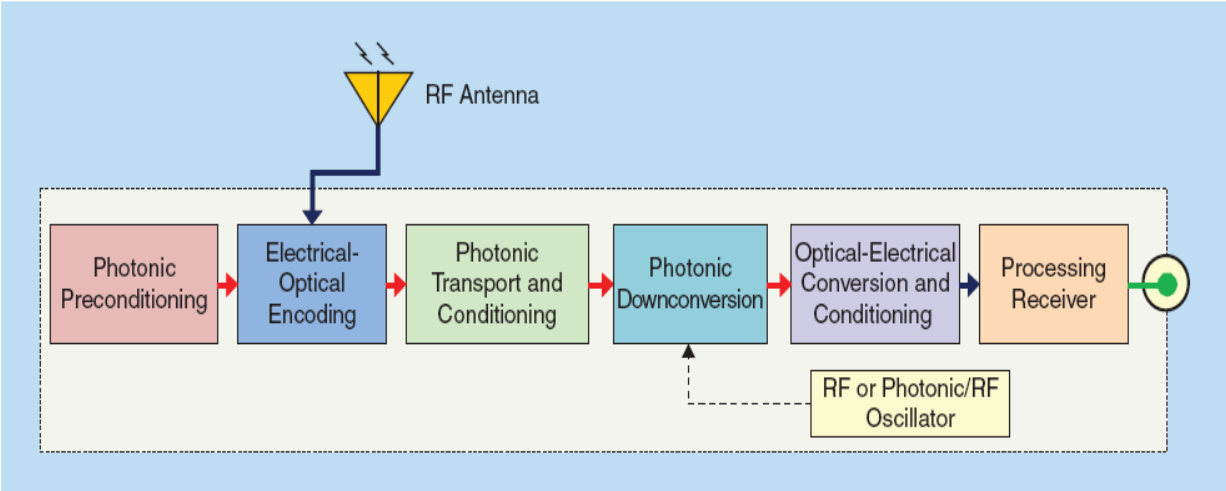

Fig. 1.3 Microwave Photonic Block Diagram [12]

Filtering [15], differentiation [16], integration [17], Hilbert transformation [18], mixing [19], and phase shifting [20] are the microwave signal processing functions which are executed in the optical domain. These capacities can be executed in light of integrated optics, free-space optics and fiber optics. For instance, a microwave photonic filter can be executed by utilizing an all-fiber [15] or an integrated delay-line module [21] with a finite impulse response. A Hilbert transformer and a differentiator can be executed by utilizing a fiber Bragg grating (FBG)

1.4 Silicon Photonics

The present work is concerned with hybrid integration of optoelectronic devices on a silicon platform, i.e. silicon photonics. Silicon photonics is new exciting frontier that has captured the imaginations of people worldwide. It is important to know its background development and its basic research method. This chapter starts with the current research status of silicon photonics and presents the larger picture and goals of the development of silicon photonics. Silicon photonics has a potential for on-chip optoelectronic interconnects for an assortment of economic and technological reasons [22]. A key advancement was the accessibility of rapid silicon-on-insulator (SOI) wafers [23] with the proper dimensions for near-IR waveguiding: a silicon layer of around 200-250 nm on a buried oxide layer of 1-3 µm. Many critical devices have been demonstrated and improved in the past years: electro-optic modulators to convert data from the electrical domain to the optical domain [24-25]; low-loss waveguides and fiber couplers [26]; filters and switches [27-28]; epitaxially grown germanium-on-silicon photodetector [29]; and heterogeneously integrated III-V compound semiconductors for on-chip laser sources [30-31].The flexibility to present CMOS based industry and cost viable applications as compared with III-V compounds are the primary force for the advancement in the field of silicon photonics. That is why; one of the benefits of silicon photonics is the ability to leverage an already mature and large-scale manufacturable process for the realization of optical integrated circuits.

On realizing the silicon photonic devices, considerable work has been done. Passive devices like splitters [32], disk resonators [33], ring resonators [34], and slot waveguide have been revealed. Various examples of SOI assisted passive devices are shown as Fig. 1.4.

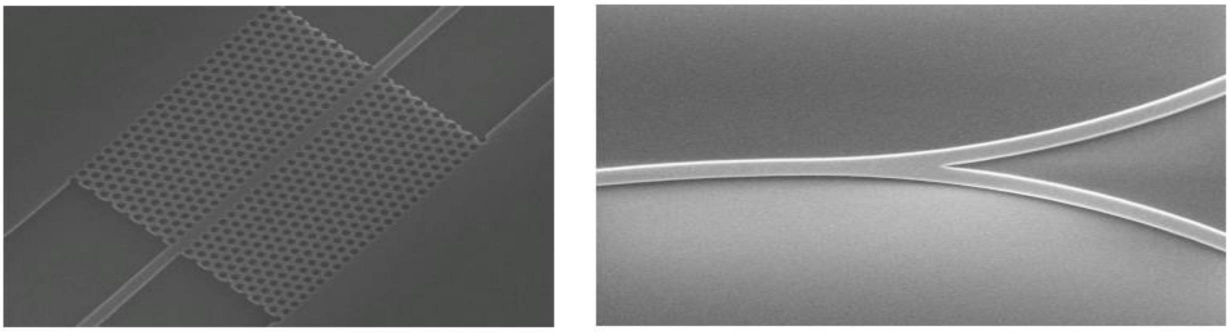

Fig.1.4 Passive devices of silicon photonics [35]

Ultimate potential of silicon photonics lies not only with the monolithic integration of optical communication devices, but also with the driver and receiver circuits. This can provide thelarge bandwidth-density and the minimization of electrical parasitics from traditional microelectronic packaging. Economically, the silicon photonic platform benefits from the semiconductor industry's massive investment in silicon material processing and the economies of scale from piggybacking on top of existing CMOS manufacturing.

Within the silicon photonics community, the current debate revolves around the precise implementation of silicon photonics that will achieve the best ratio of benefits to costs. In one approach, chip packaging, silicon photonic chips and microelectronic chips are fabricated independently and combined by using traditional packaging techniques such as wire bonding or flip-chip bonding. Figure 1.5 shows a recent demonstration of silicon photonic integration by using the chip packaging approach. The key advantage of this approach is that the best-available fabrication process can be used for each chip: highly optimized CMOS processes for the circuits, and specialized photonic fabrication for the optical chip. However, the use of traditional packaging means that the chip-scale bandwidth density cannot fundamentally be improved very much, and electrical parasitics will ultimately limit the system performance.

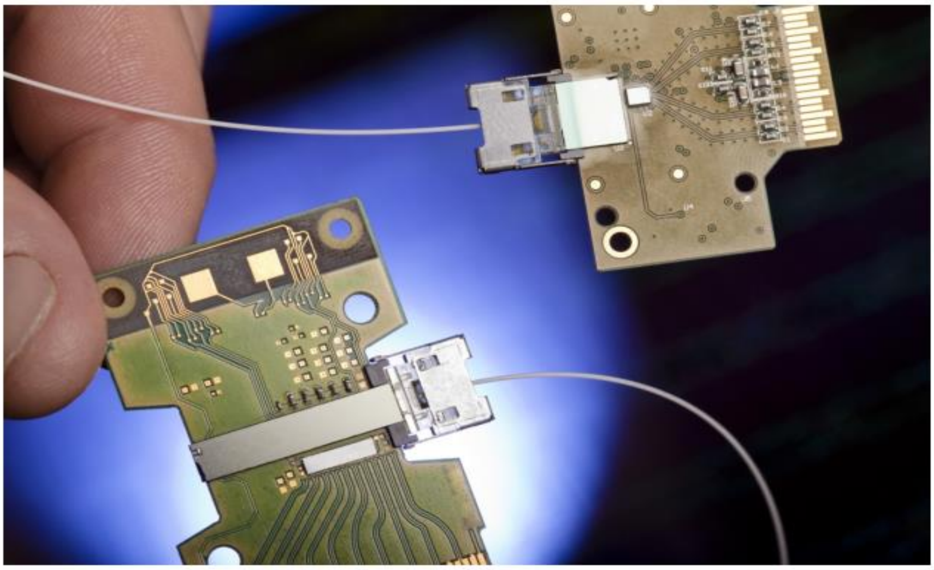

Fig. 1.5 Photograph of Intel silicon photonic integration by using chip packaging [36].

The silicon photonic chip with III-V lasers, silicon modulators, and silicon multiplexer (large central chip) is flip-chip bonded to a circuit board next to a small CMOS chip with transmitter circuits. Similar integration is performed at the receiver end to demonstrate a 4 × 12.5 Gbps link [37].

Another approach, 'monolithic front-end integration' places the optical and microelectronic devices in the same SOI layer of crystalline silicon on a single chip [38]. This approach offers the tightest integration of optics and electronics to minimize electrical parasitics and maximize bandwidth density. However, it also places severe limitations on the performance of transistors within this process. A sub-micron silicon waveguide requires a lower cladding of at least one micron to maintain low-loss operation at a wavelength of 1550-nm. In contrast, due to both thermal and electrostatic limitations of SOI transistors have consistently scaled to smaller buried oxide thicknesses on the order of 100-nm. Using a thick buried oxide SOI substrate fundamentally limits transistors to gate lengths greater than 100 nm, which is a tremendous limitation on performance and scalability. In principle, this monolithic integration could be combined with chip packaging to provide some monolithic circuit functionality while leaving the highest performing circuits to an externally packaged chip, but this solution is not ideal as overall performance will again be limited by the packaging. Additionally, there has been work to integrate waveguides in the front end of a bulk-Si or thin-SOI substrate [39-41], but this requires processing steps that interact with the silicon transistor layer in some fashion. Now, the groundwork for an intermediate approach lying between the two mentioned above is: monolithic back-end integration [42]. In this approach, a separate layer of silicon photonic devices would be monolithically integrated in a plane that is separate from the transistor layer. In this way, the transistor layer can be formed with little or no change to its optimized fabrication process, eliminating the main challenge with front-end integration. At the same time, monolithic integration results in a dramatic improvement in bandwidth density and parasitic compared to the chip packaging approach. Metal vias can connect electro-optic devices directly to the circuits sitting below.

The work in this thesis focuses on the development of high performing silicon platform for direct integration of various HCG/1-D photonic crystal assisted compact photonic devices to form a hybrid chip which is designed to receive the optical modulated signal from one end and direct it to free space by using various optoelectronics/photonics devices at terahertz frequencies from another end of silicon chip. The current silicon photonic research still has gaps before commercialization. For example, the current mainstream chip fabrication is based on 300mm wafers. However, before our work is launched, there is no report of 300-mm Fab Photonic fabrications. This is mainly because of the processing substrate: 300-mm SOI with thick buried oxide has not been ready until very recently. The main SOI wafer manufacturer, SOITEC, has developed a prototype of 300-mm SOI wafer with 2 microns of thick buried oxide. Although high speed modulator and Ge detector have been reported to have integrated on Silicon waveguide, major issues still exist with the laser source on silicon substrate.

1.5 Silicon-on-Insulator (SOI)

Silicon has unique features as a photonic medium. It is transparent in the range of optical telecommunications wavelengths (1.3 and 1.55μm) and has a high index of refraction, which allows for the fabrication of high-index-contrast submicrometer structures. Another key feature of silicon integrated circuit technology is that it facilitates the execution of dense on-chip integration of silicon–based optics with electronics. In order to achieve compact devices with loss-less environment (subwavelength dimensions), a higher refractive index contrast is required. For this purpose, SOI based strip waveguide innovation can be exploited [43]. The use of crystalline silicon (C-Si) rather than amorphous Si or poly Si as the core of waveguide minimizes the absorption losses and scattering [44]. The passive submicrometer size structures, for example, efficient couplers [45], ultra-low-loss strip waveguides [46], microning resonators [47] and nanocavities [48] on SOI have been shown. However, the active waveguide devices (modulators and switches), however, have been proposed only on large micrometer-size SOI waveguides [49].

The increased demand for High Performance, Low Power and Low Area among microelectronic devices is continuously pushing the fabrication process to go beyond for the technologies of ultra deep sub-micron (UDSM) technologies. Currently, chips are being designed in 45nm, 32nm, 14 nm and 10 nm process nodes with high performance. The performance and power goals for certain applications in these advanced nodes could not be achieved with conventional silicon (bulk CMOS) process leading to an alternative, Silicon on Insulator (SOI) process [50]. Silicon on Insulator fabrication process helps in achieving greater performance and offers less power consumption compared to the Bulk Process

SOI wafers is defined by three layers structure: the Si-substrate, followed by a silica (SiO_2) which acts as an insulator layer (around 1-µm thick), and a top active crystalline Si-layer. With a specific end goal to achieve single mode propagation in top Si layer the thickness of that layer should be normally between 200-nm and 300-nm. The prominent advantage of SOI innovation is the presence of high contrast of index of refraction (n) for distinctive materials such as silicon (n_{Si} = 3.45), silica (n_{SiO2}= 1.45), and air (n_{air}=1). This high contrast of index of refraction permits us to design compact, wavelength-scale structures, for example, tight bends or single mode nanophotonic waveguides with compact mode size and strong field confinement. SOI wafers with high quality and large size are traditionally accessible. SOI-based photonics has the ideal similarity with the standard microelectronics process. The incredible advances of SOI based photonic devices have been made since 2004. A Si-based optical modulator working at gigahertz (GHz) and pulsed stimulated emission from Si diode were effectively exhibited [51-52].Fig. 1.6 demonstrates the cross section of SOI wafers.

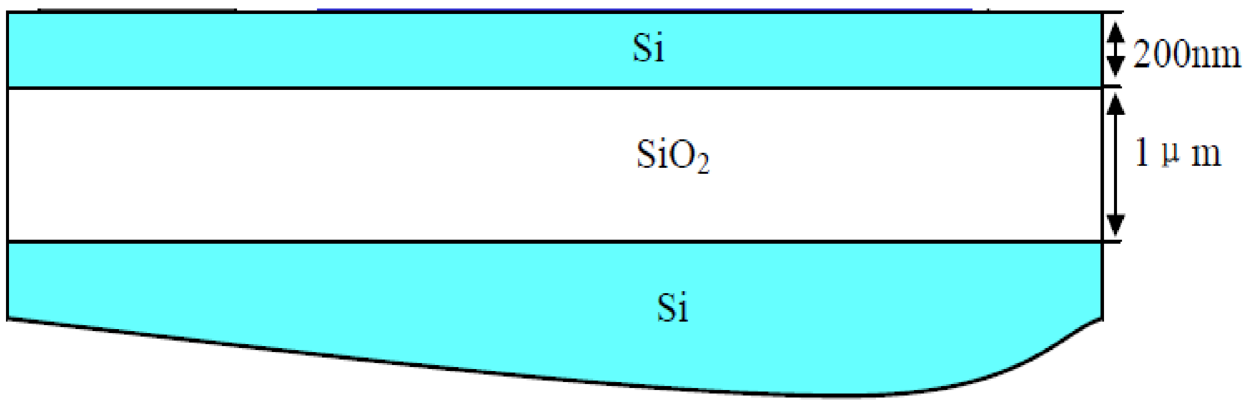

Fig. 1.6 Cross section of SOI wafer

In this work, SOI wafer is modified by employing high-contrast grating (HCG) on top silicon layer and we named it as “Engineered Silicon-on-Insulator (E-SOI)”. Very little work has been reported on HCG (having strong optical confinement based SOI active devices despite their high demand to manipulate light beams for information processing (e.g., coding–decoding, routing, multiplexing, timing, logic operations, etc.) in high-density integrated-optic circuits. This engineered SOI substrate is a potential candidate for powerful integration of photonic/RF devices because the presence of HCG on SOI can improve the performance of photonic devices. Engineered SOI structure contains a silicon waveguide formed by a central silicon region enclosed by silicon on insulator structure on the lower side and high contrast grating structure on the upper side. The presence of vertical index contrast in SOI and the in-plane index contrast in HCG modify the performances of the integrated optoelectronic devices. The compact size novel structures on engineered SOI substrate will open new class of compact terahertz devices. It will be possible to realize easily-tunable functions such as polarization dependence, resonance, confinement, and sharp bends.

1.6 Terahertz Photonics

Terahertz (THz)radiation, which is also characterized as ‘electromagnetic spectrum’ having frequency range between 0.3 - 20 THz is creating enthusiasm among researchers for the spectroscopy and imaging for medical diagnostics applications, security and defence, non destructive evaluation and high bandwidth communication. Terahertz radiation can penetrate dielectric materials without bringing any harmful ionization of the material. For instance, for sensing applications, the terahertz imager can accomplish very higher imaging resolution than millimeters- wave counterpart.

For spectroscopy, the terahertz radiations are widely utilized to produce unique fingerprints by utilizing the molecules vibration for a particular frequency. These examples are of remote gas sensing [53] and biomedical spectroscopy [54-55]. By providing exceptionally short wavelength, the terahertz range in lower side is very beneficial for indoor millimeter wave radar cross section (RCS) which is used in aircrafts and tanks[56]. The terahertz spectrum also has good efficiency in ultra fast wireless communication by giving wide bandwidth in the new spectrum region [57-58]. Designing detectors and highly efficient compact source are necessary in order to amplify the utilization of electromagnetic spectrum. However, in these transition spectrum regions, many challenges exist in achieving reliable and compact sources. To bridge this gap, various research efforts have been given with extensive approaches from high-frequency electronics and photonics [59-60].

Silicon has not been viewed as a promising arrangement because of the limited device performance and the expansive propagation losses combined through a resistive silicon substrate in terahertz regime [61]. This problem will be solved by making fully integrated THz transceiver in silicon. However, during the last decade, there is advancement in the nano- scale silicon technology which substantiated innovative achievements in RF and millimeter- wave integrated circuit (IC) technology. Therefore, there will be a new platform in the avenues of sensing, imaging, ultrafast wireless communication and spectroscopy etc due to “THz-IC” technology. Thus, the present research analyzes the realization of the fully integrated compact hybrid optical antenna for sensing and communication applications.

Generally, the terahertz region signifies the unique frequency range which lies between the infrared and microwaves in the electromagnetic spectrum as displayed in Fig. 1.7

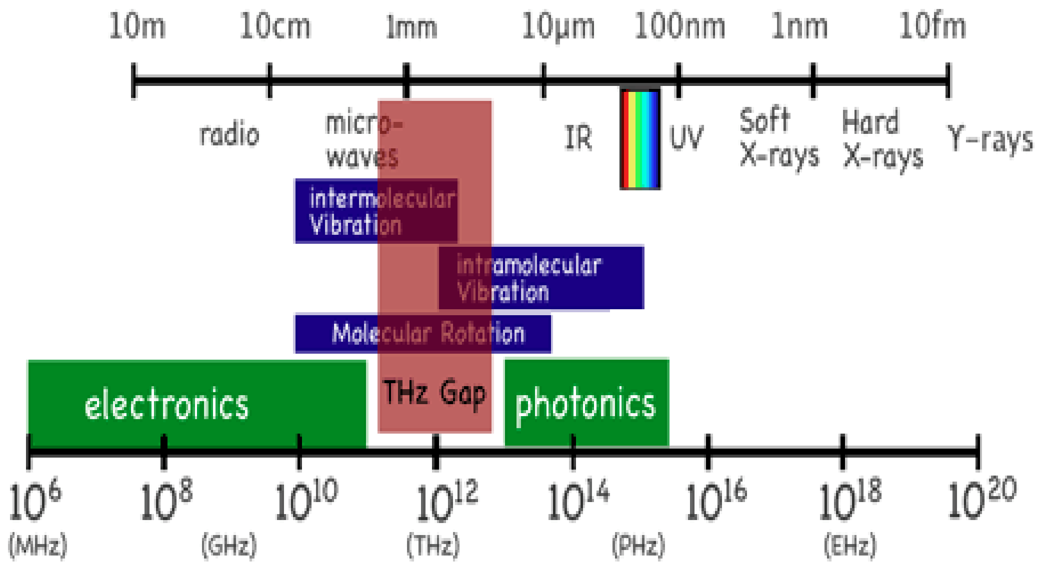

Fig. 1.7 Terahertz regime put in a transition region amongst microwaves and infrared in the electromagnetic spectrum [62].

THz Photonics has entered a new phase of research in recent years. The performance of THz sources has been significantly enhanced so that they now have considerably higher output powers, narrow pulses (both in frequency and time domain) higher output and wider range of frequency. Moreover, the increase in their degrees of freedom makes THz sources just as convenient as visible or infrared sources. At long last, terahertz waves utilized to get vital information which is not accessible by utilizing infrared signal or X-ray. Now days, a number of measurement techniques are employed for fundamental material research which are based on THz radiation, for instance, THz wave is utilized to control the superconductivity and spin of materials.

1.7 Photonic Crystal

Photonic Crystals are the fast emerging field of nanotechnologies which provides a technique to cope with low-light extraction efficiency. Light extraction efficiency is basically an enhancement in light efficiency which can be improved by use of photonic crystals. The enhancement of the extraction efficiency in light through the use of photonic crystals requires a structure design that optimizes the interaction of the guided modes with the photonic crystals. A photonic crystal is a periodic variation between low and high-index material whose length scale is in the range of the light wavelength. If the contrast of index of refraction between low and high-index material is large, light will be strongly scattered and distort the dispersion or band structure of the medium. This may lead to the formation of bandgaps and light with a frequency in a band gap is forbidden to propagate inside it. Photonic crystals (PhCs) are found in one, two, or three dimensional with periodicity of materials having different index of refraction which are shown in Fig 1.8. Some novel photonic crystal based structures have been described to improve the extraction of low-light from high index materials [63-64].

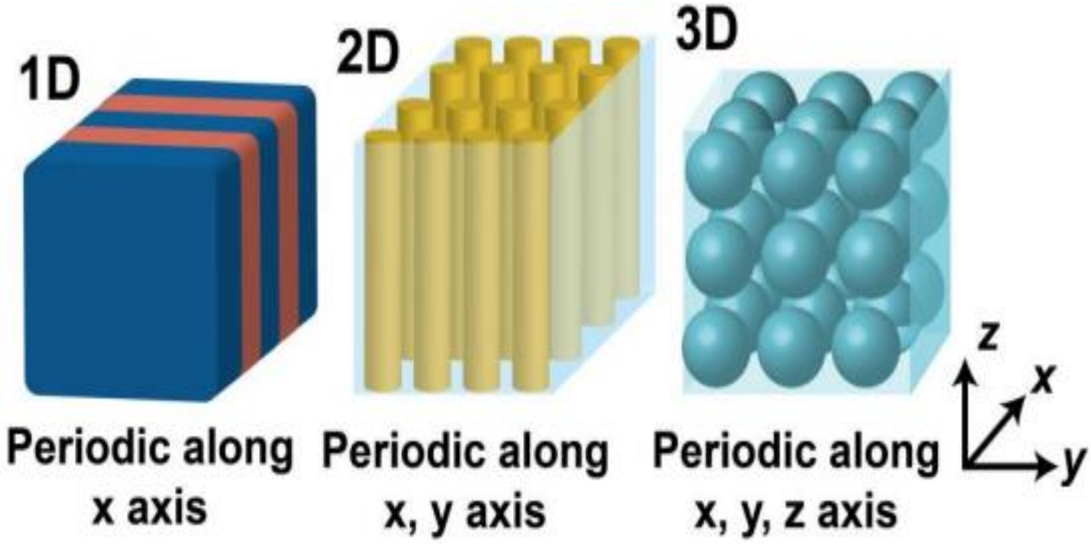

Fig. 1.8 Principal layout of a one-, two- and three dimensional photonic crystal structure (from left to right) [65].

A photonic crystal is a periodic variation in the index of refraction whose length scale is on the order of the wavelength of light. If the periodic variation of the index is large, light will be strongly scattered and distort the dispersion or bands of the medium. This may lead to the formation of bandgaps in the photonic band diagram, where no modes exist for frequencies in the bandgap. Light with a frequency in a band gap is forbidden to propagate inside it. Incident light having a frequency in a bandgap will be reflected from the photonic crystal. A photonic crystal is a perfect mirror for frequencies in a band gap. By surrounding a region of space on all sides with a photonic crystal a cavity will be created with resonances in the band gap. A single defect in the photonic crystal can create a small photonic cavity, while point defects will create cavities and line defects will create waveguides. Photonic crystals enable one to engineer the photonic properties of defect cavities, waveguides, and the materials themselves. In the future, photonic crystals will surely contribute to close the THz technology gap.

The focus of this work is to utilize the 1-D photonic crystal as a high-index contrast grating to cover the THz technology gap for the applications in future microwave/millimeter wave wireless communication system based on photonic network. The properties of a 1-D PhCs structure are utilized for efficient coupling of light into the inside medium of hybrid chip to make high performance, highly efficient, low loss environment on this hybrid chip.

1.8 High-index Contrast Grating (HCG)

A high-index contrast grating is a periodic structure along single layer in subwavelength dimensions where the material used in grating has a high contrast of refractive index with their surroundings. The word subwavelength relates to the period of the grating, having value among one optical wavelength in the grating material and that in its surrounding materials. HCG has numerous well defined features that are not working in conventional gratings. These attributes incorporate broadband ultra-high transmission, ultra-high reflectivity and very high quality factor resonance, for optical beam surface-normal or in oblique incidence to the grating surface. The transmission and reflection phase of the optical light across the high-index contrast grating can be engineered to cover a full 2π range while sustaining a high transmission or reflection coefficient.

HCG as a high reflective mirror is attractive for an extensive variety of applications such as integrated optoelectronic device, which includes filters, splitters, lasers, couplers and so forth [66].The HCG is polarization sensitive by its nature of one-dimensional (1D) periodicity. Incident beams with E-field polarization along and perpendicular to the grating bars are referred to as transverse electric (TE) and transverse magnetic (TM) polarizations, respectively. Fig. 1.9 demonstrates the scheme of a HCG design, where air acts as a material with low refractive index placed on top and among the grating grooves; another material with low refractive index underneath the grating grooves, a plane wave is incident on grating bars with an oblique angle.

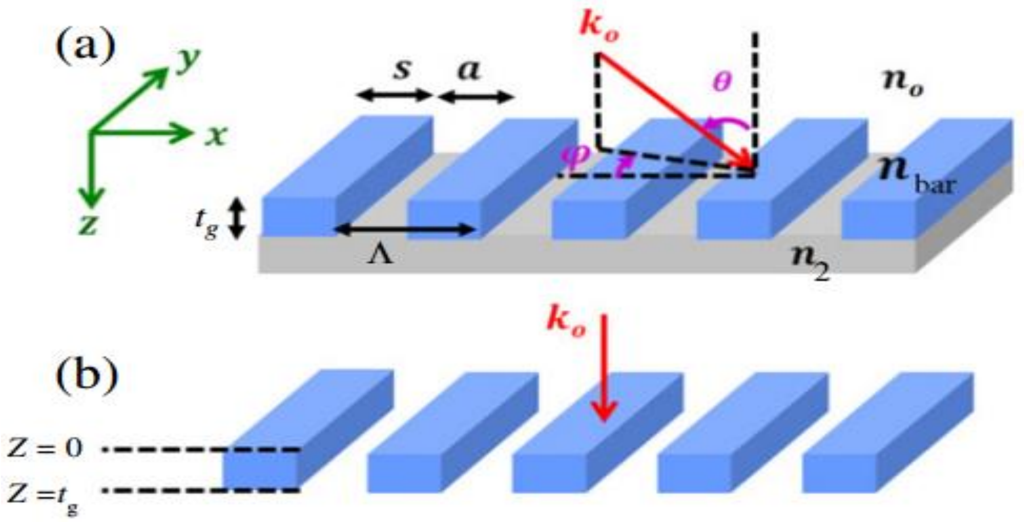

Fig 1.9 (a) The scheme of High-index Contrast Grating. The grating includes low-index medium n_o, encompassed by a dielectric bars having high refractive index n_{bar}. A second material of low refractive index material (n_2) is underneath the grating grooves. An incident plane wave from the top of grating with an oblique angle, a air gap width; s, bar width; Λ, HCG period; t_g, HCG thickness. (b) A surface normal incidence on HCG having refractive indices n_{bar} = 3.48, n_2 = 1.47, n_o = 1, [67].

The essential parameters of high-index contrast grating design includes the high-index materials refractive index n_{bar}, thickness t_g, period Λ, width of grating bar s and duty cycle, C. The duty cycle (C is characterized as the proportion of the high-index material width with period, i.e., C = s/Λ. HCGs made up with high contrast of refractive index on top of a low index insulation layer can accomplish a bandwidths larger than 100-nm and reflectivity as high as 99.9 % altogether with strong polarization selectivity amongst TE and TM mode. These attributes are exceptionally intriguing for substituting the Bragg mirror used in vertical cavity surface emitting lasers (VCSEL) devices [68].

Highly reflective subwavelength gratings have encouraging applications in VCSELs which were monolithically connected as a substitution of traditional distributed Bragg reflectors (DBRs) and as a way to build a tunable VCSEL also to give controlled polarization [69-71]. Also, HCG was appeared to act as an optical resonator with a large quality factor [72] under a different design condition. Because of the inhomogeneous profile of refractive index, and because of the way that the wavelength is practically identical to the grating periodicity, the current rigorous design for the analysis of electromagnetic through gratings [81-83] is genuinely complex, which makes it hard to understand, for example, ultra-high broadband reflectivity, in a way that will permit to forecast and design this phenomenal and surprising characteristics of HCGs.

In this work, we design a HCG based hybrid chip that gives remarkably high reflectivity over a wide bandwidth at λ of 1.55-μm. To improve the quality factor of the chip, the dimensions of HCG structure are adjusted through optimization algorithm. The strong confinement of the electromagnetic fields of the optical modes in a small region is conceivable because of high reflectivity applications of HCG for enhancing nonlinear effects, which are of high significance for potential nonlinear optical applications. The HCG-empowered guiding of optical waves on a SOI based hybrid chip causes a high efficient, loss less environment with high current for feeding an antenna with low return loss and enhanced features. On the basis of the HCG based hybrid chip for smaller losses compensation with high gain can probably be helpful for efficient on-chip light propagation.

CHAPTER – 2

Literature Review

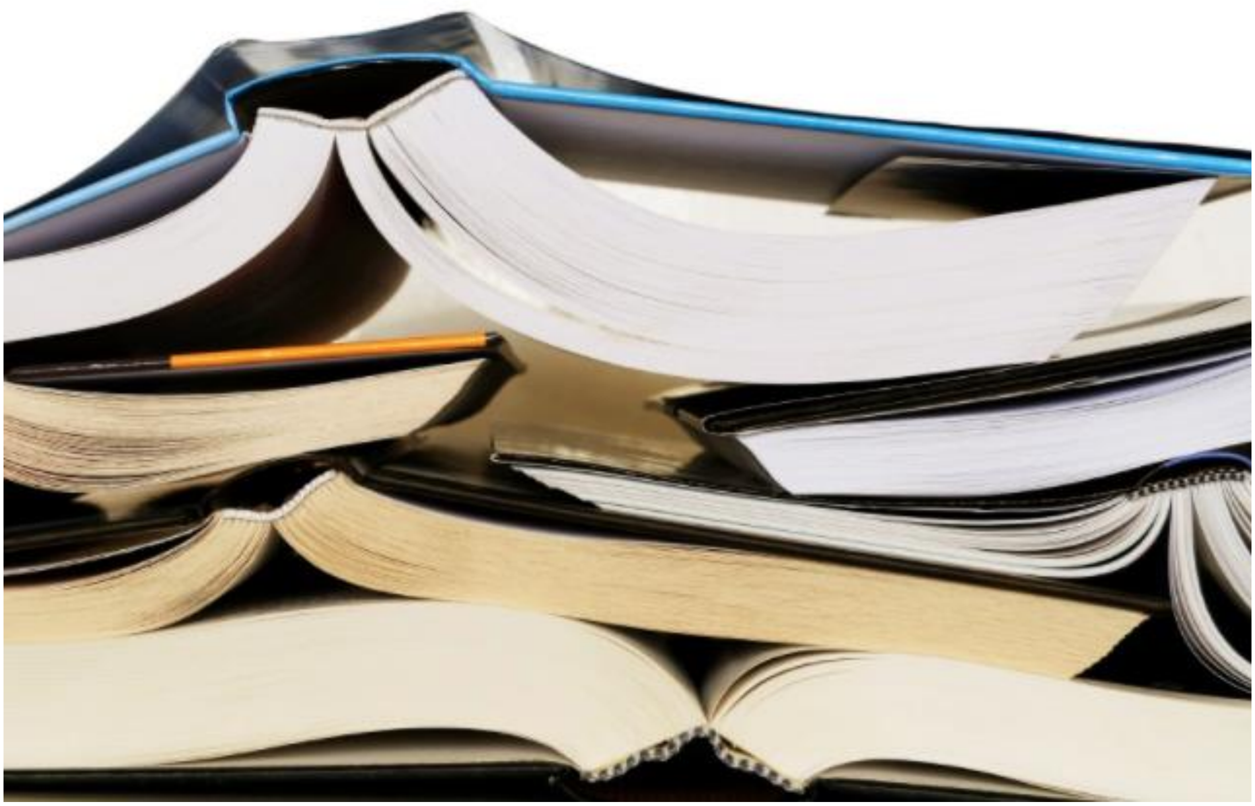

Chapter 2
Literature Review

2.1 Introduction

This chapter partially highlights the literature cited on the terahertz photonics research that have great potential for integration of on-chip optoelectronic devices in terahertz range, which has emerged as a highly efficient, low loss and cost effective approach for on-chip interconnection by designing high performance optoelectronic devices and eliminating packaging issues. The chapter also discusses the recent advancements and issues involved in various other technologies such as on-chip photonics interconnect, silicon-on-insulator (SOI) technology, high-index contrast based grating (HCG),1-D photonic crystal, silicon photonics, photodetector and antenna system.

2.2 Literature Review

The present status of THz innovation for generating, detecting, and analyzing terahertz waves is not as cutting edge as infrared photonics or high-frequency electronics. This innovative hindrance is by and large considered as the 'THz gap'. To solve such a problem, many extensive research efforts are underway to close this terahertz gap by developing additional innovative designs of compact optoelectronic devices which works very efficiently under THz regime to remove this THz gap in photonics. Recently completely incorporated THz transceiver in silicon has not been viewed as a promising arrangement because of the large propagation losses and limited device performance coupled through a resistive silicon substrate in terahertz regime. In this manner, by progressive accomplishments in RF and millimeter-wave integrated circuit (IC) innovation amid a decade ago with advancement of the nano-scale silicon innovation, some novel designs of optoelectronic devices in THz are proposed for developing loss less environment in THz regime. Considering the effect of the RFICs in its low-cost, compactness and mass production, the "THz-IC" will open another period in imaging, detecting, spectroscopy and ultrafast remote correspondence. This theory investigates the acknowledgment of the completely incorporated THz transceiver for sensing and communication applications by on-chip interconnection of high performance compact optoelectronic devices i.e. Hybrid Optical Antenna.

The goal of proposed hybrid design is to be superior device in terms of photonic microwave/RF generating, direct feeding, transmitting and receiving as compared to other types of the conventional antenna operating in high frequencies. The hybrid systemis a promising candidate for the low-loss optoelectronic interconnect configuration to future microwave and millimeter-wave wireless communication system based on photonic network. Thus, the primary inspiration in this thesis is to propose a hybrid mechanism which has moderately low transmission loss by simplifying the RF/MW system especially in high frequency wireless system as compared to the other conventional optical antenna. But still several issues are present in the hybrid antenna (such as high gain, improved radiation efficiency and the ideal terahertz transceiver models for silicon technology to accomplish desirable system requirement) which have to be resolved before implementing it into the system or network. On the basis of above said issues the comprehensive literature review and gaps in present study are described in following sections.

S. Ghosh et al. - 2011 [76] investigated how the transverse localization of light in evanescently coupled, disordered, lossless waveguide lattices depends on the shape and size of an input beam. It also demonstrated that by employing different input excitation conditions to nature of input light coupling to different localized modes of a disordered medium. It carried out a numerical study on various aspects of transverse light localization in a disordered waveguide lattice. It also reveals a waveguide-like propagation of the localized state inside such a disordered discrete medium but also showed that a specific localized state is independent of the spatial profile of the input beam. It was concluded that the results should be of interest for realizing waveguide-like propagation even in the presence of structural disorders and refractive index perturbations.

D. Taillaert et al 2006 [77]presented theoretical and experimental results on compact grating couplers for coupling between standard single-mode fibers and integrated waveguides by utilizing eigen mode expansion method with perfectly matched layers (PML) boundary conditions. By optimizing the grating period, filling factor and etch depth, the coupling efficiency to the fiber is approximately 37% was calculated for an etch depth of 70 nm and a filling factor of 0.5 and grating period of 630 nm at wavelength of 1550 nm. Grating couplers can be put anyplace on a circuit and can easily be incorporated. It was also exhibited that the >30% coupling efficiency with a 1 dB data transmission of 40 nm on standard wafers and which can be enhanced to >90% utilizing an advanced grating design and layer stack. It was also analyzed various suitable methods of increasing the coupling efficiency and calculated the coupling efficiency of 44% by including SOI with top cladding, coupling efficiency of 53% by using SOI with optimal th_{buffer} and 79 % coupling efficiency by using SOI with bottom mirror.

By employing an extra poly-silicon layer, coupling efficiency can further increase that changes its diffraction properties and reshapes the grating structure to enhance the fiber coupling effectiveness. This proposed plan was exhibited by **G. Roelkens et al. 2006 [78].** The maximum coupling efficiencies is calculated as 78% at a 1.55-μm wavelength with a 3dB optical bandwidth of 85-nm.

O. Mitomiet al. - 1994 [79] revealed in the past studies is the utilization of tapered couplers. The core shape and size of compact waveguide is progressively in the tapered form which is practically identical to the core of the incident fiber to enhance the efficiency among the SOI based photonic waveguide mode and the fiber optic mode in traditional adiabatic waveguide tapers. The long tapering area of waveguide core (i.e. one millimeter or more) is required with a specific end goal to avoid radiation loss. Then again, inversely tapered waveguides with a 100-nm tapered core size to a little tip of 10-nm can abbreviate the length of tapering on the order of several micrometers. Another option of taper procedure is to manufacture another top waveguide layer of the compact high-index contrast waveguide. The top placed waveguide layer has a low contrast of index and is intended to be single mode with an extensive core size practically identical to the optical fiber core size. Firstly, the proficient coupling of light happens among the incident mode of fiber and the mode of auxiliary waveguide. At that point, the optical signal is directed from one layer to the next by methods of vertical and/or horizontal tapering of the both waveguides. Further, **S. H. Tao et al. - 2008 [80]** demonstrated a double-tip coupler which is more efficient for fiber-waveguide coupling than a single SiN taper. It composed of two inversely and laterally tapered SiN waveguides and achieved 2 dB higher coupling efficiency per coupling facet than a single-tip coupler with the same tip width of 180 nm. This type of coupler finds important applications for constructing highly dense and efficient photonics integrated circuits.

S. Galoda et al. - 2007 [81] discussed THz imaging that will combined with spectroscopic sensor of unsafe or explosive materials, may give robust and complete real-time security screening without the requirement for different frameworks and detection techniques. With THz radiation, not only image concealed objects as well as analysis of the reflectance, absorption and transparencies of various materials so all the more precisely recognize the concealed objects are possible.

J. Grade et al. - 2007 [82] described terahertz (THz) region, generally occupied between microwave and infrared bands having range 0.3–20 THz in electromagnetic spectrum, is rich with rising conceivable outcomes in imaging, wireless communications and sensing applications.

It exploited endogenous contrast mechanisms since it is non-ionizing and it has specific strength for biological applications. This range from screening people at the sub-cellular level for concealed weapons to cutting edge biomedical diagnostics. By the utilization of these applications electronic methods for producing, sensing and controlling terahertz light which includes scanning probesand broadband antennas.

The benefits from the combination of optical technology with electronic technologyoffering high bandwidth, low energy consumption and wavelength parallelism which were demonstrated by **S. J. Ben Yoo et al. - 2012 [83].** It alsodiscussed THz signal processing and bandwidth information based on RF-photonic technologies. It further emphasized the integrated circuits to RF based photonics approaches by which highly-stable terahertz bandwidth data and signal implementation can take place. Further, it also discussed an RF-photonic based lattice filter which is helpful for making shapes of reconfigurable filter in the RF space without including power hungry RF hardware.

R. Honnungar et al. – 2012 [84] proposed a plan for n-bit stage shifter which operate at a wavelength of 1.55-µm. The proposed design considered was for the realization in the domain of integrated optics, in this manner helping for scaling down. Since the realized optical phase shift is independent of input RF frequency when utilized as a part of applications of MW Photonic such as beam squinting, beam steering issue is effortlessly kept away from. By heterodyning, the created optical phase is passed on to the RF signal. Consequently these sorts of phase shifters would have the upside of scaling down, high EMI and low power losses.

B.M.A. Rahman et al. – 2014 [85] evaluated different sorts of useful dielectric and metal covered waveguides and introduced the optimized plans of MMI-based power splitters, Quantum Cascade Lasers and limited band channels. A thorough full-vectorial finite element method has been utilized to concentrate the definite modular properties of metal clad waveguides and dielectric working in the range of THz frequencies. It was demonstrated that the impact of material loss can be lessened by utilizing porous core. It is additionally expressed that plasmonic loss occurred in a hollow-core waveguide can likewise be diminished by utilizing a thin yet advanced dielectric over-layer. By utilizing a new slot-type electrode, the differential loss of higher order modes could be essentially expanded to lessen mode hopping.

Later on, various research endeavors are utilized in the range of THz sources, detectors and waveguides and for the effective usage of THz frameworks, low loss and financially reasonable waveguides are fundamental. **A. Agrawal et al. – 2012 [86]** introduced an

Equiangular Spiral Photonic Crystal Fiber (ESPCF) outline for use in the Terahertz regime for demonstrating the very low confinement loss and ultra low bending loss. It is additionally discussed that the ESPCF has excellent modal confinement properties, together with a few parameters to permit the improvement of the execution over a scope of critical attributes.

J.K Thind et al. – 2015 [87] proposed a design of line-defect photonic crystal waveguide (PCW) based upon graphene for acknowledging low power by means of on-chip delay lines which was electrically controllable. They proposed two designs: by applying graphene within the core area (line imperfection) and another with graphene on the area cladding boundary and were analyzed with plane wave extension strategy. This strategy is reasonable for evaluating the moderate light properties of PCW. The utilization of grapheme layers improves the moderate light impact of PCW. Graphene creates surface plasmon polariton (SPPs) with the presence of guided mode in the PCW which expands guided mode group index. This subsequent impact further slows down the light wave within the photonic crystal waveguide.

Now, the integration of nano-optoelectronic devices with these PhCs waveguides are carried out which were introduced by **K. Nozaki et al. – 2013 [88]** and reported first nano-PD in light of a PhCs waveguide which includes a ultrasmall absorption layer of InGaAs material having length of 3.4-μm, and show a dynamic reaction with a 10-Gb/s eye design and high DC responsivity (~1 A/W). It was inferred that the proposed outline of PhCs embedded in PD offered high efficiency and a quick reaction, and with considerably smaller than previous InGaAs-enabled waveguide photodetector due to the solid confinement of the carriers and photons, which recommends the strength for acknowledging photoreceivers that do not require electrical amplifiers. This ultra-small nano-photodetector ought to provide least-power optical links and optical signal processing combined with CMOS based hardware.

Another class of planar optics has developed utilizing gratings in subwavelength dimensions having huge contrast of refractive-index, referred to as HCGs which prompted an abundance of new properties. HCG gives ultra-broadband high reflectivity (>99%) and amazing quality-factor resonance (Q > 107). HCG will be a phenomenal novel layout for chip-scale optics. **Connie J. Chang-Hasnain - 2009 [89]** investigated the current advancement in a single layer HCG structure in subwavelength dimensions. It fuses into a VCSEL structure empowered, lithographically defined polarization control, simple fabrication, single-transverse-mode control and large aperture. It showed an extensive manufacturing tolerance in HCG based VCSELs byvariation of ±20% in the dimension of uniform HCGs and variation of±30% in the dimension of arbitrary size HCGs. The emission wavelength of VCSEL is insensitive to the HCG lithographical variations, which makes it particularly appealing for outlining and fabricating VCSELs for a settled and attainable wavelength for specific applications. A compact size HCG (3×3-μm^2) is sufficient to hold lasing, demonstrating an extensive tolerance in lithography arrangement. These outcomes demonstrate a process that gives cost-viable and better throughput manufacturing process.

Y. Zhou et al. - 2009 [90] proposed a novel HCG based ultra-low loss single-mode hollow core waveguide structure in subwavelength dimensions which provides high reflectivity through HCG based cladding boundaries at a little glancing angle and demonstrated an extremely low propagation loss (<0.01 dB/m) utilizing both FDTD and RCWA numerical method. Hollow-core waveguides are exceptionally encouraging for accomplishing fiber-like nonlinearity, low-loss and scattering as a result of the disposal of the core material. It is additionally examined that the transmission principle in a HCG based waveguide device design is not the same as a conventional photonic crystal based slab waveguide. The value of loss is less than the three orders of magnitude the most reduced loss in the present chip-scale hollow-waveguides with a greatly wide broad bandwidth (~100nm) and a large fabrication tolerance.

W. Yang et al. – 2012 [91] proposed 2D hollow-core waveguide on a silicon substrate that accelerates a updated plan of light propagating from loss-less environment, permitting for an entirely novel applications. In proposed design, 2D waveguiding was achieved by transverse guiding which was provided by HCG reflections and lateral confinement which were achieved by varying the HCG dimensions laterally. It was discussed that sidewall-free HCW design is a strong candidate for utilization in low-power, compact, fast on-chip gas/fluid sensor arrays and lab-on-a-chip applications.

A.G. Kirk - 2005 [92] analyzed a compact double-grating coupler structure that achieves coupling between two stacked high-index-difference SOI waveguides. A coupling efficiency of 29% has been achieved in coupling light from one waveguide to another with 12.9 µm long binary gratings which can further be enhanced by applying Fabry–Perot (FP) resonance between two gratings. To analyze and optimize the proposed structure, a rigorous analytical method based on the EEM has been employed along with the FDTD model was also used to verify the final design. It was also discussed that vertical FP resonance between two gratings enhances coupling efficiency, which makes control of the distance between the two waveguides critical if high efficiency is to be obtained.

T. Srinivas et al. - 2013 [93] presented a design of lab-on-a-chip sensor for detecting the changes in index of refraction and changes in the concentration of species contained in the analyte. The proposed design of sensor contained collinear input and output waveguide which were separated by a microfludic channel. As the optical light is passed though this fluidic gap, their occurs a optical power loss due to the light absorption in the fluidic gap and mode-mismatch among the input and output waveguides. This approach of sensing can yield excellent refractive index and absorption detection limits which leads to enhancement in sensitivity. The least possible detection limits of molar concentration and index of refraction which were obtained are 0.0272 nM and 10^{-7} RIU respectively.

J.B.Lask - 1986 [94] portrayed wafer bonding for SOI advancements, in which just thermally developed oxide was available between the wafer sets. Bonding happens after addition into oxidizing surrounding. It was additionally suggested that wafers are drawn into close contact subsequently of the gaseous oxygen between them being devoured by oxidation, in this way creating an incomplete vacuum.

D. Feng et al. - 2009 [95] showed a rapid Ge photodetector coordinated with a vast cross-segment SOI waveguide. A butt-coupled Ge horizontal p-i-n junction was utilized to empower fast operation. The exhibited device has an extremely minimal active area of just 8 µm2, a 3 dB bandwidth of more than 32 GHz and responsivity as high as1.1 A/W. Importantly the device can promptly be incorporated with superior wavelength-division-multiplexing channels in light of expansive cross-area SOI waveguide to frame monolithic integrated silicon photonics collectors for multichannel terabit information transmission applications.

D. Ahnet el. – 2007 [96] exhibited rapid and high effectiveness Ge based PIN photodetectors which is monolithically incorporated with top coupled silicon nitride and silicon oxynitride waveguides. The little size of the waveguide-coordinated devices brings about low supreme dark current. The coordination of waveguides with photodetectorcan beat an exchange off issue between the efficiency and bandwidth capacity of the photodetector by having a carrier-collection way and a photon-absorption way perpendicular to each other. Subsequently, the waveguide-incorporated Ge-photodetector can accomplish the execution beyond the level conceivable with free-space enlightenment, particularly at wider wavelength where absorption in Ge is less productive.

Folkert Horst et al. - 2009 [97] exhibited ultracompact incorporated optical echelle grating wavelength-division-multiplexing demultiplexers for on-chip optical systems. It is extremely powerful against process and plan variations, and is, in this way, appropriate as building block for on-chip WDM systems. It is additionally supported by the amazing execution of the "Extraordinary" device, which gives the two stigmatic point outline that accomplish a high channel number and little channel spacing with an extremely reduced footprint. It will additionally work on improving the devices presented here by replacing the corner mirrors by absolutely reflecting flat mirrors, e.g. in light of a Bragg grating. Besides, our future plans will consider techniques for flattening the passband without presenting extra losses fabricated utilizing high-index-contrast silicon-on-insulator photonic waveguide innovation.

Silicon photonics is considered as an intriguing stage for optoelectronic interconnects due to the feasibility to acknowledge complex and smaller optical systems and the CMOS suited manufacturing process. **T. Spuesens et al. - 2012 [98]** proposed an epitaxial structure, which comprises two layers, one for a detector and another for a laser, thus empowering exceptionally reduced joining of sources and detectors. A micro disk lasers and waveguide integrated photodetector utilizing this epitaxial structure were totally manufactured in a 200-mm thick CMOS pilot line and the outcomes considered about here are for a bonding layer having 130-nm thickness. The maximum efficiency among the waveguide and the microdisk laser was figured to be approx. 15% at130-nm thick bonding layer. Other basic parameters, for example, the waveguide width and the lateral offset over the microdisk laser, detector length and top contact size were differed through a scope in the plan. Fiber based coupling are utilized to gather the laser light and to infuse optical light into the photodetector. The maximum value of coupling efficiency for the fiber coupler was calculated to be around 27% at wavelength of1580-nm. The deliberate 3 dB bandwidth of around 60-nm is achieved by this fiber coupler.

An exact model of coupled-multiple on-chip interconnects for the dynamic crosstalk analysis driven by a CMOS inverter was proposed by **V. R. Kumar et al. – 2014 [99].** The proposed design catches propagation delay; peak voltage and waveform shape quite well and is pertinent to asymmetric drivers and line arrangements too. In this way, with consistent progressions in FDTD modeling and also CMOS technology, the proposed model will involve a huge part in execution investigation of on-chip interconnects.

Later on, the trend is forcing researcher to find alternative solution to form on-chip photonic antenna link which permit immunity from electromagnetic interference, give an amazingly wide working data transfer capacity, and permit long cable keeps running with at least loss. **M.L. Vanblaricum - 1994 [100]** presented the sorts of photonic connections and modulator systems accessible to the antenna engineer. It also discussed about recent improvements in laser technology permit photonic-based connections to have high dynamic range and low noise figures.

G. Tzeremes et al. - 2004 [101]exhibited a variety of RF modulator/photodetector incorporated specifically to a variety of antennas to shape a novel smart antenna plan, in which integration of devices direct the radio transmission power level through a software enabled control system. The optical fiber specifically connects with the antenna through a photodetector which expands data transfer capacity without the requirement for signal amplification. The proposed design could empower control of quicker, more reliable and versatile wireless communication systems utilizing incorporation of microwave technologies and photonics.

O. Graydon et al. - 2011 [102] discussed the future aspects of MW based photonic linkand RoF technology. The attraction of these technologies does not stop with the use of fiberoptic medium. Photonic/optoelectronic devices, for example, resonators, interferometers and lasers can be utilized to create and implement high-frequency radio frequency signals that cannot easily be developed directly in the electronic area. It has given a thought to make on-chip integration of optical circuitry that can execute such assignments, in this manner, streamlining the mass production and packaging stages.

B.Canon - 2010 [103]intended to give a idea on the optical procedures utilized for frequency conversion, i.e. mixing, and gives the advantages and drawbacks of all systems introduced. It likewise portrayed different strategies and research brings about photonics microwave mixing, predominantly for radio-over-fiber applications. These depend on both direct and external modulation, photo-detection and the utilization of single-mode and multimode fiber, for the support of existing and rising communication systems. Execution of a few photonic components and systems with high efficiency for microwave mixing is essential in their applications to security, wireless and radar systems. It additionally demonstrated that it is conceivable to up-or down-convert over with high effectiveness microwaves and complex digital signals.

J. Marti et al. - 2009 [104]gave an outline of the most noteworthy activities that are right now occurring or have been recently evolved in the fields of radio-over-fiber and microwave photonics frameworks. These advancements have noteworthy scientific relevance and enormous application driven potential for future research and commercial items.

2.3 Research Gaps

Following gaps have been found in the literature:

1. Less work on easy-to-design and fabricate fiber-to-waveguide coupler with high coupling efficiency [76, 107].
2. Not much work has been published on performance evaluation of HCG/1-D photonic crystal embedded Optoelectronic devices on Silicon on Insulator [23, 41].
3. No report on the hybrid integrated opto-RF devices with High-index contrast grating/1-D Photonic Crystals.
4. Less work on optical waveguide – photodetector system on Silicon on Insulator with characteristics enhanced using HCG/PhCs [51, 95].

2.4 Research Objectives

On the premise of the comprehension build up from the initial study and literature review the proposed goals of the thesis are crystallized as under:

1. To improve the coupling efficiency of hybrid chip to overcome mode field mismatch, refractive index mismatch and narrow band coupling.
2. Design and simulation of optical waveguide with Photonic Crystal for improved bandwidth, propagation loss, dispersion.
3. Design and simulation of photodetector embedded with photonic crystal and to study its responsivity, gain, quantum efficiency and detectivity.
4. Design and simulation of Antenna system with Photonic Crystal; to study the effect of photonic crystal on antenna parameters e.g. bandwidth, radiation pattern, directivity, gain and return loss.

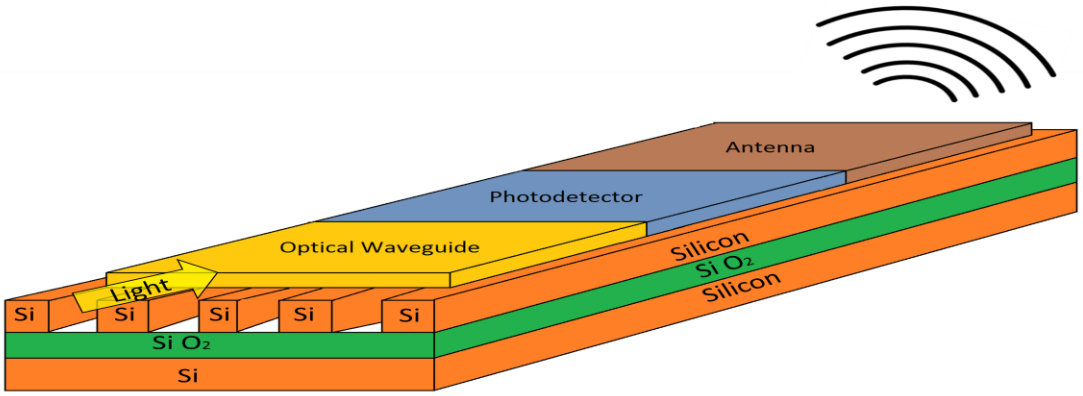

Figure 2.1:Schematic of Proposed Device Design

2.5 Thesis Organization

Chapter 1: This chapter introduces the overview of Terahertz Photonics along with Microwave Photonics with respect to major conceptual concerns.

Chapter 2: This chapter covers the thorough literature overview related to area and goals of the study. It also discussed gaps in the literature. The objectives of the thesis are crystallized here.

Chapter 3: This chapter will mainly study different efficient coupling schemes along with their various characteristic: like mode field mismatch, refractive index mismatch and narrow band coupling and will present the optimized design of grating based photonic coupler scheme that displays a high quality coupling among fiber and SOI based photonic waveguide with a wide range of wavelength. The analysis of proposed design is done by using FDTD analytical technique.

Chapter 4: This chapter will present proposed efficient design of Narrow-core Hollow optical waveguide with improvement in propagation characteristics by varying the different parameters of grating like (thickness, period and duty cycle) on the waveguide transmission properties. This chapter will also explain the impact of all grating parameters on the modal transmission loss of hollow optical waveguide by using remarkable part of high refractive-index region of silicon for controlling and manipulating the light signal across the waveguide region. Further, the utilization of proposed design of low-loss narrow-core hollow optical waveguide for the application of high performance on-chip photodetection is introduced by fixing a PIN photodetection layer in the hollow core of the waveguide. The HCG-assisted guiding of terahertz waves with loss-less environment in an intrinsic layer of PIN photodetector which causes enhanced performance in form of its responsivity and quantum efficiency.

Chapter 5: This chapter concentrates on design and analysis of 1D photonic crystal enabled multiband compact terahertz patch antenna integrated on SOI based chip. It will demonstrate that the multi-reverberation of terahertz radiation with in the copper patch placed on SOI can be successfully controlled with the presence of 1-D photonic crystals which is placed on the top of patch. The proposed design of terahertz patch antenna is appeared to operate for thirteen different frequency bands with acceptably low return losses spectra in THz region.

Chapter 6: Present chapter will remain the last chapter of thesis where summary/conclusion will be drawn, and all the more significantly recommendations on the premise of results acquired will likewise be given.

CHAPTER – 3

On-chip Coupler on Engineered SOI

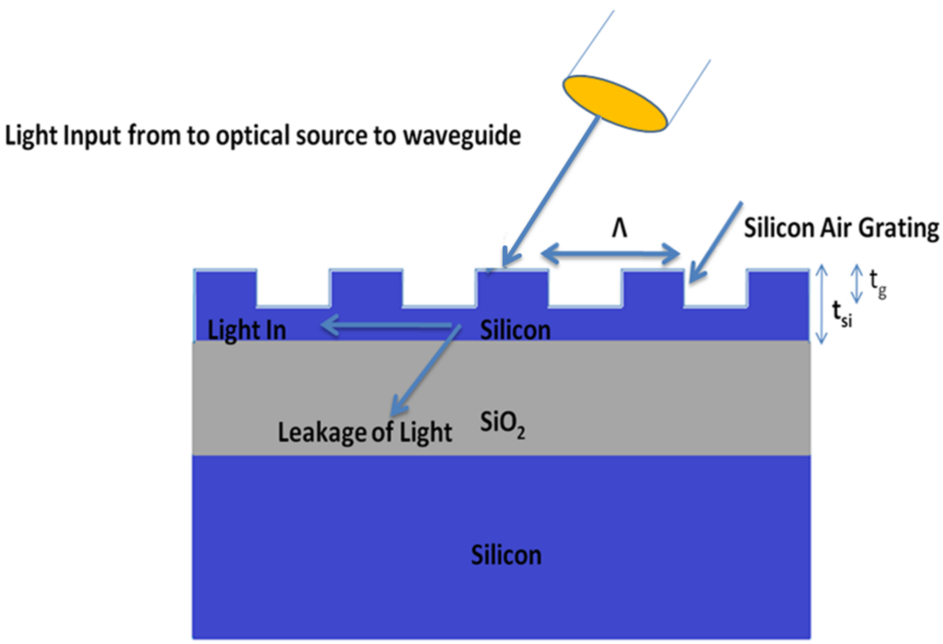

Chapter 3

On-chip Coupler on Engineered SOI

3.1 Introduction

In this chapter, the first research objective, i.e. to improve the coupling efficiency of hybrid chip to overcome mode field mismatch, refractive index mismatch and narrow band coupling has been investigated. The goal of this research objective is to give an overview of existing coupling approaches for the telecommunication range and to reveal the most efficient one to overcome a long-standing issue to connect an optical fiber with an on-chip photonic integrated circuit (PICs) and to build up an efficient fiber-to-waveguide light coupler. For this work, different schemes to improve the coupling efficiency of photonic waveguides have been discussed which incorporate the different configurations of tapered, direct, lens and scatter for improving coupling efficiency in terms of low losses, including scattering S, reflection R, and absorption A and presented a novel fiber-to-hybrid chip coupler, named “grating based photonic coupler approach” to achieve better coupling efficiency of hybrid chip through which the light fed from the top of a chip can bend 90° with low reflection and is then efficiently coupled into an on-chip silicon photonic waveguide within a short propagation distance.

Now, a great deal of efforts have been done to realize confinement of light in subwavelength dimensions by making use of silicon photonic waveguide, photonic crystals and plasmonic waveguides for increase the density of integrated optical fiber communication system. With a specific end goal to retain the condition of single mode, the dimensions of waveguide are decreased to subwavelength dimensions (e.g. 200-nm by 350-nm).Nowadays, silicon photonic waveguide are pulling in more consideration in light of their feasibility, cost viability and generally high integration density. Silicon based photonic waveguides are traditional waveguide shaving high contrast of refractive index (> 2).

A notable challenge for silicon photonic waveguide is to acquire effective coupling between the highly confined modes in a photonic integrated circuit (PIC) or an integrated optical waveguide and the large-width mode in the optical fiber utilized to couple light all through the chip. Because of the huge mismatch between the effective indices and mode sizes, direct coupling would bring about in sensational losses. However, this makes the coupling both to and from optical fiber non trivial because the presence of large mode-size mismatch among the single mode fiber and the SOI based photonic waveguide that disallows the efficient coupling of light between them (450-nm width compared to 10microns of diameters as described in

Fig.3.1).They have a very small overlap of modal fields that prevent the efficient coupling. Several solutions have been proposed to overcome this challenge.

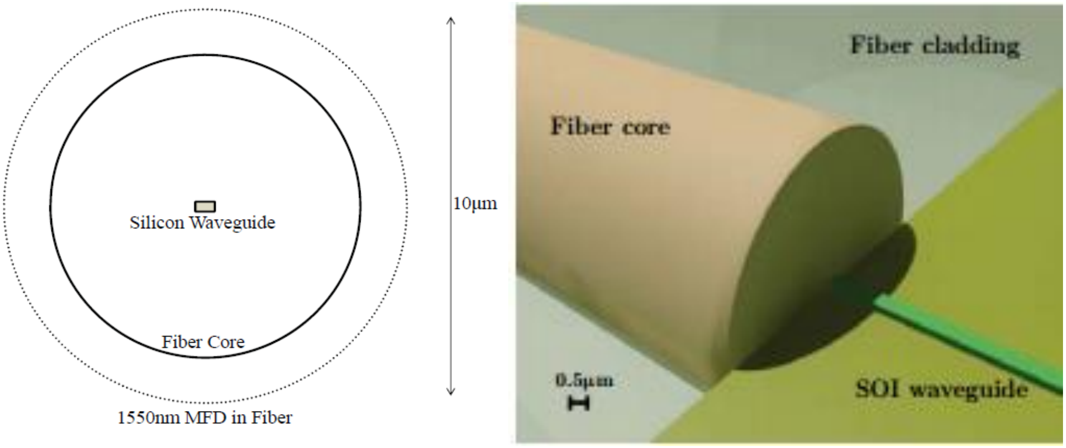

Figure3.1 Comparison of coupling scale differences [105]

Various lateral coupling techniques, for example, the proposed design of inverted tapers or 3-D tapers [106] to acknowledge coupling of light without loss between single mode fiber and SOI based photonic waveguides. Although, lensed fibers or high numerical aperture fibers are still required for proficient coupling of light, with mechanical alignment tolerances stand under 1-μm [107]. In addition, the long coupling length on the order of many micrometers to few millimeters and complex manufacturing process likewise form this technique of lateral coupling less appealing. However, none of the approaches provides sufficient efficiency for coupling into sub-micrometer silicon photonic waveguides within a compact dimension.

Table 3.1 demonstrates the better clarity of progress of grating based fiber to waveguide couplers in terms of type of grating and their coupling efficiency.

Table-I

Sr No	Type of Grating	Year	Efficiency
1	Polymer Strip waveguide based grating [108]	1997	42%
2	Top mirror [109]	2002	95% (theoretical)
3	Rear reflector [110]	2004	>70%(theoretical) 33% (measured)
4	Slanted grating [111]	2007	59% (theoretical) 16% (measured)
5	Bottom mirror [112]	2007	69%
6	Metal grating [113]	2007	60% (theoretical) 34% (measured)
7	Chirped grating [114]	2008	34% (measured)
8	Slot-waveguide based grating [115]	2008	61% (theoretical)
9	2D polarisation diversity grating [116]	2008	23% (measured)

10	2D focusing gratings [117]	2009	27%(measured)
11	Apodized Waveguide Grating Couplers [118]	2010	84% (theoretical) 76% (measured)
12	Silicon horizontal multiple slot waveguide[119]	2013	60.1%(measured)
13	Fully etched apodized grating coupler [120]	2014	87 % (measured)

To take advantage of the CMOS technology, all the existing structures must be designed/fabricated in SOI wafers which also include top and bottom mirrors, rear reflectors and slot waveguide based gratings and are made of CMOS compatible materials. Chirped and slanted gratings are of great interest in the research field, but the required fabrication techniques are not suitable for mass production yet. 1D focusing gratings have already been tested in commercial applications. Polarisation diversity gratings have also been well studied and tested, so they arise as a good solution to the coupling problem.

A different approach which involves launching of light vertically onto the chip instead of horizontally by means of HCG enabled photonic couplers. A photonic coupler is a device that makes its possible coupling of light from optical fiber or from free space to a nano-waveguide. It can be comprehend as a focusing device, a kind of an optical funnel as shown in Fig. 3.3(a) that squeezes/crushes light into a small spot. This approach only relies on normal process steps to produce a good structure, and has the significant benefit of avoiding the end facet all together. Vertical photonic coupling also eliminates the need for precise chip cleaving or polishing. These vertical photonic couplers have been shown to have low-losses similar to the other enhanced coupling methods.

By matching a thin and a thick waveguides that have various modal distributions is possible by means of photonic coupler that can be also understand as a mode convertor, a device that changes a mode of the thin waveguide to a mode of the thick waveguide as shown in Fig. 3.3 (b).

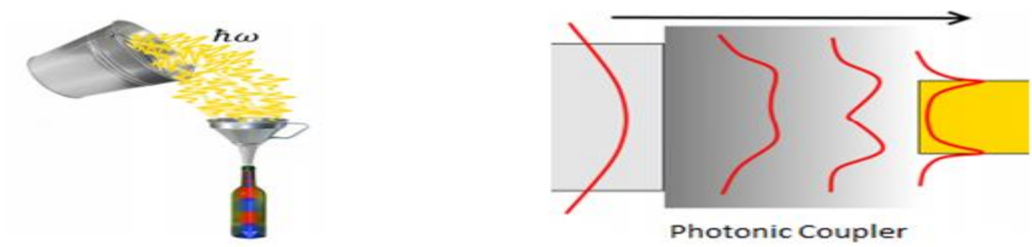

(a) (b)

Figure 3.2 Photonic Coupler concept: (a) A masterful perspective of the issue of coupling light from a wide microscopic fiber to a nanoscopic waveguide, (b) a centering device or a mode convertor [121].

3.2Structure of On-chip HCG enabled photonic coupler

The anticipated design of the on-chip HCG based photonic coupler is shown in Fig.3.4. It is composed of Silicon-on-Insulator (SOI) waveguide which comprises of top silicon layer followed by silicon dioxide layer on a silicon substrate.

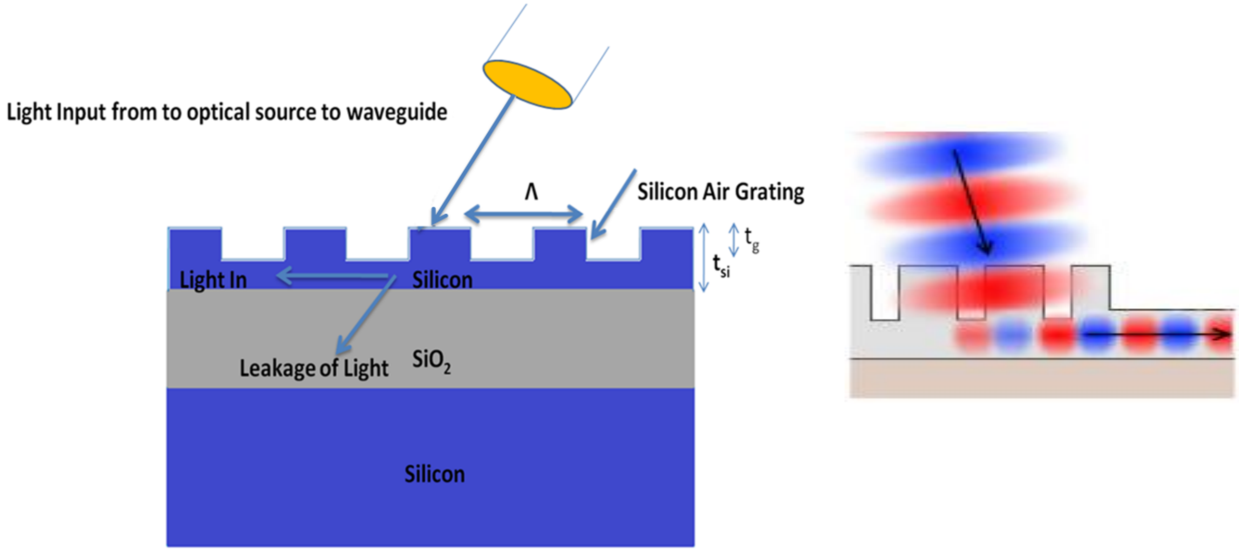

Figure 3.3 Grating based photonic coupler

A grating (called as HCG) is formed onto the top silicon layer of SOI in z-direction and the bars of grating are invariant in the x direction, however the width of SOI based photonic waveguide is limited. On top silicon layer of SOI, there can be air or an index-matching layer (refractive index nearly taken to 1.44). Perfectly matched layers (PML) boundary conditions are employed as PML can absorb radiation travelling towards the wall without introducing any additional parasitic reflections regardless of incidence angle, wavelength, and polarization of the incident light. The schematic diagram is shown in Fig.3.4.The material utilized have characteristics as the index of refraction of air, Si and $SiO_2$is considered as n_{air}= 1, n_{si} = 3.48 and n_{SiO2} = 1.45 respectively. Inset of Fig. 3.4describes the transmission of EM field inside the HCG enabled waveguide on SOI.

The purpose of this design is to investigate a technique to obtain maximum coupling efficiency between fiber and waveguide mode. To achieve this objective, an HCG enabled SOI waveguide is designed and analyzed to obtain maximum coupling from the outside world, i.e. a single mode fiber. The utilization of a HCG based waveguide stage permits a high-efficient and broadband optical coupling by using finite-difference-time-domain numerical technique. An optical light having wavelength of 1.55-µm with TE polarization is vertically introduced from fiber mode into a grating enabled SOI waveguide and is desired to be maximum in-coupling so as to maximize the coupling efficiency between fiber and waveguide mode.

In grating literature, the part of the power i.e. coupled-in or out by the grating grooves is characterized as coupling efficiency. The oxide layer thickness affects the coupling efficiency as depicted in [112]. The downward radiated wave partially reflects at the oxide–substrate interface. The oxide thickness should be chosen such that the reflected wave interferes constructively with the directly upward radiated wave. In this work, the thickness of oxide-layer is settled to 1-μm. An important part of the power is still radiated into the substrate, since the oxide–substrate interface is not a perfect reflector.

3.2.1 Coupling theory:

The modeling of the grating based photonic coupler is illuminated by a focused Gaussian beam from the end facet of a fiber which is represented as [122]:

$$|E(\rho, z)| = \frac{w_o}{w(z)} \exp\left(-\frac{\rho^2}{w^2(z)}\right) \qquad (3.1)$$

where ρ is the radial distance from the center axis of the beam, z is the axial distance from the beam's waist, $w(z)$ and w_o are the beam radius and beam waist radius of the Gaussian wave.

$$w(z) = w_o\sqrt{1 + \frac{2z^2}{kw_o^2}} \qquad (3.2)$$

where k = 2π/λ is the wave number for a wavelength λ.

Now, the field present in the grating enabled waveguide is expanded in plane waves and is expressed as:

$$E_x(y, z) = \sum_{-\infty}^{+\infty} E(\rho, z) \exp(j\beta_m z) \qquad (3.3)$$

where $\beta_m = \beta_o + \frac{2\pi m}{\Lambda}$and $\beta_o$and $E(\rho, z)$ are to be determined and Λ is the period of the gratingenabled coupler.

For the grating enabled photonic couplers the index of refraction may be represented as [123]:

$$n^2(x,y,z) = n'^2(x,y) + \Delta n^2(x,y) \sum_{-\infty}^{+\infty} F_m \exp\left(-j\frac{2m\pi}{\Lambda}z\right) \quad (3.4)$$

where n' is the index of refraction of a uniform reference design and the second term express a periodic index perturbation i.e. because of the presence of grating.

The general working of grating based photonic coupler is characterized by the Bragg condition:

$$n_{eff} = n_{top}\sin(\theta_c) + m\frac{\lambda}{\Lambda} \quad (3.5)$$

wheren_{top}relates to index of refraction of the material placed on top of the grating, n_{eff}represents effective refractive index of the grating, $\theta_c$shows thesmall coupling angle of 8^0, λ relates to wavelength of incident light, m is the particular diffraction mode and Λ representsthe period of grating. The above Eq. (3.5) describes the grating modes of operation at a specific coupling angle; however it does not give any valuable data regarding the efficiency of a proposed structure.

The different strategies have been created to ascertain the coupling efficiency among waveguide and single mode fiber through equations and analysis. However, computer simulation is mandatory to model a suitable class of grating structures. Utilizing the FDTD technique, the coupling to a waveguide can be ascertained with an Overlap Integral. The coupling to a waveguide is determined with the following integral by knowing the electromagnetic field distribution at the position of the fiber end facet [124],

$$\gamma = \frac{\left|\iint E * H_{fib}^*\right|^2}{Re\ \iint E * H^*.\iint E_{fib*}H_{fib}^*} \quad (3.6)$$

where E_{Fib} and E denote the electric field distribution of the fiber and the waveguide, respectively; H_{Fib} and H are the corresponding magnetic field distribution; the asterisk indicates the complex conjugate. γ describes the overlap between the fiber mode and waveguide mode. γ must be multiplied by the in-coupled power efficiency for calculating the fiber to waveguide coupling efficiency. If the field distribution of fiber mode and waveguide mode are normalized, the coupling efficiency to fiber becomes

$$\eta = \left|\iint E * H_{fib}^*\, dS\right|^2 \quad (3.7)$$

where S is the surface of the fiber. This equation is correct just in uniform media; however, it is exact here due to the index matching layer and the way that a fiber is a weakly guiding structure. The coupling efficiency can be additionally simplified to constant A that shows the normalization of the Gaussian wave by neglecting the smaller field components.

$$\eta = \left| E(x)E(y = y_0, z)Ae^{\frac{(x-x_0)^2+(z-z_0)^2}{w_o^2}} e^{jn\frac{2\pi}{\lambda}z\sin(\theta_c)} dx\, dz \right|^2 \qquad (3.8)$$

where θ_c is the small angle at which the fiber is inclined to surface normal direction of grating to avoid second order reflections. Coupling efficiency depends on wavelength of light and also dependent on angle θ_c as shown in above equation. x_o and z_o defines the alignment positionof the fiber which is placed above grating in x and z-direction, respectively. If fiber is inclined vertically, i.e. $\theta = 0^0$, the whole exponential term will become unity. The fiber end facet is kept near to the grating groove (< 10μm).

While Eqn. 3.8 gives a way of finding the coupling efficiency for a fiber to a silicon waveguide; it does not contain terms for the grating structure itself. Structural parameter sinclude the silicon top layer height, grating period, grating thickness, duty cycle, and silicon dioxide thickness - all of which have a significant effect on the coupling efficiency [125]. In fact, they are not omitted, but appear by affecting the *E(y,z)* term. Using an appropriate field modeling package such as optiFDTD by Optiwave, CAMFR, Lumerical FDTD solutions etc., the power coupled in by the grating enabled photonic coupler as a result of an incident power in the waveguide can be calculated, and then fed into Eqn. 3.8 to get the system's coupling efficiency.

3.3 Analysis of Grating Enabled Photonic Coupler

A grating empowered photonic coupler having uniform grating teeth can provide as maximum value of theoretical coupling efficiency of around 80% on the grounds that the input wave has exponentially reducing power along the direction of propagation z,

$$p = p_o exp^{-2\alpha z} \qquad (3.9)$$

where, α is known as the coupling quality or leakage factor of the grating [126]. It ought to be noticed that the above given equation is correct just for a long grating with small α.

accordingly, the consequences of above equation have been utilized as a beginning point and expands optimization of the best grating structure.

The design of grating based photonic coupler is realized in a 220-nm thick silicon layer of SOI. As a key segment of the configuration, the grating assumes a part of photonic coupler. The proposed design having uniform grating is intended for vertical coupling scheme with a certain angle of 8^0, the period of grating, Λ of which ought to fit Bragg condition:

$$\Lambda = \frac{\lambda}{N_{eff}} \qquad (3.10)$$

where, N_{eff} relates to the effective refractive index of the grating region and λ is the light wavelength in vacuum. As per the basic principle, the period of grating is accessible suitable for vertical coupling. At that point a series of computations were performed to locate the ideal grating thickness (t_g),grating period (Λ) and duty cycle (C = W/Λ, where W is width of high-index material in a period) respectively by utilizing the FDTD technique.

3.3.1 Effect of Silicon di-oxide Layer Thickness

As seen in literature [127], the silicon dioxide layer has a huge impactto calculate the coupling efficiency of a photonic coupler accordingly of its part in reflecting light that leaks throughthe coupling structure. Here, the design has been analyzed by varying oxide layer thickness of 1-µm and 3-µm on the efficiency of the grating enabled photonic coupler. As a result of increasing the oxide layer thickness from 1-µm to 3-µm, the coupling efficiency improved by 9 % at 1550-nm. This suggests the increased oxide layer thickness should take into consideration marginally more efficient coupling at the cost of some bandwidth.However, the standard thickness of oxide layer is assumed 1-µm in commercialized SOI wafers. Accordingly, oxide layer thickness in this work is fixed at 1-um as used by commercialized SOI wafers and analyzed the result of grating enabled photonic coupler;thepurpose of analysis is to confirm the impact of the thickness ofoxide layer rather than to optimize it.Fig. 3.5 shows the impact of thickness of oxide layer on the coupling efficiency of grating enabled photonic couplerby varying the wavelength from 1500-nm to 1650-nm.Here, it is concluded that thicker (3-µm) oxide layerhas a larger efficiency at all wavelegths as compared to the1-µm oxide layer. The values of efficiency at both oxide layer thickness (t_{SiO2}= 1 and 3-µm) by varying light wavelength of 1500, 1525, 1550, 1575, 1600, 1625 and 1650 are 0.575, 0.606, 0.631, 0.61, 0.575, 0.559 and0.548 and 0.584, 0.626, 0.689, 0.625, 0.598, 0.566 and 0.559 respectively. From the above, thecalculated value of maximum efficiency are 63.1 % and 68.9 % for 1-µm and 3-µm oxide layer thickness at wavelength of 1550-nm respectively which described that efficiency has been increased by 9 % as shown in Fig. 3.5. This suggests the increased oxide layer ought to allow marginally more efficient coupling at the expense of some bandwidth.

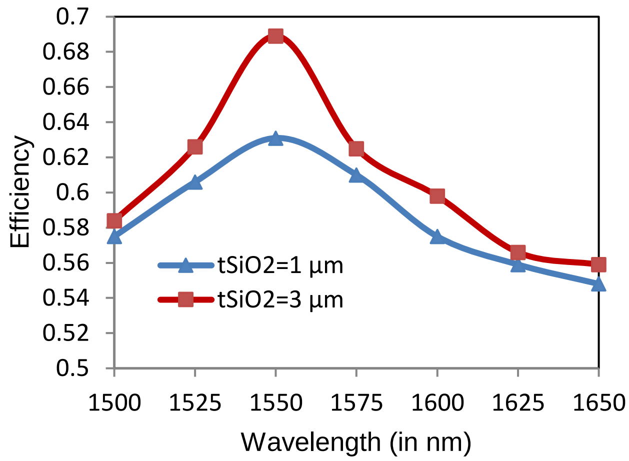

Figure 3.4 Effect of oxide layer thickness on coupling efficiency

3.3.2 Effect of Top Silicon LayerThickness and Grating Thickness

The grating thickness, t_g (thickness of the etched rectangular grating), grating period, Λ and duty cycle, C (ratio of the high-index material width with grating period) are the parameters that actually define the grating. Whereas the thickness of top silicon layer, t_{si}(guiding Si layer thickness buried over Silicon di-oxide layer) and thickness of oxide layer, t_{SiO2} (oxide cladding layer thickness) were set by the chosen SOI wafers, these parameters must be chosen to maximize efficiency, bandwidth, and have the correct center wavelength. The effect of t_{SiO2}on the coupling efficiency has already been seen from Fig. 3.5. Now, the effect of t_{si}, and t_g also plays a major role in order to achieve maximum coupling strength [128]. The overlap of mode among waveguide and fiber will not be good by choosing t_{si} in range less than 200-nm.t_{si} should be close to about 220-nm,as either increased or decreased in its dimensions reduces the confinement of power in waveguide direction, hence decreases the coupling strength. Further, by applying the shallow grating depth of around 50-nm, as desired very less amount of power is reflected back at the SOI waveguide input surface, however an abundant amount of light power get radiated through the propagation direction of waveguide. This radiated power throughout the SOI waveguide length which is needed to be condensed, therefore, the highest coupling efficiency could be acquired. Accordingly, the analysis of t_g occurred for depths of 50-nm to 80-

nm in10-nm increments. 10-nm was selected as the increment size as it was esteemed a sensible level of exactness that could be achieved through reactive ion etch (RIE) in the fabrication process. By increasing t_g above 80-nm, the transmitted power will reduce, which increases the reflected power at input of SOI based waveguide and towards the substrate. As the t_g changes, the effective refractive index and the reflectivity of the given area will also change. More etching will cause a lower effective index, and likewise less etching will cause a higher effective index. As a result of designing parameter values instead of merely checking the effect of a single change, initial simulation of t_g revealed a greater number of simulation runs were necessary to accurately gauge its efficiency effect. Fig. 3.6 shows that grating thickness, t_g of 80-nm gives maximum efficiency of 63.1 % at t_{si} of 220-nm.

Fig. 3.6 shows the impact of top silicon layer thickness by varying from 100-nm to 350-nm, t_{si} and grating thickness, t_g (50-nm to 80-nm) on the coupling efficiency (%) between fiber and SOI waveguide where it is shown that maximum value of coupling strength is achieved at t_g= 80-nm which have the values of 58.3%, 58%, 56.2%, 58.8%, 58.2% and 57.1% at t_{si} of 100-nm,150-nm, 200-nm, 250-nm, 300-nm and 350-nm respectively and it is further shown that maximum coupling efficiency is at t_{si} of 220-nm which has the values of 50.5 %, 51.8 %, 55.2% and 63.1%for each t_g of 50-nm, 60-nm, 70-nm and 80-nm. Therefore an ideal value t_g and t_{si} should be chosen which here is taken as 80-nm and 220-nm respectively at λ = 1.55-µm, with the goal that maximum light can be taken out of the plane of waveguide as shown in Fig.3.6.

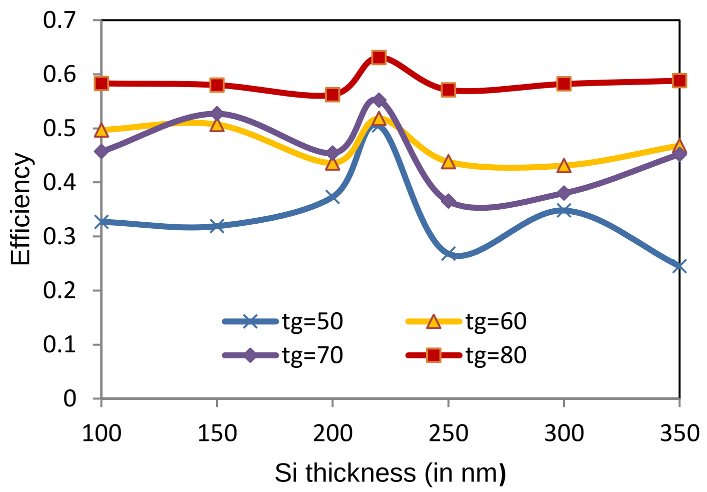

Figure 3.5Coupling efficiency with variation in t_g from 50-nm to 80-nm and t_{si} from 100-nm to 350-nm.

3.3.3 Grating Periodicity

After establishing the possible maximum grating thickness, the grating periodicity isanalyzed. Fig 3.7 shows the calculated results that was done for wavelength from 1500-nm to 1650-nm at grating period of 300-nm, 500-nm, 700-nm, 900-nm and 1000-nm on the coupling efficiency where it is shown that the maximum value of coupling efficiency of 63.1 % occurs for Λ of 700-nm at 1550-nm. A smaller interval of period have been used for this analysis, this interval was sufficient tosee the behavior as periodicity varies. It is shown by the plot that the maximum coupling efficiency achieved at each wavelength for Λ of 700-nm which have the values of 57.5%, 60.6%, 63.1 %, 61%, 57.5%, 55.9% and 54.8% at λ of 1500, 1525, 1550, 1575, 1600, 1625 and 1650-nm respectively and it is also examined that maximum coupling strength is at λ of 1550-nm which has the values of 49.5 %, 61 %, 63.1 %, 60.3 % and 59.1% for each Λ of 300-nm, 500-nm, 700-nm, 900-nm and 1000-nm. It is further concluded that the plot of Λ=700-nm has the maximum coupling efficiency at each λ.

The effect of Λ for calculating the coupling efficiency is similar to the effect of t_g and the major difference between the potential genuine impacts of t_g and Λ is that the Λ can be definitely characterized utilizing electron beam lithography, while there is natural error in characterizing the t_g. This implies that the Λ is known to be very near to the attainable value and unaltered by manufacture errors.

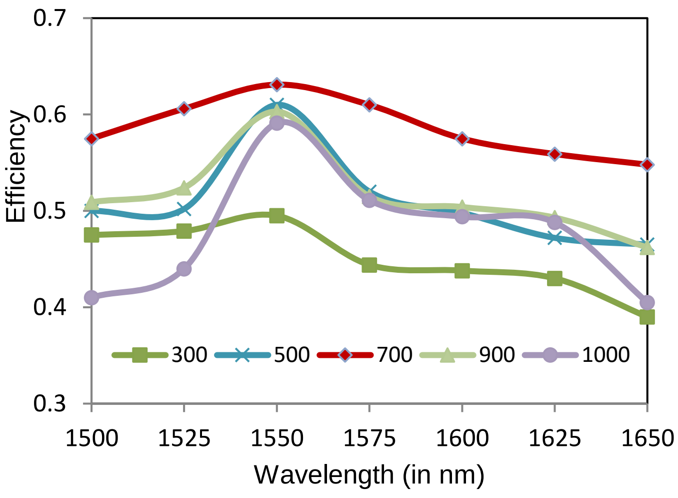

Figure 3.6 Effect of grating period and wavelength on Coupling Efficiency of grating based photonic coupler.

3.3.4 Effect of Duty Cycle

Duty cycle (C), characterized as proportion between the widths of the etched sections and areas without etching additionally assumes a critical part towards increasing coupling strength. The effect of grating thickness and grating periodicity are optimized in previous section, duty cycle, or the percentage of period of grating possessed by un-etched silicon, still the main parameter of grating to be modeled. To provide a decent specimen of execution, an efficient baseline coupler is required to be obtained. Fig 3.7 shows a best optimized grating period of 700-nm that provides the highest performance at all wavelengths (1500-nm to 1650-nm) and provides maximum coupling strength of 63.1% at λ of 1550-nm. Integrating the results of Fig. 3.6 and 3.7, optimized values of Λ of 700-nm, t_g of 80-nm and t_{si} of 220-nm, maximum value of coupling efficiency of 63.1 % is found for different values of duty cycle as appeared in Fig. 3.8. Duty Cycle between 0.1 and 1 were tested at 10% intervals. It is shown by the plot that the maximum coupling efficiency achieved at each wavelength for C of 0.5 which have the values of 0.575, 0.606, 0.631, 0.61, 0.575, 0.559 and 0.548 at λ of 1500, 1525, 1550, 1575, 1600, 1625 and 1650 respectively and it is shown that maximum value of coupling efficiency is at λ of 1550-nm which has the values of 0.177, 0.0494, 0.631, 0.613, 0.602 and 0.595 for each C of 0.1, 0.3, 0.5, 0.7, 0.9 and 1.It is concluded that the maximum coupling efficiency is obtained at C= 0.5 in comparison to any other value of duty cycle. The best curve centre was obtained using a 50% duty cycle.

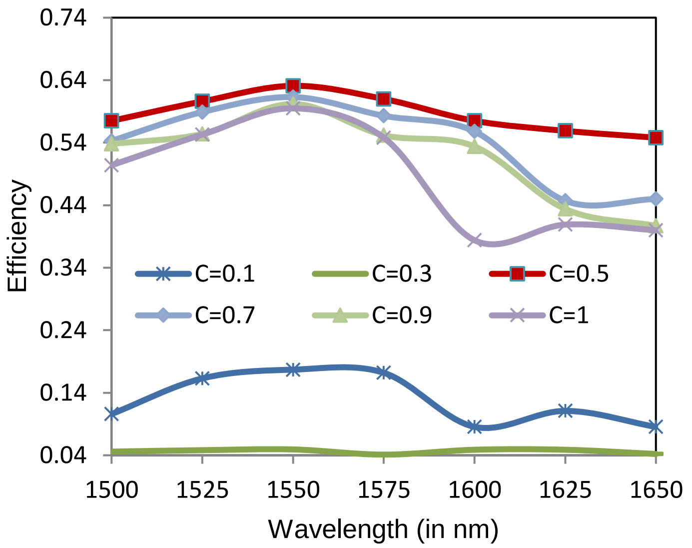

Figure 3.7Effect of C from 0.1 to 1 and λ between 1500 to 1650-nm on coupling efficiency of grating based photonic coupler.

3.3.5 Optimized Grating Design

From the analysis done in previous sections, the optimal grating design for a 220-nm top Si layer, 1-µm oxide layer wafer, 700-nm grating period, 80-nm grating thickness, and 50% duty cycle is designed to work. This design is appeared in Fig. 3.9.

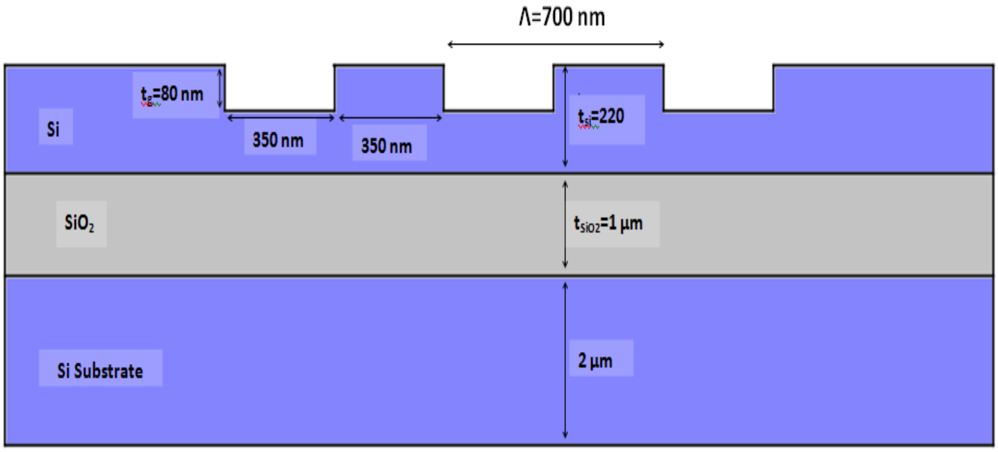

Figure 3.8 Optimized grating profile design

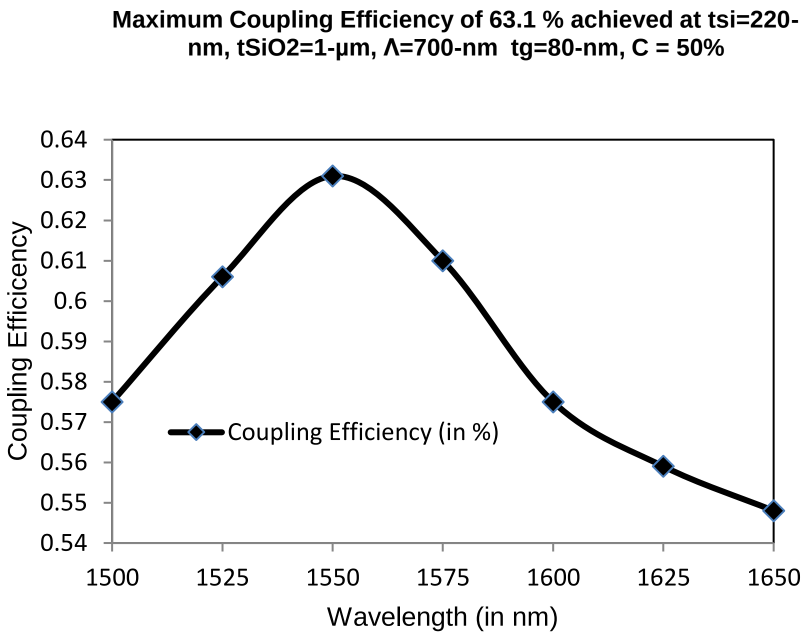

Figure 3.9 Optimized grating coupler simulated performance

The performance of the optimized grating design is shown in Fig. 3.10 where it is observed that the minimum and maximum coupling efficiency achieved with this proposed grating based photonic coupler design are 54.8 %and 63.1 % at λ of 1550-nm and 1650-nm respectively.

3.4 Summary

This objective focuses on the design of compact grating based photonic couplers in the strong coupling regime. An overview on the background of the main aspects related to fiber-to-chip coupling efficiency has been reported in this chapter. Some issues regarding different fiber-to-chip coupling schemes were first introduced and the efficient coupling techniques insensitive to polarization are strongly recommended. Different configurations to raise the fiber-to-chip coupling efficiency were discussed. Micro/ nano photonic devices on SOI assume a vital part in integration of large-scale photonic device due to the high contrast of index of refraction among SiO_2 (1.46)and Si (3.45).The need for efficient coupling by high index contrast silicon photonic waveguides was also discussed. The fiber-to-waveguide coupling problem in silicon photonic waveguides was then analyzed by modeling the two main coupling loss contributions: the mode size difference and the refractive index mismatch between the fiber and the waveguide mode. After calculating the coupling losses between the fiber and the waveguide, it is concluded that efficient coupling techniques are needed because obtained coupling losses were extremely high. Then, the most important grating based photonic coupling techniques (out-of-plane coupling) is introduced, that yields a significant improvement in coupling strength between an SOI waveguide and a single mode optical fiber, which emphasizes the fact that the strong confinement of the electromagnetic fields of the optical modes in a small region can be efficiently exploited for enhancing nonlinear effects, which are of high importance for potential nonlinear optical applications. On the basis of the proposed grating based photonic coupler design for smaller losses compensation with high gain can probably be useful for efficient light coupling.

CHAPTER – 4

Grating Enabled Hollow Waveguide for efficient photodetection

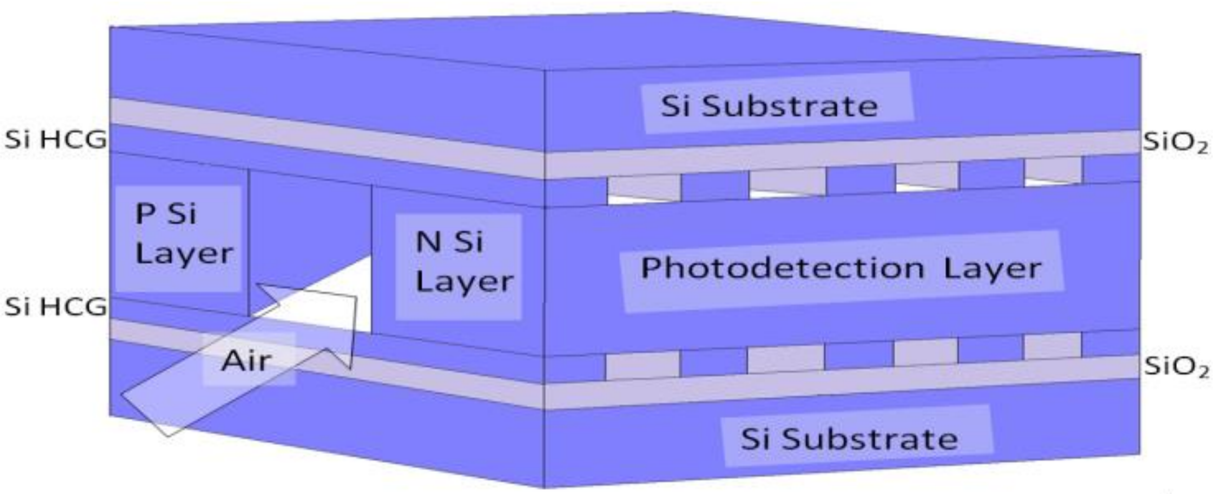

Chapter 4

Grating Enabled Hollow Waveguide for efficient photodetection

4.1 Introduction

In the chapter 3, we proposed a novel design for grating enabled photonic coupler for broadband coupling with higher efficiency. In this chapter, our prime focus is to propose a design and analytical treatment of narrow–core hollow optical waveguide in engineered SOI for developing a low-loss medium by employing top and bottom HCG's mirrors at hollow core for the application of on-chip photodetection. The proposed design of narrow–core hollow optical waveguide in engineered SOI allows a loss-less and efficient environment for the signal to be propagated within the hollow core of the waveguide because of the existence of highly confined surface modes through HCG's mirrors. The presence of top and bottom HCG's mirrors within the waveguide acts as cladding boundaries for guiding and manipulating the light on a compact platform. The resulting HCG based device design enables the field to be strongly restricted in the active layer by making it highly efficient and responsive device. This strong optical confinement within the narrow-core hollow optical waveguide allows the signal to be easily detected by applying PIN photodetection layer in hollow core with limited footprint. In this work, a novel design of HCG enabled low-loss narrow-core hollow optical waveguide embedded with PIN photodetection layer is presented which demonstrate propagation of highly confined optical modes at near-infrared wavelength in hollow optical waveguide and their detection with an on-chip integrated PIN photodetection layer. Firstly, we will start with the introduction of the monolithic optoelectronic integrated circuits.

The monolithic integration of optoelectronic circuits is encouraging for future optical fiber communication system because of the good reliability, small size, and remarkably reduction in interconnections for the applications high speed information [129-130]. It is viewed that the future interconnects technology required an energy cost of around 10 fJ/bit for a single fiber optic link [131].Superior photodetector remain a vital part as which decides the total utilization of power and the complete execution of the optical medium [132-134]. Hollow-core waveguides (HW) are highly promising for achieving fiber-like ultra-low loss, nonlinearity and dispersion because of the elimination of the core material. The basic principle of hollow-core waveguide is to guide the optical beam propagating through air by multiple reflections at the cladding mirrors. A hollow-core waveguides can be the building block for low-loss monolithic optoelectronic/photonic integrated circuits. An integrated platform based on hollow core waveguide can permit on-chip cost-viable systems having capacity to monolithically integration of electronics with light sources, detectors. There have been advances in hollow-core waveguides, ranging from waveguides using a metallic shell, to ones using a distributed Bragg reflector (DBR), to ones with photonic crystals (PhCs), etc [67]. Demonstration of HCG based hollow waveguide has opened another plan of light propagating for low-loss waveguide, considering a totally new scope of applications. The impact of HCG enlightens us to give very high quality factor resonance, broadband ultra-high reflectivity, and broadband ultra-high transmission for surface-normal light wave [135].

A light can be efficiently controlled and manage on a compact platform by means of HCG enabled hollow optical waveguide. In this work, a proposed design of narrow-core hollow optical waveguide in engineered SOI with a compact foot-print (1-µm x 10-µm x 10-µm) is presented with two parallel HCGs mirrors for accomplishing the superior detection of light inthe PIN photodetector (PD) intrinsic region. The HCG-enabled guiding of optical light with low propagation loss in intrinsic region of PD enhances the responsivity (R) of 0.8 A/W and quantum efficiency (QE) of 64 %. The existence of HCGs mirrors in the proposed waveguide design can build the light intensity thereby resistance inside the intrinsic layer of photodetector reduces because of the more generation of electron-hole pair which further increases the generated photo-current within the photodetector that enhances the R and Q.E of on-chip PIN photodetector. Light propagation and detection within the grating empowered hollow optical waveguide in engineered SOI are executed with FDTD numerical technique by assuming a TE-polarization light with wavelength of 1.55-µm and a width of photodetection layer is considered as1-µm. In the proposed plan, HCG empowered narrow-core waveguide for superior photodetection design has been appeared as good sensing applicants on account of their better sensitivity and inherent benefits of multi-parameter sensing. The subsequent configuration enables the field to be tightly restricted in the intrinsic layer of PIN photodetector through HCG based waveguide design device by making it highly efficient and responsive device.

4.2 Proposed Configuration

The proposed scheme of HCG enabled narrow-core hollow optical waveguide in engineered SOI for superior photodetection is appeared in Fig. 4.1(a) in which a PIN-photodetection layer having width 1-µm is presented among two parallel placed HCGs(in subwavelength dimensions) mirrors of proposed hollow-waveguide. HCG assisted hollow optical waveguide greatly reduce dispersion and non-linearity accordingly decreases the loss within the waveguide mode [90]. Therefore, the presence of guided modes inside the waveguide reaches to the intrinsic layer of PIN photodetector where they 'senses' the existence of two parallel placed HCGs mirrors as cladding boundaries to PIN-photodetector. Accordingly, the optical power of guided modes totally transmits into the active intrinsic layer of PIN photodetector where it begins to generate a photocurrent by absorbing the guided modes power within the PIN-photodetection layer. Hence, the optical power from proposed waveguide mode transformed into electrical signal which will transmit by means of photodetector hardware to the electronic chip.

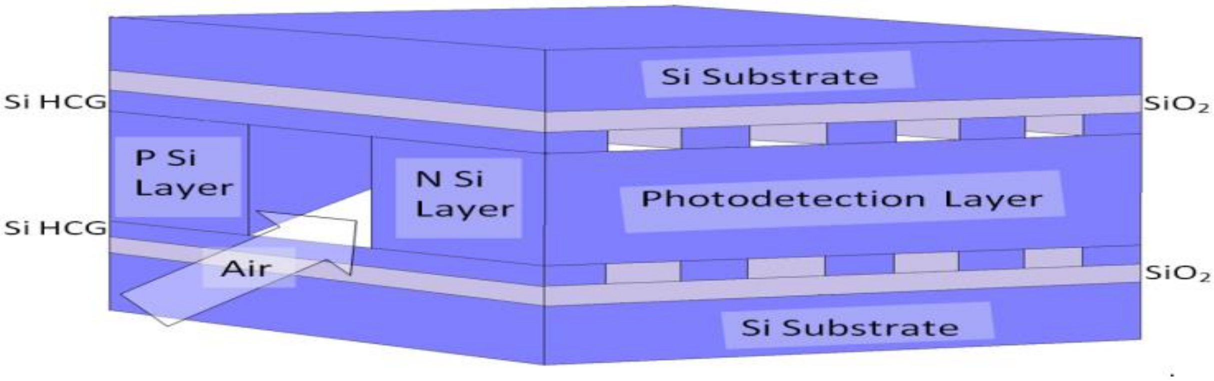

(a)

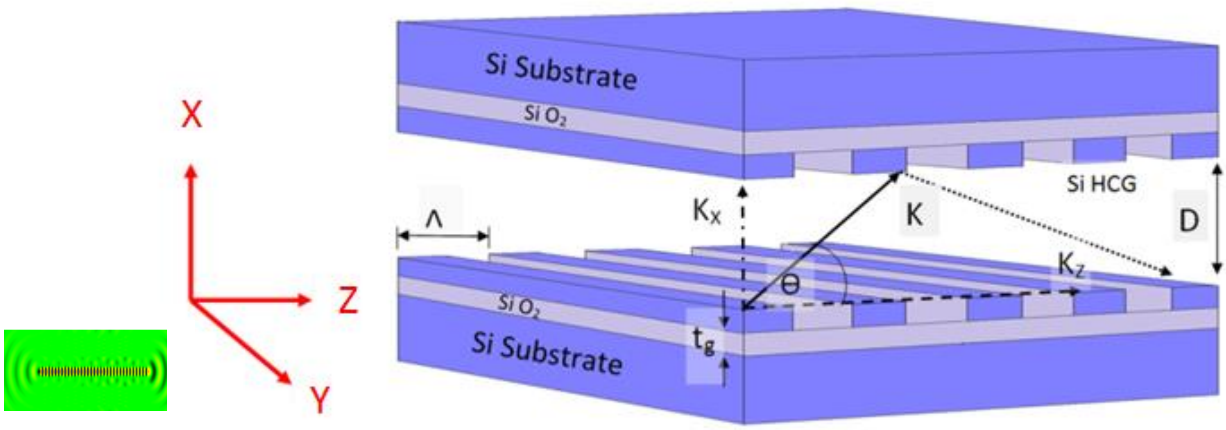

(b)

Fig.4.1 (a) Scheme of proposed narrow-core hollow waveguide in engineered SOI for superior on-chip photodetection. (b) Scheme of HCG enabled hollow optical waveguide in engineered SOI; the air-core is put among two parallel HCGs mirrors with 1-μm separation gap. The longitudinal confinement has been achieved through HCGs by which light is propagated with zig-zag reflections. The HCG configuration gives ultra-high reflectivity over a large bandwidth; therefore, the optical light can be tightly confined in the hollow-core of waveguide in z-direction. HCG period, duty cycle and thickness are indicated by Λ, C and t_g respectively.

The proposed scheme for HCG enabled narrow-core hollow waveguide is appeared in Fig 4.1(b) in which two parallel placed HCGs mirrors are completely fenced by material having low refractive index. HCGs are typically made of semiconductor materials having high refractive index contrast (>2). The fundamental parameters of grating are utilized to manage the optical light inside the proposed hollow waveguide i.e. period (Λ), duty cycle (C)and thickness (t_g). As the incident light wave is introduced on a periodic grating structure, the wave is getting transmitted and reflected into the multiple diffraction orders. In spite of the fact that, when the period of the grating is not as much the wavelength of light, expect zeroth order mode all higher order modes are evanescent in the air [91]. In this manner, broadband ultra-high reflectivity is accomplished because of the presence of high contrast of index of refraction between the grating grooves and their surroundings which is valuable for establishing a tightly confined light wave inside the proposed waveguide area consequently increases the efficiency and decreases the waveguide loss. In this way, a HCG empowered hollow waveguide can improve the coupling efficiency between the optoelectronic devices. Inset of Fig. 4.1(b) demonstrates the propagation of EM field inside the proposed waveguide which shows that light is linearly transmitting with lossless medium throughout the waveguide length because of the existence of surface modes emerge with both HCG's mirrors that can additionally enhances the execution of PIN-photodetection layer.

4.3 Analysis of Transmission Modes within Proposed Waveguide

The proposed design of narrow-core hollow optical waveguide provides a loss-less transmission due to the presence of two parallel placed HCGs mirrors on SOI which acts as high reflective cladding boundaries of the hollow optical waveguide. This novel waveguide design considered as potential applicant for efficient coupling stage for on-chip integration of optoelectronic circuits due to the existence of in-plane index contrast through HCG and vertical-index contrast through SOI. This section presents the analytic formulation for propagating modes in the waveguide. Due to the symmetry of the HCG waveguide, the modes can be classified as even and odd modes. The position of the hollow core center is x=0. Here, the waveguide is decomposed into three regions: inside the core ($x<D/2$), the grating region ($D/2<x<D/2+t_g$) and outside the grating ($x>D/2+t_g$) whereD relates to the height of waveguide The electric and magnetic fields for a TE mode are written using Maxwell's equations in each of the regions. By matching the boundary conditions at the interface, a set of homogeneous equations relating the field amplitudes in each region. Axial propagation constant and the mode profiles can be solved by looking for solutions when the determinant of the homogeneous system becomes zero.

As the optical wave is incident on the surface of periodic grating having high refractive index contrast, multiple diffraction orders will emerges and that provides a solution of infinite set of plane waves and can be described within the hollow-core of the waveguide [91].

$$(E_y)_{core} = \sum_m \rho_m \cos(k_{xm}\, x) e^{i(k_z + mk_g)z} \qquad (4.1)$$

where ρ_m is the mode density, z is the axial distance and Bragg wave number $k_g = \frac{2\pi}{\Lambda}$, k_{xm} and k_z are the lateral and axial wave numbers respectively related by the expressions

$$k_{xm}^2 + \left(k_z + mk_g\right)^2 = k_0^2 \quad (4.2)$$

where k_o is the free space wavenumber.

In the grating region, the field is given by the sum of infinite number of harmonics in both the high index and low index regions. These solutions are of the form

$$(E_y)_{grating} = \sum_n A_n \cos(\beta_n\, x + \Phi_n) e^{i\Gamma_n z} + B_n \cos(\beta_n\, x + \Psi_n) e^{-i\Gamma_n z} \quad (4.3)$$

Periodic boundary conditions are applied to relate the wave numbers in the grating region (β_n, Γ_n) to the bloch wavenumber k_z. The electric field outside the waveguide region is similar to that inside the core comprising of multiple-diffraction orders

$$(E_y)_{outside} = \sum_m \tau_m\, e^{ik_{xm}x}\, e^{i(k_z + mk_g)z} \qquad (4.4)$$

The desired HCG is needed to get high reflectivity throughout the length of the waveguide; therefore, the TE polarized light wave is completely confined in the z-direction with lossless environment. The incident optical beam is propagated inside the waveguide by multiple jumps at different angles among two high reflecting HCGs mirrors which acts as a cladding layers as these layers composed of two parallel SOI enabled HCGs mirrors which are separated by a distance D. At every jump, the propagation loss occurs of δ=1-R, where R is the reflectivity through HCGs. The existence of air as a hollow-core and high reflectivity HCGs mirrors as cladding boundaries of the proposed waveguide, the propagation loss per unit length over distance L is calculated as:

$$Loss\left(\frac{dB}{m}\right) = \frac{-10}{L} \;.\,log\left(\frac{P_t}{P_i}\right) = \frac{-10}{L} \;.\,log(R^N) \;= \frac{-10}{L} \;N\,log(R)$$
$$= \;-10\;\frac{tan\theta}{D}\;\;log(R)$$

Where N is the number of bounces in distance Land N=$\frac{L\tan\theta}{D}$.

$$Loss\left(\frac{dB}{m}\right) = \frac{-10tan\theta}{D} \;.\,log\;\;(R) \qquad (4.5)$$

Here θ represents the angle between the ray and the waveguide mode and D relates to the height of waveguide. Thus, these parameters are needful to find out the presence of guided modes within the waveguide region. The very interesting feature of proposed HCG enabled hollow optical waveguide design includes its compact size, low-loss within the narrow-core and strong carriers confinement. Therefore, the proposed design of low-loss waveguide utilized to design various devices such as couplers, antenna etc. The value of optimized grating parameters are used while calculating the low-loss propagation within the hollow optical waveguide: grating period (Λ) = 700-nm, C = 0.5, t_g= 200-nmand wavelength (λ) = 1.55-µm.

Finite difference time domain (FDTD) technique is utilized to determine the transmission loss within the proposed hollow waveguide. This technique allows us to study the propagation of light within the waveguide which is based upon the Maxwell equations.

Maxwell's equations are a set of four equations that describe the behavior of electromagnetic radiation. These equations were first presented by James Maxwell in 1864 and today are commonly written in differential form as:

$$\nabla \times H = \frac{\partial}{\partial t}D + J \qquad (4.6)$$

$$\nabla \times \mathrm{E} = -\frac{\partial}{\partial \mathrm{t}}\mathrm{B} \qquad (4.7)$$

$$\nabla.\mathrm{D} = \rho \qquad (4.8)$$

$$\nabla.\mathrm{B} = 0 \qquad (4.9)$$

E and H are the electric and magnetic field strengths respectively, D the electric displacement, B the magnetic flux density, and J and ρ the current and charge density [67]. Since we are working in photonics, we are only interested in source-free situations so ρ = 0 and J = 0. The equations simplify further if our material system is isotropic:

$$D = \epsilon E \qquad (4.10)$$

$$B = \mu H \qquad (4.11)$$

where ϵ, the material permittivity and μ, the permeability, are scalars. In the end, we are left with

$$\nabla \times E = \frac{\partial}{\partial t}\mu H \qquad (4.12)$$

$$\nabla \times H = \frac{\partial}{\partial t}\epsilon E \qquad (4.13)$$

$$\nabla . E = 0 \qquad (4.14)$$

$$\nabla . H = 0 \qquad (4.15)$$

which the finite difference time domain (FDTD) technique solves.

Fig 4.2 describes the effect of wavelength (λ) by varying from 0.6 to 1.7-µm and grating period, Λ (500-nm, 700-nm and 900-nm) on the propagation loss α (dB/m) of proposed waveguide which shows that grating period of 700-nm has low propagation loss at each wavelength. The values of propagation loss occur at 700-nm grating period are 1.41, 1.26, 1.27, 1.8, 1.33, 1.22 and 1.58 dB/m at each wavelength of 0.6-µm, 0.8-µm, 1-µm, 1.2-µm, 1.4-µm, 1.55-µm and 1.7-µm and it is also shown that the value of minimum propagation loss occurs at λ of 1.55-µm which have the values of 1.42, 1.22 and 1.6 dB/m for each Λ of 500-nm, 700-nm and 900-nm. It is further bringing out that the propagation loss (in dB/m) of proposed narrow-core hollow optical waveguide is ultra-low at λ of 1.55-µm for each period.

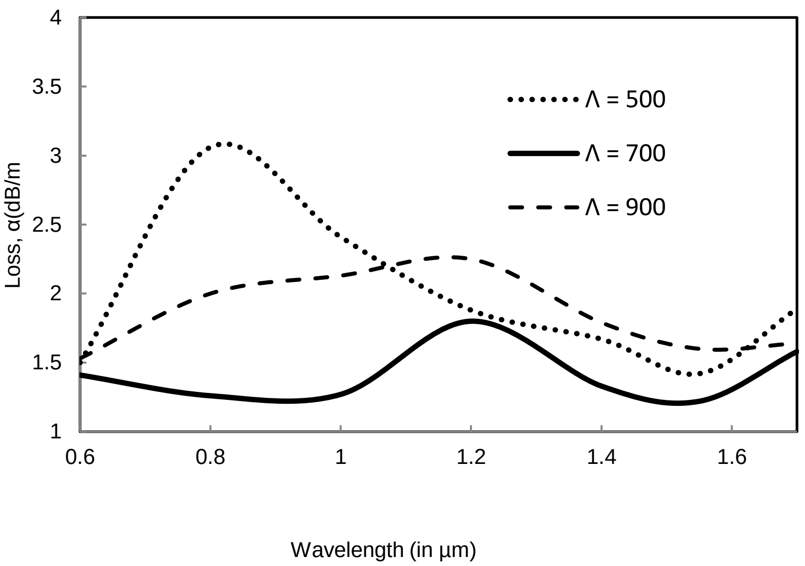

Fig.4.2 Dependence of wavelength (λ) on the propagation loss of hollow-waveguide at periods

of Λ= 500, 700 & 900-nm with t_g= 200-nm, C = 0.5.

The presence of HCG mirrors as cladding boundaries of hollow-waveguide supports lateral surface modes that will combine within the hollow-core of the waveguide with a least loss in the hollow-core. By using narrow-core and optimized grating parameters makes it able to improve the photodetection through the surface modes which get combined with the guided modes of the proposed waveguide. The optical light having λ of 1.55-µm with TE polarization is introduced into 1-µm air-core of the proposed waveguide along the propagation direction of HCG enabled hollow waveguide and calculated the loss within the waveguide mode having value of 1.22 dB/m by utilizing the FDTD numerical technique.

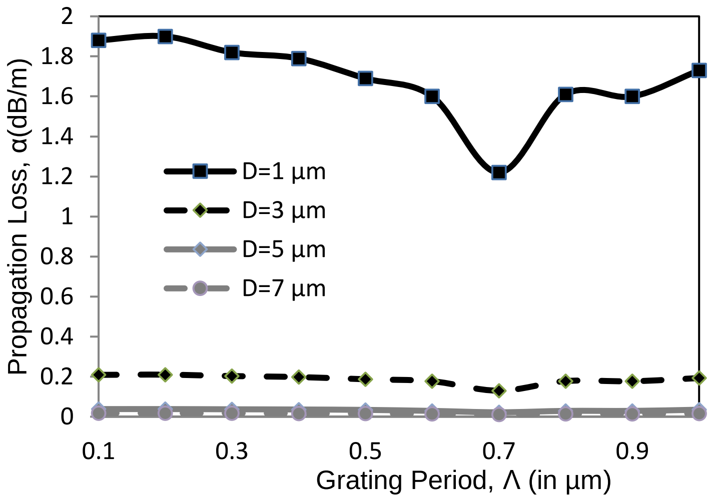

Fig.4.3 Propagation loss (in dB) of hollow optical waveguide by varying period from 0.1-µm to 1-µm and air-core thickness of 1-µm, 3-µm, 5-µm and 7-µm at t_g= 0.2-µm, C = 0.5, λ=1.55-µm.

Fig 4.3 demonstrates the effect of grating period Λ by varying from 0.1-µm to 1-µm and thickness of core size D, (1-µm, 3-µm, 5-µm and 7-µm) on the loss of proposed waveguide which shows that minimum value of loss occur at Λ of 0.7-µm for each core size thickness D. At each core size thickness of 1-µm, 3-µm, 5-µm and 7-µm the values of propagation loss occur are 1.22, 0.13, 0.022and 0.012 dB/m at grating period of 0.7-µm and it is also optimized that propagation loss for D = 1-µmare 1.88, 1.9, 1.82, 1.79, 1.69, 1.6, 1.22, 1.61, 1.6 and 1.73 dB/m at each Λ of 0.1, 0.2, 0.3, 0.4, 0.5, 0.6, 0.7, 0.8, 0.9and 1-µm. From the above values, it is found that the maximum and minimum value of propagation loss within hollow waveguide at air-core thickness of D=1-µm are 1.9and 1.22-dB/m at Λ of 0.2-µm and 0.7-µm respectively. Moreover, it is bringing out that loss occur within the waveguide having value of 1.22-dB/m at air-core thickness of D =1-µm is ultra least loss in contrast with earlier revealed outcomes.

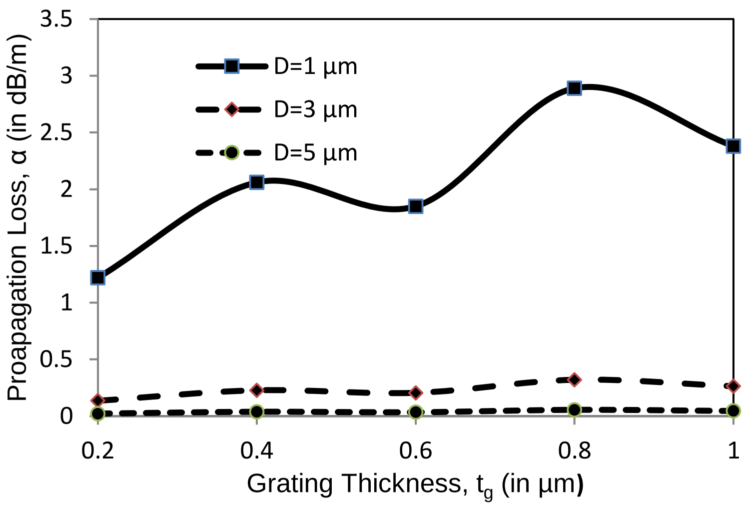

Fig.4.4Propagation loss by varying grating thickness t_g from 0.2 to 1-µm and air-core thickness D on 1, 3 and 5-µm at Λ= 0.7-µm, C = 0.5, λ=1.55-µm.

Fig.4.4 describes the impact of loss within the waveguide by varyinggrating thickness, t_g from 0.2-µm to 1-µm at air-core thickness, D of 1-µm, 3-µm and 5-µm of the narrow-core hollow optical waveguide where it is shown that the minimum value of loss is obtained at t_g of 0.2-µm for each core size thickness D. The values of minimum propagation loss occur at t_g of 0.2-µm are 1.22, 0.136 and 0.023 dB/m at each core size of 1-µm, 3-µm and 5-µm and it is also optimized that propagation loss value for narrow-core (D = 1-µm) are 1.22, 2.06, 1.85, 2.89 and 2.38 dB/m at each t_g of0.2-µm, 0.4-µm, 0.6-µm, 0.8-µm and 1-µm. The values of minimum and maximum propagation loss for core thickness (D) of 1-µm, 3-µm and 5-µm are 1.22, 0.136 and 0.023-dB/m and 2.89, 0.321 and 0.056-dB/m respectively. Hence, it is concluded that the value of minimum propagation loss obtained at t_g of 0.2-µm in comparison to any other value of grating thickness.

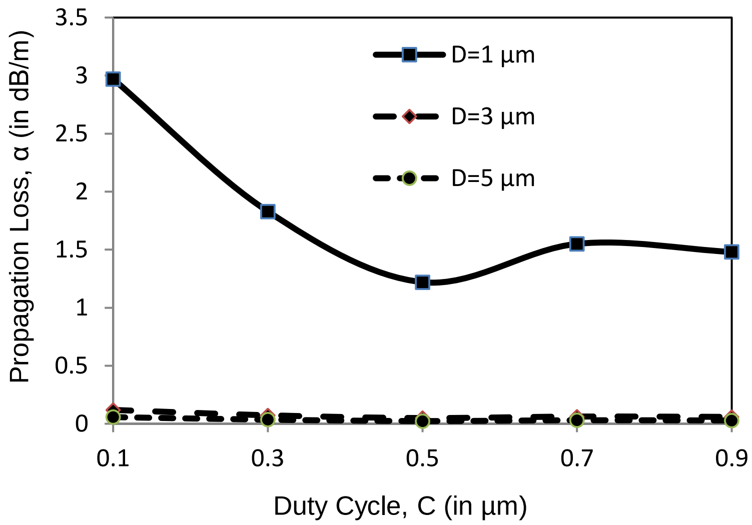

Fig. 4.5Variation of Duty cycle from 0.1-µm to 0.9-µm and air-core thickness on the

propagation loss of waveguide at Λ= 0.7-µm, t_g= 0.2-µm, λ=1.55-µm.

Fig. 4.5 demonstrates the impact of duty cycle by varying from 0.1-µm to 0.9-µm and air-core thickness (D) of 1-µm, 3-µm and 5-µm on the propagation loss of hollow-core waveguide which optimized that loss has a minimum value of 1.22-dB/m at duty cycle of 0.5-µm for each core size thickness D. The values of minimum propagation loss at duty cycle of 0.5-µm are 1.22, 0.049 and 0.023 dB/m at air-core thickness (D) of 1-µm, 3-µm and 5-µm. It is further observed that the propagation loss valuesat air-core thickness (D) of 1-µm are 2.97,1.83, 1.22, 1.55 and 1.48 dB/m at C of 0.1, 0.3, 0.5, 0.7 and 0.9.From the above results, it is further concluded that the value of minimum loss is obtained at duty cycle of 0.5-µm for each air-core thickness, D.

From the previous results explained above, it is observed that the optimized values of grating parameters of Λ of 700-nm, t_g of 200-nm and C of 0.5 are obtained and the minimum loss of 1.22-dB/m is calculated at λ of 1.55-µm. Fig. 4.6 shows the effect of air core thickness D at 1-µm, 3-µm, 5-µm, 7-µm, and 9-µm on the propagation loss of the proposed hollow waveguide where it is shown that the value of propagation loss reduces by incrementing the air-core thickness D. In this work, the air-core thickness of 1-µm is taken for the proposed design of hollow optical waveguide and it is bringing out that the propagation loss of1.22 dB/m is least at the air-core thickness (D) of 1-µm. Moreover, it is examined that the values of loss within the waveguide at D of 3-µm, 5-µm, 7-µm, 9-µm and 15-µm are 0.136 dB/m, 0.049 dB/m, 0.023 dB/m, 0.011 dB/m and 0.006dB/m respectively.

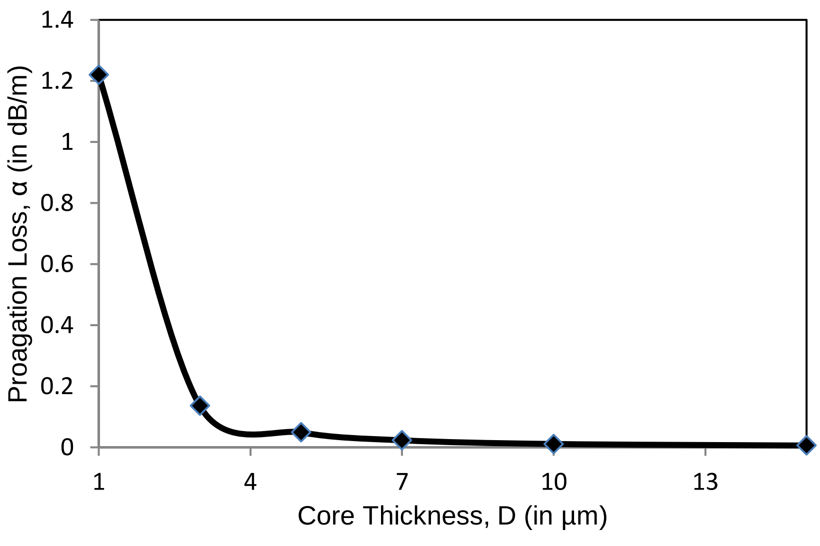

Figure 4.6 Effect of air-core thickness, D from 1-µm to 10-µm on propagation loss of waveguide at Λ = 700-nm, t_g= 200-nm, C = 0.5, λ=1.55-µm

4.4Optimized Hollow Optical Waveguide Design

From the analysis done in the previous sections, the optimal narrow-core hollow optical waveguide design for a 200-nm grating thickness, 700-nm grating period and 50% duty cycle designed at λ of 1.55-μm to work. This design is shown in Fig. 4.7.

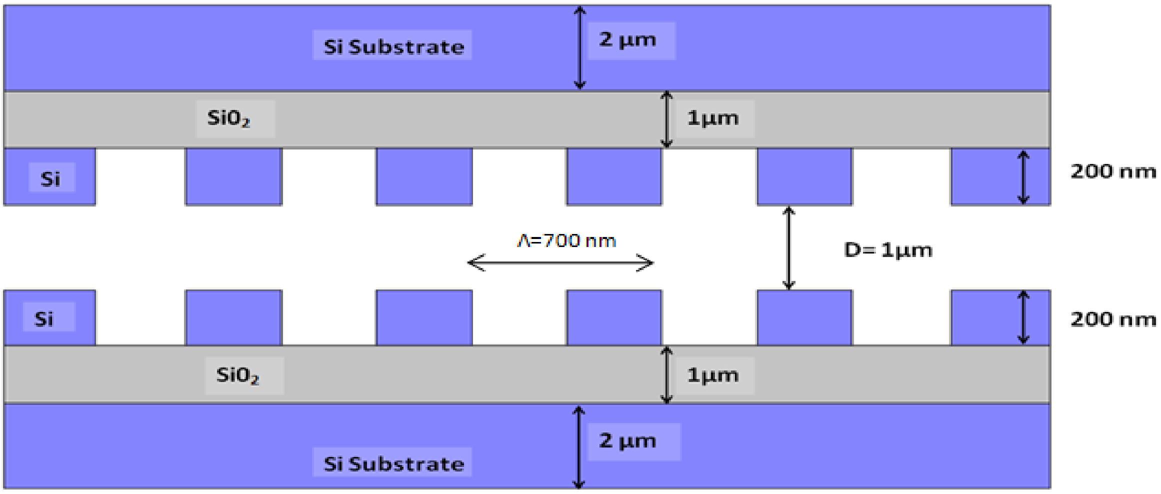

Figure 4.7 Optimized Hollow Optical Waveguide profile design

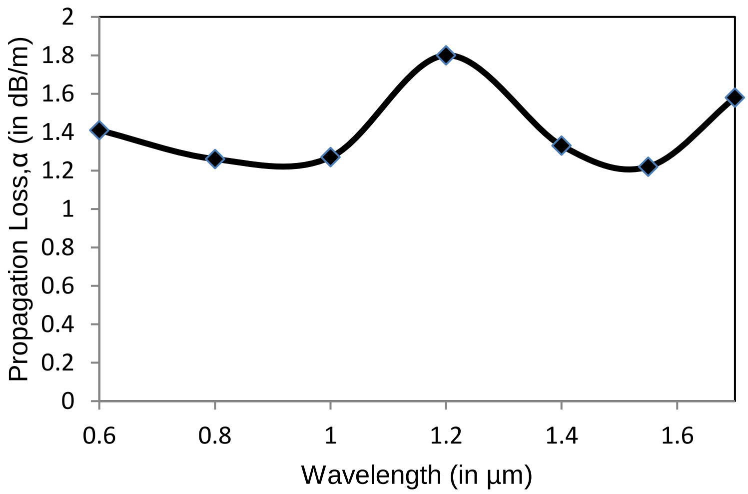

Figure 4.8Optimized narrow-core hollow optical waveguide performance at Λ=700-nm,t_g= 200-nm, C = 0.5.

The performance of the optimized low-loss narrow-core hollow optical waveguide design is shown in Fig. 4.8 where it is examined that the maximum and minimum values of loss achieved within the proposed waveguide are 1.8 -dB/m and1.22-dB/m at λ of 1.2-μm and 1.55-μm respectively. In literature, the propagation loss has been calculated by the previous researchers for hollow core waveguide [90, 91, 136, 137] which demonstrated the propagation loss values of 0.006 dB/m, 0.37 dB/cm, 0.55 dB/cm and 0.2 dB/cm for core thickness of 15-µm, 9-µm, 5-µm and 20-µm respectively.

Ref [90] proposed the same structure of HCG assisted hollow core waveguide and validated our results for 15-µm core thickness having the same value of propagation loss of 0.006dB/m. In contrast, Yang Ref [91] has explored experimentally and theoretically a novel 2D HCG hollow-core waveguide where grating bars run along the direction of guided wave and calculated propagation loss of 0.37 dB/cm at 9-µm core thickness which is very high than the results found in our work i.e. calculated value of propagation loss is 0.011dB/m by optimized best grating parameters.

Here, first time we have utilized this low-loss HCG based hollow waveguide for achieving highly responsive and efficient photodetection by integrating it with PIN photodetection layer. The presence of surface modes at the core-cladding boundaries of hollow waveguide improves the overall performance of coupled device by pushing the generated photo carriers into the detection layer for making it highly responsive and efficient device. However, the previous research efforts have been utilized for passive and discrete low-loss HCG based hollow core waveguide.

4.5 Need of Hollow Waveguide Integrated Photodetection Layer

The highly confined light for absorption in conventional waveguide with dimensions in subwavelength and smaller than the diffraction limit becomes challenging in a volume of semiconductor. In a simplified case, we can imagine sending a beam of light with a wavelength of 1.55-µm carrying an optical signal onto a cube of semiconductor with dimensions of 1 µm x 10 µm x 10 µm which creates a issue regarding the photodetector efficiency which depends on how well light can interact with the active region of the device.

The smallest spot size area that could be achieved with a diffraction limited optical beam propagating in free-space is around $\lambda/2$, where λ is the optical wavelength [137-138]. Because the cross-sectional area of the photodetector is only 10 µm x 10 µm, only a small region of the optical beam can interact with the semiconductor, since its cross-section is much smaller than the incident field pattern, leading to a loss in sensitivity for a photodetector with subwavelength dimensions.

In recent years, high-contrast grating (HCG)based hollow optical waveguide have been suggested as a method to manipulate light at very compact platform i.e. at nanoscale [139], and provide the much needed on-chip confinement for routing of information. Fundamentally ,the surface modes created by collective oscillations of electrons near the surface of HCG and these electronic oscillations lead to an electromagnetic wave induced by their displacement, which in turn excites nearby electrons. Surface modes propagate at the HCG based core-cladding boundaries in subwavelength dimensions.

In this work, we focus on the on-chip photodetection of highly confined surface modes in HCG enabled narrow-core hollow optical waveguide. These modes can propagate in the loss-less environment of proposed waveguide and achieve strong confinement in a gap region of $\lambda^2/100$ cross-sectional area, which is much smaller than the free-space diffraction limit. The integrated waveguides can route and localize optical signals in confined spaces, and their integration with nanoscale photodetector could lead to low capacitance devices that can operate with low energy levels and good sensitivities. Silicon-based PIN photodetection layer integrated on-chip with low-loss narrow-core hollow optical waveguide is optimized for detecting optical signals in subwavelength dimensions with high responsivity and larger quantum efficiency by investigating the best use of surface modes present at the boundaries of top and bottom HCGs mirror. The enhanced photo generation in the active region and the collection efficiency of the generated photo carriers is improved due to the presence of surface modes at the core-cladding boundaries pushes the generated photo carriers between the active layer and away from silicon-oxide interface as a way of confining light in subdimensions so as to increase interaction between the optical signal and the semiconductor material. This method has the potential of reducing the size mismatch between optics and electronics.

4.6 Design and Analysis of Hollow waveguide embedded Photodetector

The performance of PIN photodetection layer can be examined by leakage power and radiated/absorbed power within the active intrinsic layer of PIN photodetector. The output optical wave is directly combined from HCG assisted hollow optical waveguide to PIN photodetection layer that embedded among two parallel placed HCGs mirrors. The absorbed power in the active intrinsic layer of PIN photodetector is exhibited as [140]:

$$P(z) = (1 - R)\mathrm{P_{inc}}(1 - \mathrm{e}^{-2\alpha z}) \tag{4.6}$$

where R demonstrates the reflected power of the incident light. The leaky mode description of the electromagnetic field is utilized to determine the leakage of the from guided mode power. The proposed waveguide design is able to maximize the absorbed/radiated power inside the active layer of PIN-photodetector thereby decreasing the leakage power because of the presence of tight carrier confinement inside the intrinsic layer of PIN-photodetector, in this manner, the generated photocurrent become larger. Therefore, it can largely improve the on-chip responsivity (R) and quantum efficiency (Q.E) by utilizing the proposed design of low-loss narrow core hollow optical waveguide structure. All the grating parameters(Λ, t_g and C) of proposed waveguide design are considered and varied for getting the high performance photodetection and found the best optimized grating parameters (i.e. Λ =700-nm, t_g =200-nm and C =0.5) which are able to make a superior and highly efficient on-chip device. The existence for these optimized value of grating parameters is due to the presence of two parallel placed HCGs layer in subwavelength dimensions having periodicity of grating is not exactly to the light wavelength. Because of subwavelength dimension of grating, the incident beam while reaching to the top boundary of both HCGs mirrors splits into two modes and further these two modes cancel to each other destructively at the output plane of both HCGs mirrors. In addition, the ratio of standing wave is very less at t_g of 200-nm which implies that t_g of 200-nm causes very low-losses. Further, by increasing the value of t_g, the proportion of standing wave inside the grating structures also increases which results into high standing wave ratio due to the radiations turning out after reflections from grating bars is distributed. In this manner, a low-loss environment is obtained inside the waveguide due to the presence of 100% reflectivity through both HCGs layers.

The efficiency of photodetector is defined in terms of its responsivity. The photodetector responsivity is characterized as the proportion of generated photocurrent through photodetector to the input optical power introduced inside the photodetector which is appeared by the equation [134]:

$$R = \frac{I_{ph}}{P_{ph}} \tag{4.7}$$

where I_{ph}= is the density of generated photocurrent and P_{ph} is input power density of optical light source having wavelength of 1.55-µm. The photodetector quantum efficiency based upon the responsivity by utilizing the following equation as:

$$Q.E.(\eta) = 1240 * \frac{R}{\lambda(\text{in nm})} \tag{4.8}$$

Hence, when a PIN photodetection layer is embedded inside the proposed low-loss narrow-core hollow optical waveguide and having optimized values of grating parameters, a superior photodetection will shows which enhances on-chip R of 0.8 A/W and QE of 64 %.

4.6.1. Propagating Modes in Various Configuration

The role of HCG based hollow optical waveguide for detecting the optical signal has been studied in the previous sections. Here, we analyze and optimize different techniques for integration of photodetection layer in different waveguides. The different configuration of integration of photodetection layer with conventional waveguide, SOI based waveguide and HCG enabled hollow optical waveguide are analyzed. Propagated field pattern for all three configurations and the calculated curve for absorption of power are shown in Fig. 4.9, 4.10 and 4.11 respectively. The optical signal propagates in the waveguide hollow core region and is incident on an integrated silicon PIN photodetection layer, which lies in the same plane as the waveguides. The silicon photodetection is used to convert highly confined modes with a wavelength λ of 1550-nm into an electrical signal. The cladding boundaries of the waveguide act as reflector as well as a feed-in excitation for antenna. The presence of photocurrent in each waveguide structures are calculated by using FDTD numerical method.

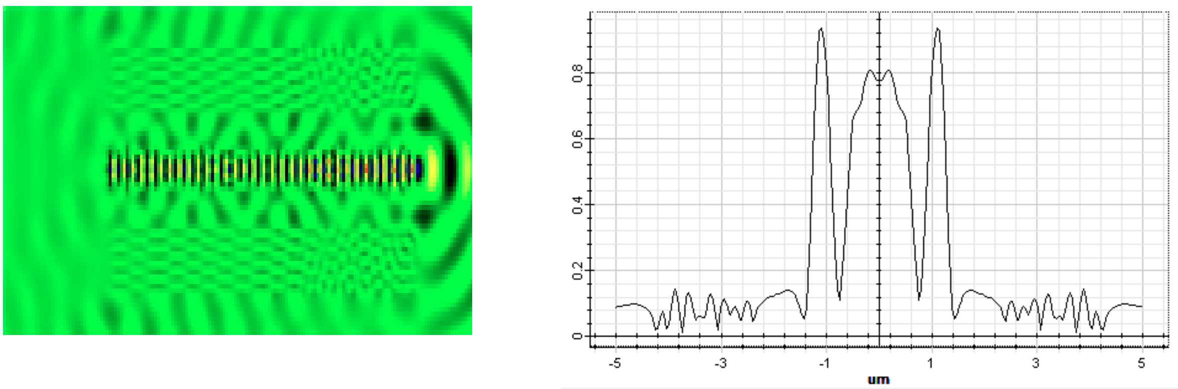

(a) (b)

Figure 4.9Photodetection layer integrated with conventional waveguide, a) Analytical Configurations for field inside the conventional waveguide core having core thickness (D) = 1-µm. b) Measured absorbed power of 0.87 nW.

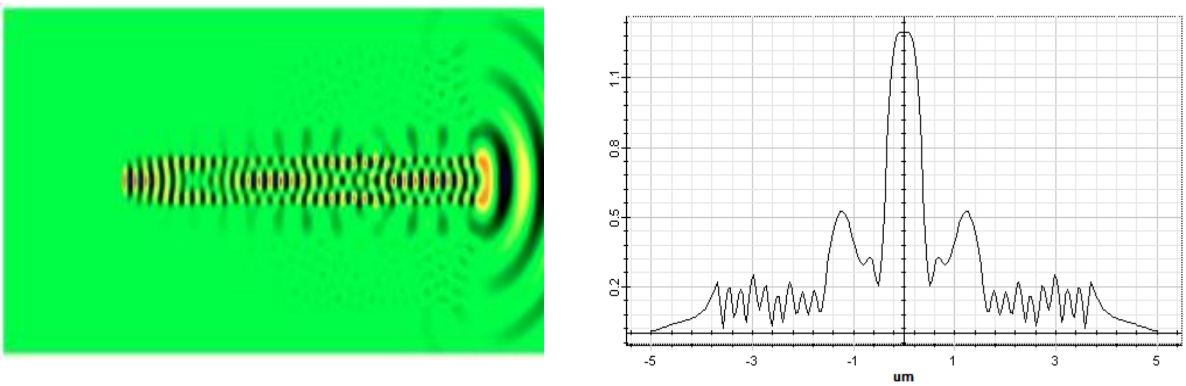

(a) (b)

Figure 4.10 Photodetection layer integrated with SOI based hollow waveguide a) Analytical Configurations for field inside the SOI based hollow waveguide core having core thickness (D) = 1-µm. b) Measured absorbed power of 1.32 nW.

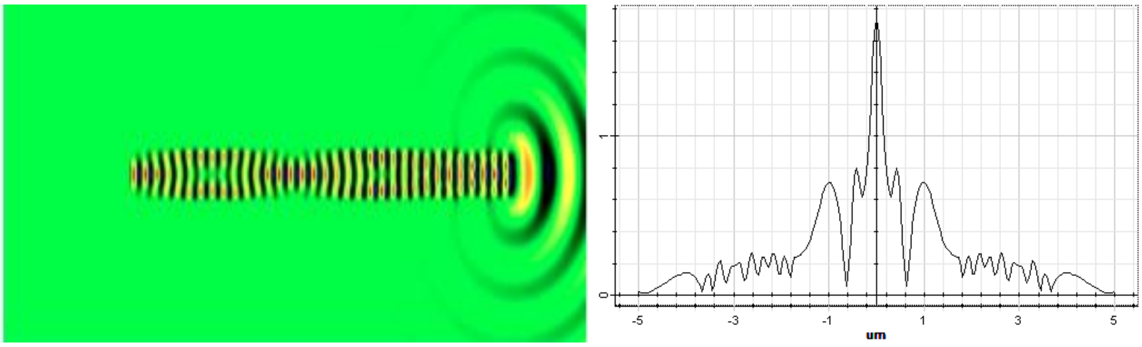

(a) (b)

Figure 4.11 Photodetection layer integrated with HCG enabled hollow waveguide in SOI a) Analytical Configurations for field inside the HCG enabled hollow waveguide core having core thickness (D) = 1-µm, Λ=700-nm, tg= 200- nm, C = 0.5, b) Measured absorbed power of 1.8- nW.

The responsivity of photodetector is to be determined by utilizing Eq. 4.5 that gives the total optical power that reaches/absorb into the photodetection region. Consequently, the incident optical power having 2.6-nW optical power, the evaluated power within the device is 1.8-nW. The generated photocurrent with TE polarized light wave is calculated as 2.33-nA. The responsivity which is characterized as the proportion of generated photocurrent through photodetector to the input optical power introduced inside the photodetector is calculated as 0.8 A/W for HCG enabled hollow waveguide in SOI by utilizing the described FDTD numerical method. However, the theoretical value of responsivity for λ of 1.55-µm is 1.2 A/W with the supposition of Q.E of 100%. The calculated responsivity corresponds to 64% Q.E which is the maximum reported performance for a hollow core waveguide for efficient photodetection with such a narrow-core. Such HCG enabled hollow waveguide integrated with PD has never been reported before. However, the performance of PD depends on the material systems and structures adopted. Table 2 summarizes the performances of typical PDs made from various material platforms. The performance is characterized in terms of responsivity and quantum efficiency which is summarized as below:

Table-II

Material	Responsivity (in A/W)	Quantum efficiency (in%)	Year	Reference
InGaAs	0.17 at1550 nm	13.5	2002	141
Ge	0.53 at 1550 nm	42.4	2008	142
Ge	0.75 at 1550 nm	59.9	2013	143
Si	0.5-10 at 1100-1700 nm	40	2009	144
Si	0.15 at 1550 nm	1	2008	145

Therefore, the revealed responsivity is strongly accepted for on-chip photodetection of light wave. Further, the measured responsivity for SOI based hollow waveguide is 0.63 A/W corresponds to the 53% Q.E which is very low while comparing with HCG enabled hollow optical waveguide in SOI device. Similarly, the measured responsivity for traditional waveguide is 0.30 A/W corresponds to 24 % Q.E which is extremely low in contrast to HCG enabled hollow waveguide in SOI.

Fig 4.12demonstrates the responsivity curve of the PIN photodetection layer by varying cladding thickness (t_{clad}) from 100-nm to 1000-nm for traditional waveguide and SOI based hollow waveguide and HCG enabled hollow optical waveguide in SOI where it is shown that minimum and maximum values of responsivity with HCG enabled hollow optical waveguide in SOI are 0.63 and 0.8A/W at t_{clad} of 900-nm and 200-nm respectively. By assuming the SOI based hollow optical waveguide device, it is shown that minimum and maximum values of responsivity are calculated as 0.4and 0.63 A/W at t_{clad}900-nm and 200-nm. Further, the traditional waveguide configuration, it is shown that minimum and maximum values of responsivity are calculated as0.12and 0.30 A/W at t_{clad}100-nm and 600-nm.

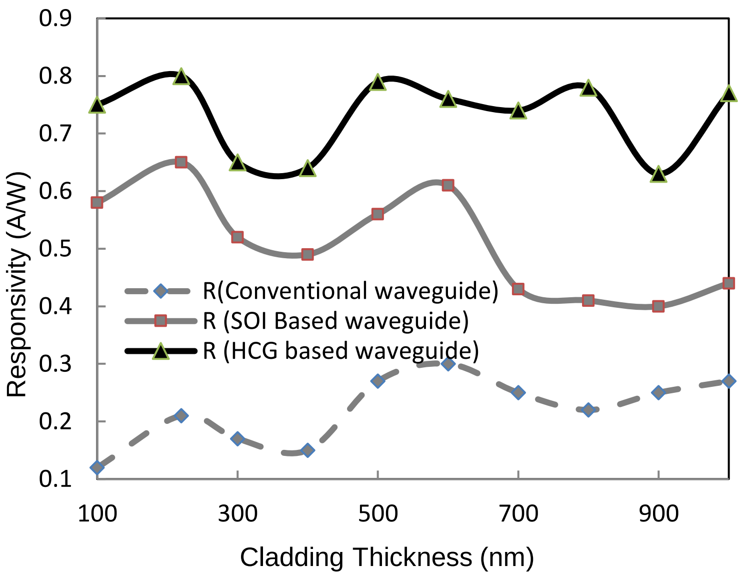

Figure 4.12 Responsivity of photodetector by varying cladding thickness t_{clad} from 100 to 1000-nm at λ of 1.55- µm for traditional waveguide, SOI based hollow waveguide and HCG enabled hollow optical waveguide with Λ= 700-nm, C = 0.5.

The values of responsivity by varying cladding thickness of hollow optical waveguide at 100-nm, 200-nm, 300-nm, 400-nm, 500-nm, 600-nm, 700-nm, 800-nm, 900-nm and 1000-nm are 0.75, 0.8, 0.65, 0.64, 0.79, 0.76,0.74, 0.78, 0.63 and 0.77 A/W (for HCG enabled hollow optical waveguide in SOI) and 0.58, 0.65, 0.52, 0.49, 0.56, 0.61, 0.43, 0.41, 0.4 and 0.44 A/W (for the SOI based hollow optical waveguide) and 0.12, 0.21, 0.17, 0.15, 0.27, 0.3, 0.25, 0.22, 0.25 and 0.27 A/W(for conventional waveguide).

4.7 Summary

A low-loss narrow-core HCG enabled hollow optical waveguide in engineered SOI is proposed for the realization of high performance on-chip photodetection. A very low propagation loss of 1.22 dB/m even at narrow-core at 1550-nm wavelength obtained by utilizing FDTD numerical technique. Further, the PIN photodetection layer having width of 1-μm is embedded within this HCG assisted narrow-core hollow optical waveguide in engineered SOI to get the superior photodetection. All the parameters of grating are examined and found optimized grating parameters having values as Λ= 700-nm, t_g = 200-nm and C = 0.5. From this proposed design the responsivity and quantum efficiency of photodetection layer are calculated as 0.8 A/W and 64 % respectively which are strongly acceptable for on-chip integration of optoelectronic devices. The reported outcomes prove the validity of photodetector with compact foot-print and superior performance. The proposed compact device of HCG enabled hollow optical waveguide in engineered SOI is useful for realizing a low-power photonic link which is therefore a potential applicant for developing a green optical link for on-chip integration. Further, implementation of interest that could tentatively explored which incorporate traditional on-chip access to 3D photonic crystals. Likewise, the method could be extendable to the visible regime.

CHAPTER – 5

Multiband Compact Terahertz Antenna on Engineered SOI facilitated by 1-D Photonic crystal

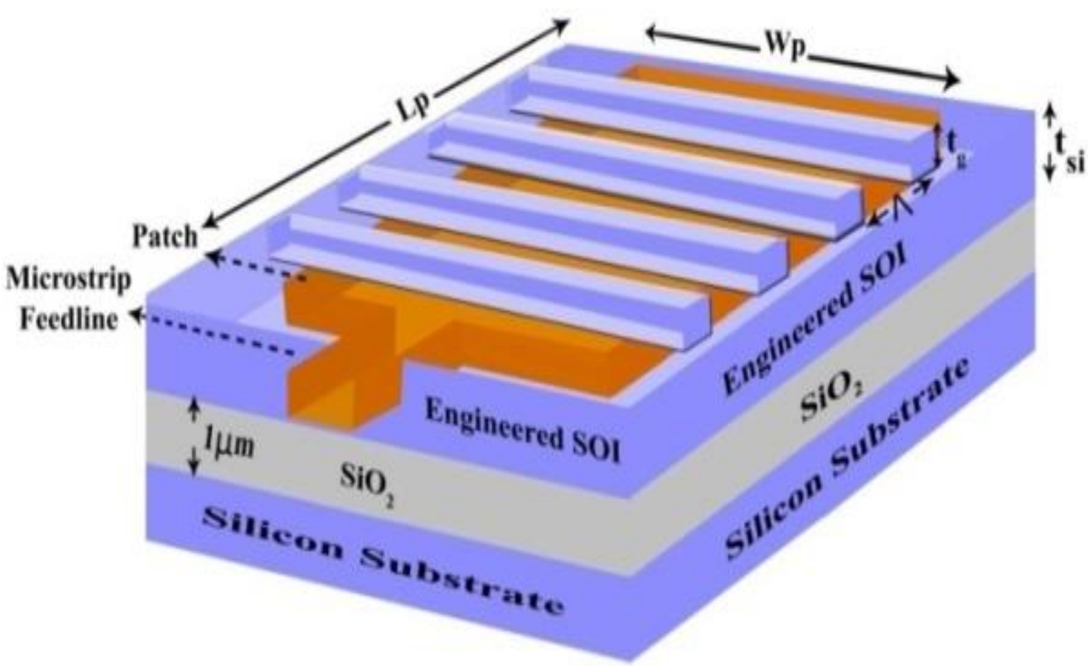

Chapter 5

Multiband Compact Terahertz Antenna on Engineered SOI facilitated by 1-D Photonic crystal

5.1 Introduction to Hybrid Optical Antenna

The effect of grating based photonic coupler for efficient coupling of optical light onto hybrid chip and ultra low-loss nature of narrow core hollow optical waveguide based on nanostructure SOI for efficient photodetection are discussed in chapter 3 and 4. It is found that a strong in-coupling, loss-less environment and high output power/photocurrent through this ultra low-loss waveguide integrated photodetector is achieved. Here this chapter deals with the introduction of hybrid optical antenna where the 1-D photonics crystal assisted compact terahertz antenna is directly coupled with the output of waveguide integrated high performance photodetector to make a highly directive, large gain and more efficient device at terahertz frequencies.

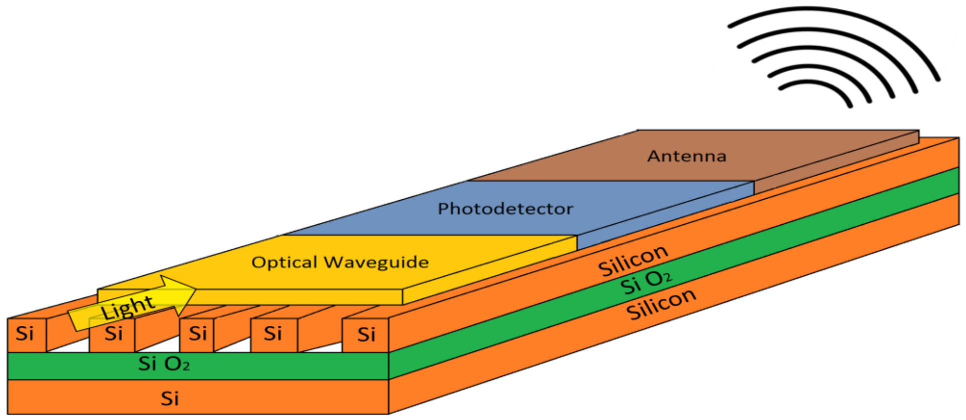

Fig.5.1Novel nanostructured SOI based hybrid optical antenna.

The schematic of nanostructured SOI based highly efficient hybrid optical antenna for future communication system is shown in Fig. 5.1, in which a Hollow-core optical waveguide, Photodetector and Antenna systems are directly coupled on-chip by making use of HCG/1-D photonics crystal to make a hybrid optical antenna for applications in future microwave/millimeter wave wireless communication system based on photonic network.This hybrid chip is designed to receive the optical modulated signal from one end and direct it to free space by using various optoelectronics/photonics devices at terahertz frequencies from another end of chip.

In the present time, Terahertz technology is in vogue and used for applications such as sensing [146] and communication [147]. In the last decade, this terahertz technology has shown the amazing advanced usage of it in the modern devices. By observing optical properties in the THz regime; different applications have been contemplated practically, for instance, medicinal diagnostics [148] and security applications [149]. After reading about classical electrodynamics process, it is found that the EM radiations can be emitted by means of electric dipole at THz region due to this region is considered as a high frequency region. To realize a high frequency antenna, particularly working at THz frequencies was challenge for the researchers. A number of new novel designs have been inspected at different terahertz frequencies, for example, metamaterial based antenna for proficient performance [150]. The normal structures operating at microwave frequencies introduce high losses due to presence of solid dielectric absorption at such high frequencies [151-152]. To solve this technical issue, new facts with different pioneering structures having rectangular silicon based waveguide have been used for the transmission at high frequencies range i.e. at THz. The reason of using 'silicon' based waveguide is that 'silicon' has the properties: (1) it has weak absorptivity i.e. A< 0.2 cm^{-1} which is adequate upto millimeter wave frequency (> 30 GHz). (2) Silicon has a high dielectric constant (11.9) which helps to execute the planner antenna on its surface in a better manner as compared to the same free space antenna. Therefore, it is exceptionally captivating to use a silicon based monolithically integrated antenna which means towards the umbrella of silicon photonic [153-154].

Various designs have been contemplated to guide and control the THz radiations. An antenna operating at THz frequency integrated on photonic crystal substrate gives an adaptable stand for the realization of various optical/terahertz components. In fact, terahertz antenna/waveguides based on photonic crystal substrate enhances the transmission spectra and efficiency of the antenna [155-157]. To provide superior performances and the hybrid integration of microelectronic devices with optical/terahertz devices; some smart designs of the above mentioned structures are examined which incorporates a low-loss single-mode SOI based waveguide [158-159] and ribbon waveguide for low-loss terahertz guiding [160].

An efficient 1-D photonic crystal has the strength to integrate the electronic and photonic devices on a single silicon chip with loss-less environment. The emerging field of photonic crystal is attractive and useful for controlling and manipulating the electro-magnetic radiations particularly on small scales due to the presence of alternating layers of material with different dielectric constants [161-164]. HCG is a physical structure having single layer along with the sub-wavelength dimensions where the material of the grating has a large contrast of index of refraction with their surroundings. HCG is the improved version of 1-D photonic crystal; therefore, it can be utilized to acknowledge a number of functionalities simultaneously such as optical coupler, splitter and switch. The usage of HCG empowers us the broadband ultra-high transmission, broadband ultra-high reflectivity and produces high Q.F. resonance for surface normal light wave [135].

Here, a compact design of terahertz antenna integrated on an engineered SOI chip is proposed. In the proposed antenna design, the presence of in-plane index contrast (above patch) through HCG and the vertical-index contrast through SOI (below patch) alter the radiation pattern of the terahertz antenna and forms multi-resonance impact with enhanced antenna gain and radiation efficiency. The low-loss propagation with multimode coupling at a compact platform results because of the presence of multilayer periodic structure of HCG for the efficient multiband operation [64]. The HCG is useful to permits the field to be tightly confined in the central area of the subsequent silicon-patch waveguide.

5.2 Proposed Configuration

The proposed scheme of HCG based terahertz patch antenna on SOI is appeared in Fig. 5.2 (a) in which a copper patch is presented between HCG (on top) and the top silicon layer of SOI (on bottom). The SOI technology is rising as a stage for integration of optical/electronic devices as the high contrast of refractive index among the oxide cladding and silicon core that makes it appropriate for some novel applications in the field of integrated photonics [94]. In the commercialized SOI wafers, the SiO_2thickness is considered as 1-μm which is the standard one. However, the thickness of copper patch and grating thickness is represented as t_{cu} and $t_g$respectively. The period and duty cycle of HCG are signified by Λ and C respectively. HCG is a periodic structure along single layer having subwavelength dimensions where the refractive index contrast among the low-index material and high-index material is reasonably high. The configuration of HCG gives remarkably wide bandwidth with high reflectivity [73]. The plan grating parameters for the design incorporate the thickness (t_g), period (Λ) and duty cycle (C).

The most vital qualities of the proposed configuration of terahertz patch antenna results an efficient radiation pattern, multiband operation on a compact-size platform, and the probability to design a low radiation loss due to the presence of high contrast of index among the HCG material. In this way, the silicon waveguide utilized to design various devices, e.g., couplers, antennas etc. The coupling of optoelectronic devices with antennas permits the arrangement of the highly confined and efficientantenna array. The utilized grating parameters are: $n_{substrate}$= 3.48 (Si), t_L = 1.47 (SiO_2), t_H = 3.48 (Si), t_g = 0.5-µm, Λ =6.5-µmand C = 0.2. The terahertzpatch antenna is effectively work at a length (Lp) of 24-µm, width (Wp) of 8-µm with thickness of 1-µm. The gap coupled microstrip feeding line technique has been utilized to accomplish the better match of feed and the resonator. The proposed structure of patch alongside microstrip feed line is integrated with engineered SOI based HCG. To accomplish the better match of resonator with feedline, the gap coupled microstrip feeding line method has been utilized. The patch inside the silicon waveguide has been fed and patch excitation is accomplished by using microstrip transmission line. The proposed terahertz antenna having size 16-µm x 37.5-µm which can be additionally reduced by utilizing unique controlling capacities of photonic crystal utilized as a part of the proposed device. Photonic crystals have different additional controlling parameters like thickness (tg), period (Λ) and duty cycle (C)that can enhance the device tolerance. There are opportunities to build the grating pitch to additionally modify the device footprints.

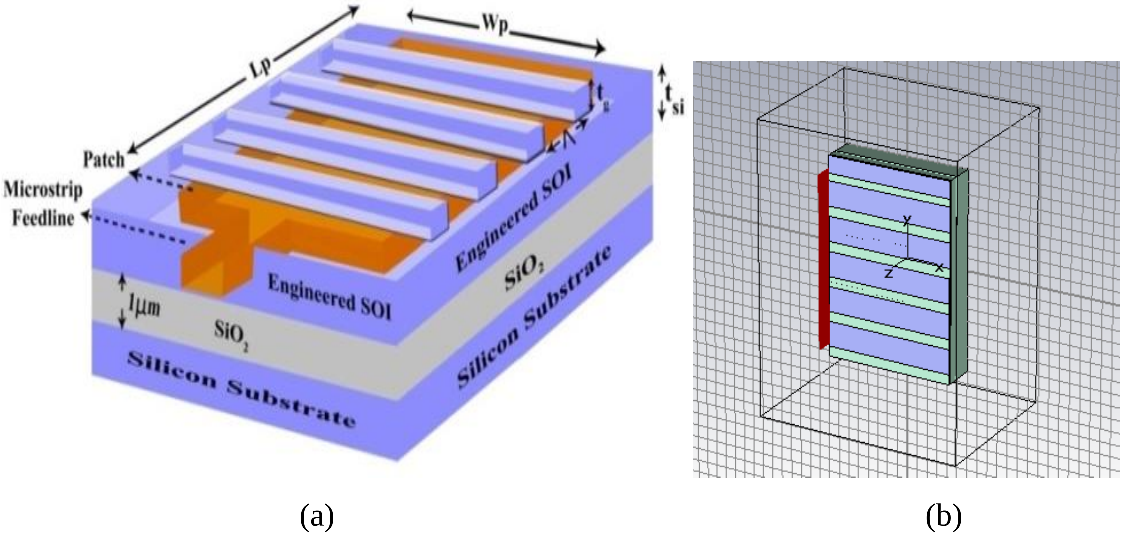

Figure 5.2 (a) Scheme of the proposed terahertz patch antenna in HCG based SOI; the copper-patch is presented among the HCG (thickness t_g) and Silicon layer of SOI (thickness t_{Si}).Thickness of SiO_2 is considered as 1-µm which is the standard one for commercialized SOI wafers. HCG duty cycle and the period are singnified by C and Λ respectively. The values of length and width of copper patch are 24 µm and 8 µm respectively; the overall size of the proposed antenna is 16-µm x 37.5-µm, (b) Designed antenna are analysed by Finite Element Method (FEM) based simulation tool CST Microwave Studio.

5.3 Design Approach and Discussion

For intense integration of photonic devices with RF devices; an engineered SOI substrate is highly efficient due to the existence of HCG on SOI substrate which can enhance the execution of photonic devices. The magnetic and electric fields for the proposed terahertz patch antenna under 1-D Photonic Crystal (HCG) by using FDTD numerical method can be composed as [165]:

$$E_z^{n+1}(i) = E_z^n(i) + \lambda\, \partial_x H_y^{n+\frac{1}{2}} \quad (5.1)$$

$$H_y^{n+\frac{1}{2}}\left(i+\tfrac{1}{2}\right) = H_y^{n-\frac{1}{2}}\left(i+\tfrac{1}{2}\right) + \Lambda\, \partial_x E_z^n \qquad (5.2)$$

Here n, n+1, $n-\frac{1}{2}, n+\frac{1}{2}$represents the time indices which are utilized to determine the new estimations of magnetic and electric field which relies upon their previously values.

Eq. 5.1 utilized to ascertain the new estimation of the electric field at time $n+1$which relies upon the previously electric field value at time n (E_z^n) and the magnetic field new value at time $n+\frac{1}{2}$ ($H_y^{n+\frac{1}{2}}$). Here $\lambda = \frac{\Delta t}{\varepsilon}$, Δt relates to temporal offsets, ε relates to permittivity and $\partial_x = \frac{\partial}{\partial x}$.

Eq. 5.2 utilized to compute the magnetic field new estimation at time $n+\frac{1}{2}$ which relies upon the magnetic field previously value at timen $-\frac{1}{2}$ ($H_y^{n-\frac{1}{2}}$) and electric field new estimation at time n(E_z^n). Here $= \frac{\Delta t}{\mu}$, μ relates to permeability.

The effect of 1-D photonic crystal (of HCG) on the parameters of optical patch antenna is discussed below.

Radiation efficiency is given by [161]

$$\varepsilon_{rad} = \frac{p_{rad}}{p} = \frac{p_{rad}}{p_{rad} + p_{loss}} \qquad (5.3)$$

where P_{rad} is the radiated power and P_{loss} is the power lost. By using a 1D photonic crystal the power lost can be minimized and power radiated is also increased there by increases the efficiency of the antenna.

The directivity of the antenna is given by

$$D(\theta, \varphi) = \frac{4\pi}{P_{rad}} p(\theta, \varphi) \qquad (5.4)$$

where P_{rad} the power is radiated into the antenna and $p(\theta, \varphi)$ is the angular power density related to isotropic radiator. The angular power density depends on the direction of (θ, φ) and by choosing a specific value of (θ, φ) the angular power density increased thereby increases the value of directivity. Therefore, a 1D photonic crystal enhances the directivity in addition to radiation efficiency due to directive guiding and low-loss of terahertz waves on SOI.The bandwidth of the antenna is given by:

$$\mathrm{B.W} = \mathrm{f_h} - \mathrm{f_l} \qquad (5.5)$$

$$\mathrm{B.W}(\%) = \frac{\mathrm{f_h} - \mathrm{f_l}}{\mathrm{f_r}} * 100 \qquad (5.6)$$

where f_h *and* f_l correspond to highest and lowest resonant frequencies which lie at -10 dB level in return loss graph. $f_r$is resonant frequency which is the lowest dB level in the return loss graph. The bandwidth (%) depends upon value of the difference between the highest and lowest resonant frequencies as compare to the main resonant frequencies; Using a photonic crystal the difference between the lower and higher resonant frequencies can be increased thereby increasing the bandwidth efficiency of the antenna. HCG can minimize the radiated power which further increases the gain and efficiency of the antenna. Accordingly, a1-D photonic crystal or HCG can improve both the gain and radiation efficiency.

Additionally, an HCG makes it conceivable to control and manipulate the multiband operation of a patch antenna operating at terahertz frequencies due to the presence of multimode coupling application through HCG which get coupled to the guided mode making multiple resonances [73].

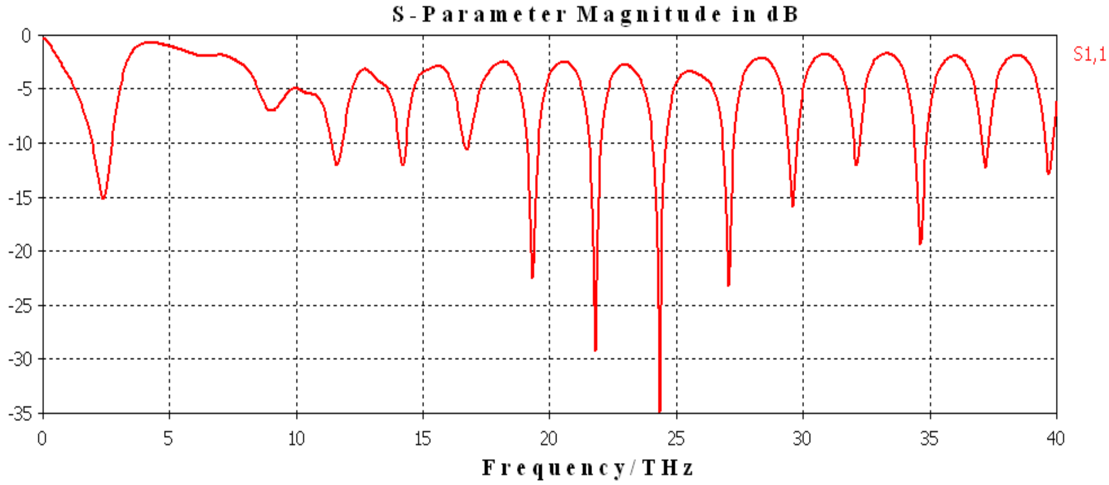

Fig. 5.3Loss spectra (in dB) versus frequency (in THz) scenario for proposed terahertz antenna; Thirteen bands are obtained at frequencies of 2.4 THz, 11.6 THz, 14.2 THz, 16.72 THz, 19.32 THz, 21.8 THz, 24.32 THz, 27.04 THz, 29.56 THz, 32.08 THz, 34.6 THz, 37.16 THz and 39.68 THz with Λ = 6.5-µm, t_g = 0.5-µm, C = 0.2.

The return loss of the proposed compact terahertz patch antenna integrated on an engineered SOI is appeared in Fig. 5.3 which shows the loss spectrum (in dB) with frequency (in THz). The proposed terahertz antenna gives return loss of less than -10dB for each thirteen bands. Therefore, the proposed patch antenna can work at thirteen different bands at the same time. The designed antenna configuration having HCG parameters are period (Λ), thickness (t_g) and duty cycle (C) having values of 6.5-µm,0.5-µm, and 0.2 respectively. The thirteen bands incorporates frequencies at 2.4 THz, 11.6 THz, 14.2 THz, 16.72 THz, 19.32 THz, 21.8 THz, 24.32 THz, 27.04 THz, 29.56 THz, 32.08 THz, 34.6 THz, 37.16 THz and 39.68 THz with return loss -15.2 dB, -12.08 dB, -12.083 dB, -10.61 dB, -22.55 dB, -29.2 dB, -34.86 dB, -23.2 dB, -15.9 dB, -12.1 dB, -19.32 dB, -12.23 dB and -12.94 dB respectively. It is further shown that the seventh band gives most minimal loss of -34.86 dB in comparison with the forth band which shows the highest return loss having value -10.61 dB.

Fig. 5.4 shows the effect on bandwidth of each low-loss band of proposed antenna at different operatingfrequencies2.4, 11.6, 14.2, 16.72, 19.32, 21.8, 24.32, 27.04, 29.56, 32.08, 34.6, 37.16 and 39.68 (in THz), where it is shown that the maximum value of bandwidth obtained at different operating frequencies are 0.632, 0.444, 0.367, 0.398, 0.98, 1.12, 1.34, 1.07, 0.459, 0.356, 0.508, 0.429 and 0.407 (in THz). It is further observed that four bands at resonant frequencies of 19.32 THz, 21.8 THz, 24.32 THz and 27.04 THz have best values of bandwidth ranging from 0.98 THz to 1.34 THz which shows that the proposed antenna exhibits a wider bandwidth at these frequencies. It is further shows that the 24.32 THz frequency band has wider bandwidth that have the value of 1.34 THz and low return loss value of -34.86 dB.

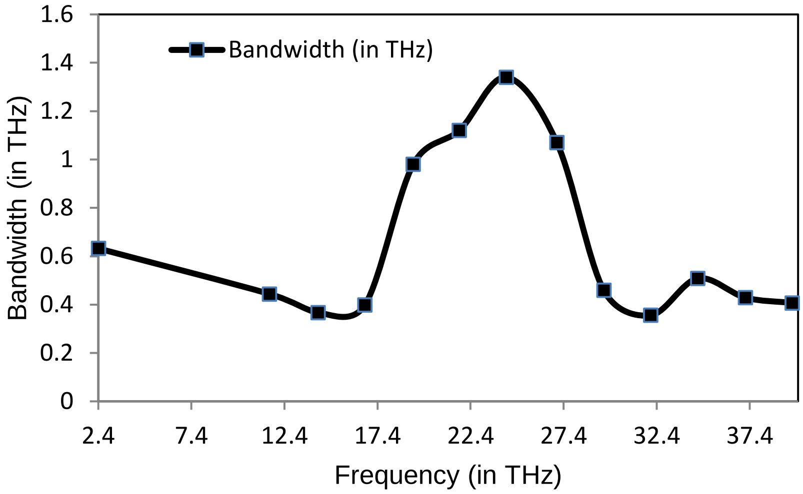

Fig. 5.4Bandwidth of the proposed terahertz patch antenna for all thirteen bands at different resonating frequencies Λ =6.5-µm, t_g= 0.5-µm, C = 0.2.

A multiband low-loss operation of terahertz antenna has been realized by making use of loss-less propagation of multiple resonances through HCG at THz frequencies. The performance of antenna is bifurcated into two broad classes such as; intermediate and output performance parameters. Input impedance, return loss and VSWR come under the class of intermediate performance parameters. The VSWR plot of the proposed THz antenna is shown in Fig. 5.5 which enlightens us regarding how much signal is reflected back to the source because of the impedance mismatch between antenna and source. The signal which is reflected back deteriorates the execution of the proposed antenna due to the availability of standing wave voltage in the feed line. Infact, the VSWR value ought to be equivalent to 1 which means that the reflection is zero with 100% power accepted. Moreover, the value of VSWR can be bearable upto 2.

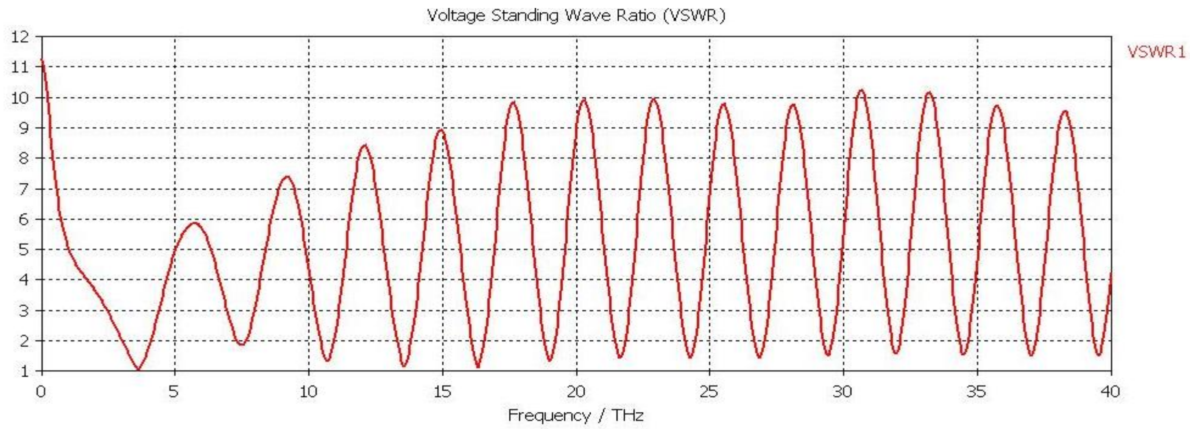

.

Figure 5.5VSWR versus frequency (THz) plot for proposed antenna

It can be observed from Fig. 5.5 that the value of VSWR of the proposed antenna lies between 1 and 2 throughout 1 to 40 THz frequency band ranges. This shows that the characteristic of the planned terahertz antenna are similar as represented in Fig 5.3 for return loss plot. It is further observed that the wider bandwidth and low return loss band of the proposed antenna shows the value of VSWR as 1.36 which lies between 1 – 2 which are adequate range of VSWR.

It has already been considered that both the parameters of antenna i.e. intermediate and output performance parameters has remarkable role for the analysis of antenna system. Therefore, radiation efficiency, gain and directivity as intermediate performance parameters of the antenna must be taken into consideration for the analysis of the terahertz antenna. This is imperative to examine the all output parameters value for low-loss band at 24.32 THz resonating frequency in light of the fact that occasionally the antenna demonstrates a decent value of VSWR and return loss; however, it does not affirm that the antenna is a good radiator until the values of all parameter be checked at this resonant frequencies.

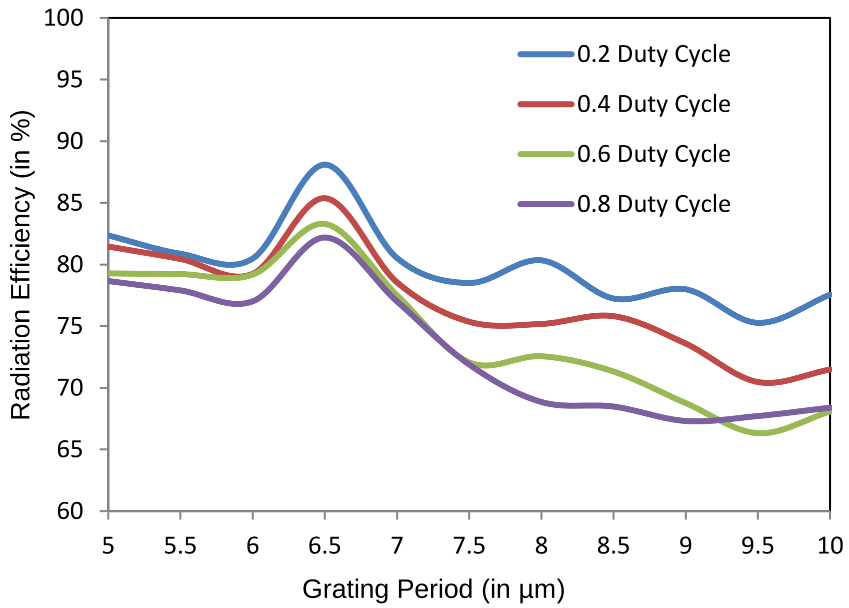

Figure 5.6Effect of grating period by varying from 5-µm to 10-µm and duty cycle between 0.2 to 0.8 on the antenna radiation efficiency (in %).

Fig. 5.6 demonstrates the impact of grating period, Λ by varying from 5-µm to 10-µm and duty cycle, C (0.2, 0.4, 0.6 and 0.8) on the antenna radiation efficiency which shows that value of maximum antenna efficiency is at period of 6.5-µm which have the values as 88.1%, 85.38%, 83.29% and 82.19% for every duty cycle of 0.2, 0.4, 0.6 and 0.8respectively further it is additionally inferred that the plot of 0.2 duty cycle has the most extreme efficiencies at every period. The maximum value of radiation efficiency of antenna for 0.2 duty cycle at Λ of 5-µm, 5.5-µm, 6-µm, 6.5-µm, 7-µm, 7.5-µm, 8-µm, 8.5-µm, 9-µm, 9.5-µm, 10-µmare 82.36%, 80.87%, 80.48%, 88.1%, 80.53%, 78.5%, 80.34%, 77.24%, 77.99%, 75.27% and 77.55%. The explanation behind optimized period of 6.5-µm is that HCG comprised of a single-layer physical structure having subwavelength dimensions with a periodicity is not exactly to the light wavelength. The incident optical wave parts into two modes while reaching the HCG top boundary and these two modes revoke each other destructively at HCG output plane because of its subwavelength dimensions. Thus, 100% reflectivity can be achieved. If the grating period is too substantial, the higher order diffraction mode will kick in, and if the grating period is even smaller, the existence of in-plane standing waves inside the device causes poor coupling and just the effective index mode is left over, and therefore, it is inferred that the period of grating at medium state demonstrates the unexpected properties, for example, narrow high Q factor resonances and high reflectivity. Appropriately, when a 1-D photonic crystal assisted enabled having period of 6.5-µm supports to realize an antenna, high reflectivity area will acquired which causes the large antenna efficiency as the efficiency is greatly depends upon the period of the grating.

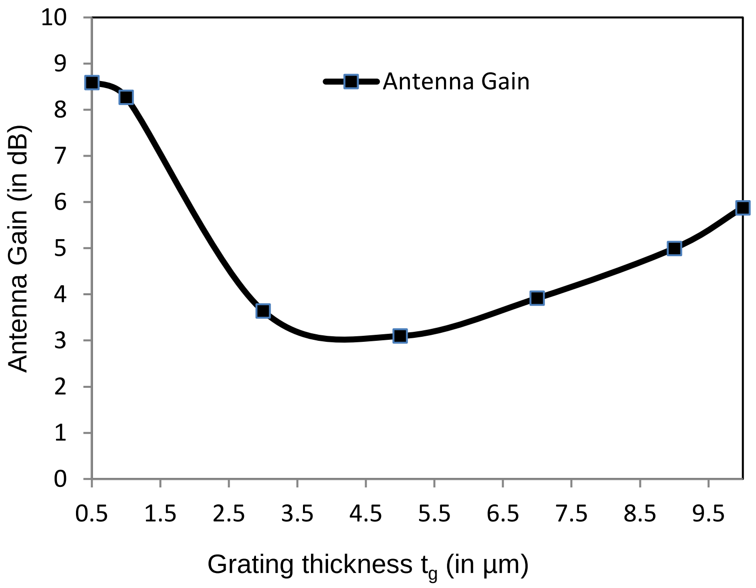

Fig. 5.7Antenna gain (in dB) with variation in grating thickness, t_g from 0.5-µm to 10-µm for low loss band at Λ =6.5-µm and C = 0.2.

Fig. 5.7 demonstrates the change in gain of antenna by varying the grating thickness, t_g (0.5-µm to 10-µm) for low loss band where it is optimized that maximum value of antenna gain is 8.588 dB at thickness, t_g of 0.5 µm. The measured antenna gain values are 8.271 dB, 3.639 dB, 3.097 dB, 3.916 dB, 4.998 dB, 5.879 dB by varying grating thick t_g of 1-µm, 3-µm, 5-µm, 7-µm, 9-µm and 10-µm respectively. The purpose behind most reduced antenna gain at 5-µm is that the presence of standing waves proportion is least at grating thickness of 0.5-µm, it implies that very low losses occurs at this grating thickness due to which high value of gain is achieved and if it additionally incrementing the thickness of grating then presence of standing waves proportion inside the grating is also increases until 5-µm due to which reflected radiations from grating is distributed that results a high standing waves proportion. After 5-µm, the proportion of standing wave again begins reducing which increases the antenna gain. It is conceivable to enhance the antenna gain by further increasing the period of grating however a compromise is made with the radiation efficiency and directivity of the proposed device.

The top silicon layer thickness of SOI assumes a critical part in the guidance and manipulation of different modes all through the HCG. Appropriate choice of the every single grating parameter (1-D photonic crystal) is vital in deciding multiband low-loss operation of the antenna system. Here, the proposed on-chip photonic crystal based planar device design has been analyzed by applying best grating parameters of period, thickness and duty cycle which have the values 6.5-µm, 0.5-µm and 0.2 respectively and it is observed that an enormous improvement has been found in the form of directivity, antenna gain and radiation efficiency having values 8.72 dB, 8.588 dB and 88.1 % respectively.

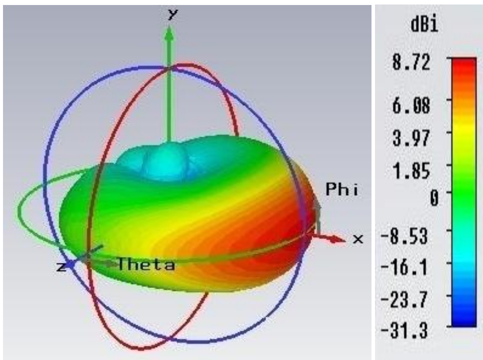

Figure 5.8 Radiation pattern plot for of proposed antenna having computed percentage of radiation efficiency of 88.1% and computed values of 8.72 dB of directivity.

The proposed terahertz antenna exhibits the minimum return loss value of−34.86 dB as compared to the reported terahertz antennas with respect to references [166,167,168] demonstrating the return loss values of −25 dB, −25.6 dB, and −31 dB respectively. Furthermore another important output parameter is gain of antenna and the proposed design represents the gain value of 8.588 dB which is appropriate in contrast to 3.502 dB gain of [169], 3.85 dB of [168], and 5 dB of [167]. All the findings of the proposed antenna are reported and finally it is concluded that the proposed antenna exhibits broadband behavior. All the calculations of the proposed terahertz patch antenna are investigated and lastly it is presumed that the proposed antenna shows broadband behavior that can also be checked with the traditional techniques which can be adaptably set with the different configurations like far-infrared Fourier transform spectroscopy (FIRFTS),THz time domain spectroscopy (THz-TDS) and vector network analyzer (VNA) [170 -171].

Overall performance of the proposed antenna by applying best grating parameters (Λ = 6.5-µm, t_g = 0.5-µm and C = 0.2) at frequency 24.32 THz is tabulated as under:

Antenna Performance	**Proposed THz Antenna with 1-D Photonic Crystal**
Return Loss	-34.86
VSWR	1.38
Radiation Efficiency	88.1%
Antenna Gain	8.588 dB
Directivity	8.725 dB
Bandwidth	1.34 THz

5.4 Photodetector coupled Antenna

The performance of HCG enabled low-loss narrow-core hollow optical waveguide for efficient photodetection and 1-D photonic crystal assisted antenna systems are individually analyzed where it is concluded that the both devices reported maximum efficiencies of 64% and 88.1 % respectively by using best optimized grating parameters of period (Λ) = 700-nm, t_g= 200-nm and C = 0.5 for photodetection device and period (Λ) = 6.5-µm, t_g= 0.5-µm and C = 0.2 for Antenna system. The microstripfeedline of antenna is utilized to feed the two slots of the antenna and at the similar time it works as the electrodes of the hollow optical waveguide embedded photodetector. The final antenna layout fed with photodetector is represented as under:

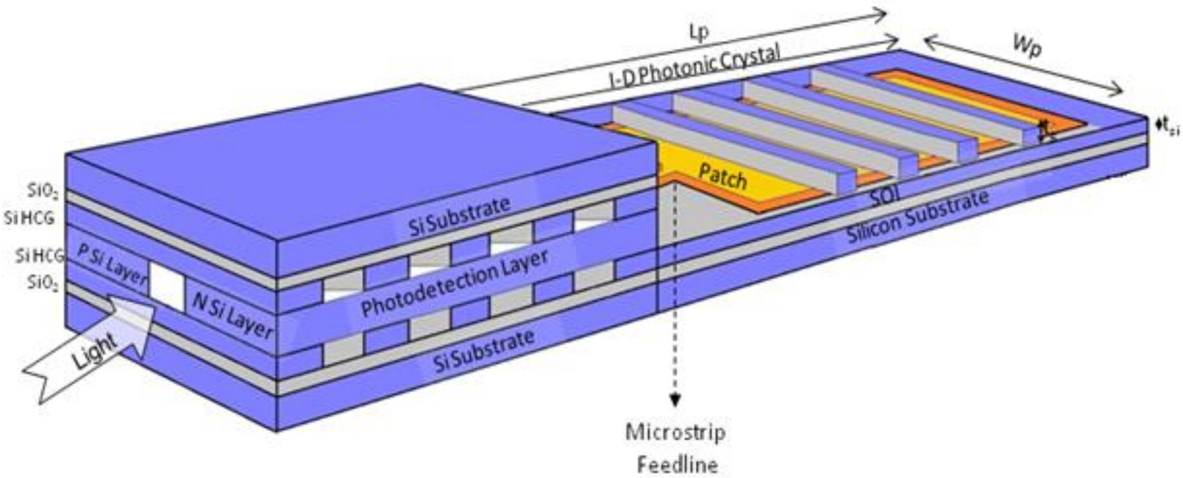

Fig.5.9 Hybrid integration of HCG assisted low-loss narrow-core hollow optical waveguide for superior photodetection with 1-D photonic crystal enabled antenna system.

Using the FDTD method, the measured optical power at the output of the photodetector coupled with an antenna system is expressed as follows [172]:

$$P_{out(PD-Ant)}(L) = P_{in}\eta_{in}\exp(-\alpha_{coupling}L)\,\eta_{out}\,10^{-\alpha_{PD}\cdot\frac{l'}{10}}T \qquad (5.7)$$

where P_{in} is the input light power at the point of entering the photodetector, η_{in} and η_{out} are the efficiencies of narrow core hollow optical waveguide photodetector and antenna system. L is the detector coupling length and $\alpha_{coupling}$ is the direct coupling rate from the photodetector to antenna system, $\alpha_{PD}$is the photodetector loss and T is the power transmittance at the output facet.

$P_{out(PD)}$, the optical output power from the reference photodetector without integrating with antenna system is given by:

$$P_{out(PD)} \;=\; P_{in}10^{-\alpha_{PD}\cdot\frac{l}{10}}T \qquad (5.8)$$

Normalizing (1) and (2), we obtain

$$\frac{P_{out(PD-Ant)}(L)}{P_{out(PD)}} = \eta^2\exp(-\alpha_{coupling}L) \qquad (5.9)$$

The efficiency of direct couple integration of high performance photodetector and antenna systems are obtained by considering two cases: (a) by varying photodetector grating period, Λ from 100-nm to 1000-nm and fix the antenna best grating period, Λ of 6.5-µm, the value of maximum value of efficiency of the integrated system is calculated as 49.95 % at a photodetector Λ of 700 nm. (b) By varying antenna Λ from 5-μm to 10-μm and fix the photodetector best Λ of 700-nm, the value of maximum value of efficiency of the integrated system is calculated as 50.01 % at antenna Λ of 6.5-μm which is shown in Fig 5.10 (a, b) as under:

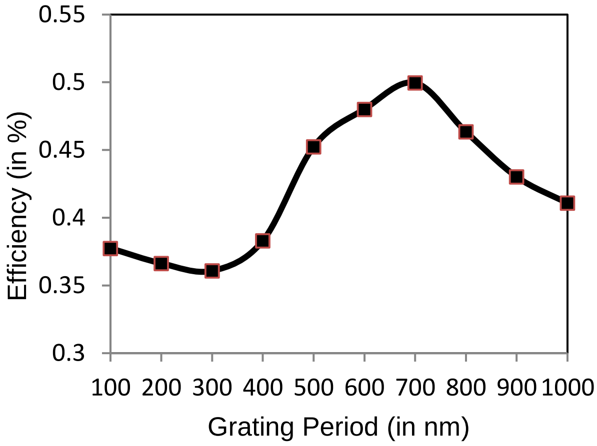

(a)

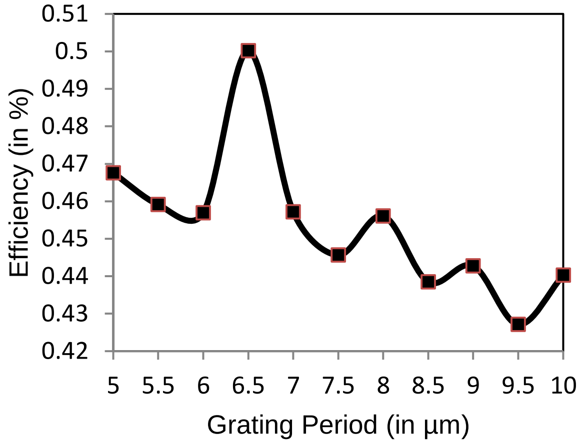

(b)

Fig. 5.10 Efficiency of Hybrid Optical Antenna

It is concluded that the output power obtained at the antenna output with the corresponding input power to the photodetector results 18% coupling loss at the interface between photodetector and antenna system. In this way, hybrid optical antenna which represent the highly efficient advanced chip for detecting, modulating and radiating the optical signal (in THz) with low transmission losses by direct integration of microstrip fed patch antenna with the hollow optical waveguide embedded photodetector transforms the MW-modulated light signal power into electrical signal at terahertz frequency. This novel work is useful to developed a "smart antenna" that is expected to be the corner stone of the high-capacity and high-speed future wideband optical communication system at terahertz regime.

5.5 Summary

A 1-D photonic crystal enabled compact design of multiband terahertz patch antenna integrated on engineered SOI is proposed. The presence of copper-patch among the top silicon layer of SOI and 1D photonic crystal (HCG) shows proficient multi-resonance impact. This proposed terahertz antenna demonstrates a low return loss for the revealed thirteen bands. The proposed antenna shows a small return losses and wider bandwidth for the reported thirteen bands. Besides, the output parameters like gain, directivity and radiation efficiency of the proposed terahertz patch antenna is additionally made improved.

The introduction of HCG to form a compact antenna working in THz region is unquestionably a topic of wide research interests. To design a small-size antenna, particularly a THz antenna on SOI substrate is a way to consider high-end hybridization of antennas with electronic processors. The proposed design of THz antenna on an SOI with its smaller size will start another class of small-size THz components. It will be conceivable to acknowledge effectively tunable functions, for example, polarization dependence, sharp bends, confinement and resonance.

The proposed compact multiband terahertz patch antenna will open new span in spectroscopy, sensing, imaging and ultrafast wireless communication. Assize of the antenna shrinks quadratically by increasing radiation efficiency for a given gain, on-chip antennas working in THz regime have incredible potential by disposing of packaging problems for cost-viable, compact terahertz antennas.

CHAPTER – 6

Conclusion and Future Scope

Chapter 6
Conclusion and Future scope

6.1 Conclusion

There has been some introductory research into how antennas can be efficiently integrated with photonic devices [173-174]. It has been shown that by careful design of the surrounding environment, highly efficient, broadband radiators can be developed on materials used to create photonic devices. This is something previously deemed not possible due to the excitation of surface waves and also the perceived impact of these high dielectric constant materials on the overall bandwidth of the hybrid antenna. The on-chip hybrid optical antenna is found to be superior in terms of photonic microwave/RF generating, direct feeding, transmitting and receiving as compared to other types of the conventional antenna operating in high frequencies. The hybrid system found potential application for the low-loss optoelectronic interconnect configuration to future microwave and millimeter-wave wireless communication system based on photonic network. Therefore, the major inspiration in this dissertation is to propose a hybrid device which has comparatively low transmission loss by simplifying the RF/MW system especially in high frequency wireless system as compared to the other conventional optical antenna. In this work, various high performance on-chip compact optoelectronic device designs are analyzed to realize hybrid antenna. Here, it is also addressed the difficulty related with the conventional antennas.

The on-chip hybrid optical antenna is found to be superior in terms of photonic microwave/RF generating, direct feeding, transmitting and receiving as compared to other types of the conventional antenna operating in high frequencies. The hybrid system found potential application for the low-loss optoelectronic interconnect configuration to future microwave and millimeter-wave wireless communication system based on photonic network. Therefore, the major inspiration in this dissertation is to propose a hybrid device which has comparatively low transmission loss by simplifying the RF/MW system especially in high frequency wireless system as compared to the other conventional optical antenna. In this work, various high performance on-chip compact optoelectronic device designs are analyzed to realize hybrid antenna. Here, it is also addressed the difficulty related with the conventional antennas.

Antennas that previously present are not appropriate for THz wireless communication due to high free space path loss and high atmospheric attenuation in THz rays. The design of antenna structures working in THz is an emerging opportunity for novel optoelectronic devices.

The novel design of optoelectronic devices for converting propagating optical waves into confined/superior electromagnetic fields is a challenging obstacle which is overcome by this advanced hybrid chip. This advanced chip helps to surpass the diffraction limit, making it possible to highly efficient coupling between the devices, low transmission loss, strong detection and to realize a high gain antenna system to visualize the optical fields on this compact chip.

The purpose of this dissertation is to design and analysis the a hybrid system which represent the highly efficient advanced chip for detecting, modulating and radiating the optical signal (in THz) with low transmission losses. The performance of various types of the grating based optoelectronic devices integrate on this chip is studied and found highly efficient compact devices by optimizing the different parameters of grating (thickness, period and duty cycle) for the application of Radio-over Fiber optical link.

The major findings obtained are summarized as follows:

1. The hybrid chip first externally receives an optical signal from fiber source by using a proposed compact grating based photonic coupler. The presence of in-plane index contrast through HCG and the vertical index contrast through SOI makes it feasible to strengthen the coupling effect resulting from the strong in-plane modifications of the guided waves in the grating region and high-index contrast in the grating. In this objective, a broadband design of grating based photonic in-coupler is presented and analyzed that yields a significant improvement in coupling strength among a single mode optical fiber and an SOI based photonic waveguide. All the grating parameters are examined to achieve maximum coupling strength and after optimization, the best grating parameters of Λ=700-nm, t_g = 80-nm, t_{si} = 220-nm and C = 0.5 are investigated. A maximum fiber-waveguide coupling efficiency of 63.1% is calculated with this device by using FDTD numerical method at a wavelength of 1550-nm with best grating parameters Λ = 700-nm, t_g = 80-nm, t_{si} = 220-nm and C = 0.5.It is further expected that enhancements in coupling efficiency between waveguide and fiber mode can be increased by employing2-D type grating based photonic couplers.

2. A compact design of narrow-core HCG embedded waveguide in engineered SOI having compact foot-print (1 µm x 10 µm x 10 µm) is presented and analyzed. The proposed waveguide possesses novel propagating characteristics because of its unique light confinement mechanism for creating a highly confined and low-loss environment in the proposed device which is used for the application of high performance on-chip photodetection. This top and

bottom grating can significantly reduce the leakage mode through the HCG based cladding boundaries without compromising the lateral index contrast. Therefore, a propagation loss of 1.22-dB/m was reported with this device which is ultra-low loss even at narrow core (D = 1-μm) at 1550-nm wavelength by using FDTD analytical technique. Further, a PIN photodetection layer is embedded within this ultra low-loss HCG enabled narrow-core hollow optical waveguide in engineered SOI for achieving superior photodetection by utilizing optimized parameters of grating as Λ= 700-nm, t_g = 200-nm and C = 0.5. The responsivity and quantum efficiency of PIN photodetection layer are calculated as 0.8 A/W and 64 % respectively which are very large sufficient for the on-chip integration of optoelectronic devices. This technology development brings us closer to the end goal of creating a highly efficient photonically antenna system by integrating all the devices such as light sources, modulators, detectors on a single chip with high density passive SOI based photonic waveguide circuits.

3. After the realization of on-chip waveguide embedded high performance photodetector for creating a highly efficient photonically antenna, a compact design of patch antenna on an engineered SOI working at THz frequencies is proposed for making an on-chip hybrid optical antenna by combining all the devices on the same chip. A copper-patch is embedded between the 1D photonic crystal and SOI to demonstrate efficient multi-resonance effect. This on-chip optical antenna causes a multiband operation with acceptably small return losses for the revealed thirteen bands and improved characteristics due to the presence of HCG-enabled guiding of THz radiations in a patch on SOI. The proposed antenna exhibits a wider bandwidth at resonant frequencies of 19.32 THz, 21.8 THz, 24.32 THz and 27.04 THz ranging from 0.98 THz to 1.34 THz and the value of return loss is -34.86 dB which is very low as compared to other terahertz on-chip antenna. Furthermore, another important output characteristics are directivity, gain and radiation efficiency of antenna and the proposed antenna represents the values 8.72 dB, 8.588 dB and 88.1%, respectively at best grating parameters of Λ = 6.5-μm, t_g = 0.5-μm and C = 0.2. These reported results show the strength of the described waveguide to create an antenna operating in THz frequency with tiny foot-print and superior execution. The anticipated novel antenna design illustrates an88.1% radiation efficiency with a period of 6.5-μm which is larger than the previous existing results on THz antenna. Further, an antenna at optical frequencies has also been analyzed and it is observed that the proposed optical antenna (at telecommunication wavelength) further improved the antenna characteristics which in terms of return loss and antenna efficiency which have the values of -43.81 dB and 95.8 %

respectively by applying grating parameters of Λ, t_g and C having values 700-nm, 200-nm and 0.5 respectively.

6.2 Future Scope

The work presented in this dissertation leaves further avenues to be pursued in future work which is drawn as:

The hybrid optical antenna will release a new span in spectroscopy, sensing, imaging and ultrafast wireless communication system. Hence, the size of the antenna shrinks quadratically due to increase in the radiation efficiency for a given gain; on-chip antennas have huge strength in THz regime by removing packaging problems for cost-viable, compact terahertz antennas. Therefore, recent progress made in understanding on-chip antennas by integrating various compact optoelectronic devices at high frequencies over the last decade is highly encouraging.

The research presented herein has successfully outlined a strategy that conquers the previous issues that limited the widespread applications of optical antenna. Although issues still remain to be resolved such as:

1. Coupling between the propagating optical light and hybrid chip can be further improved by applying some novel designs such as nanophotonic couplers.
2. Concept of slow light will add up the strong optical confinement for further reductions in transmission loss which will have a potential application in high density photonic integration and optical interconnect.
3. The work can be extended to make a speed-up and highly responsive photodetector to realize a high-power photonic device by utilization of graphene material and is consequently a better applicant for creating a green optical link for CMOS based chips.
4. Introduction of Graphene to make a nanoantenna for high speed wireless networks working in terahertz range is definitely a topic of broad research interests. To Design a graphene based small scale nanoantenna is a way to think of high-end hybridization of antennas with electronic processors. It will be probable to understand easily-tunable functions such as confinement, polarization dependence, sharp bends and resonance.

We are convinced that these issues will be solved in the near term as the field continues to attract bright researchers and the expectation that new developments in thesis field are eminent is a realistic expectation.

List of Publications:

[1] Varun Kumar, Harpinder Kaur and Mukesh Kumar, "Narrow Core Hollow Optical Waveguide with Nanostructured SOI as Ultra-low Loss Platform for Efficient Photodetection," ***Photonics Network Communication by Springer***, DOI 10.1007/s11107-017-0687-y, pp. 1-7, Jan. 2017. **(IF: 0.557).**

[2] Varun Kumar, Mukesh Kumar, "Photonic crystal assisted multiband compact terahertz antenna on engineered silicon-on-insulator," ***IET optoelectronics***, ISSN 1751-8768, pp 1-4, May 25, 2015.**(IF: 0.653).**

[3] Harpinder Kaur, Varun Kumar and Mukesh Kumar, "Slow Light in Narrow Core Hollow Optical Waveguide with Low loss and Large Bandwidth," ***Applied Optics***, Vol. 55, Issue 35, pp. 10119-10123 (2016) **(IF: 1.649).**

References

[1] E.Ozbay, “Plasmonics: Merging Photonics and Electronics at Nanoscale Dimensions”, Science, 311, pp.189-193, 2006.

[2] D. Miller, “Device requirements for optical interconnects to silicon chips”, Proc. IEEE 97,pp.1166–1185, 2009.

[3] L. Katsuo Oxenlowe, H.Ji, M. Galili, “Silicon Photonics for Signal Processing of Tbit/sSerial Data Signals”, IEEE Journal of Selected topics in quantum Electronics 18,pp.996-1005, 2012.

[4] T. Nagatsima, G. Ducournau and C.C. Renaud, “Advances in Terahertz Communication Accelerated by photonics”, Nature Photonics, 10, pp. 371–379, 2016.

[5] T. Nagatsuma, S. Horiguchi, Y.Minamikata, Y. Yoshimizu, S.Hisatake, S.Kuwano, N. Yoshimoto, and H. Takahashi, “Terahertz wireless communications based on photonics technologies”, opt. exp., 21, pp. 23736-23747, 2013.

[6] A. J. Cooper, “Fiber/Radio for the provision of cordless/mobile telephony services in the access network,” Electron. Lett., 26, pp. 2054–2056, 1990.

[7] W. Zhang, A. Wen, X. Li and S. Shang, “Microwave Photonic Frequency Conversion With High Conversion Efficiency and Elimination of Dispersion-Induced Power Fading”, IEEE Phot. J., 8, pp. 1-10, 2016.

[8] J. Marti and J. Capmany, “Microwave photonics and radio-over- fiber research”, IEEE Microwave Magazine, 10,pp.96-105, 2009.

[9] S. R. Prasad, A.A. Ghatol and A.V. Patil, “Radio over fiber technology Using electro-absorption Modulation", International Journal of Engineering Science and Technology, 2,pp.5663-5671, 2010.

[10] A. Kim,Y. J. Joo and Y. Kim, “60 GHz wireless communication systems with radio-over-fiber links for indoor wireless LANs", IEEE Transactions Consumer Electronics 50,pp.517- 520, 2004.

[11] J. Yao, “Microwave Photonics”, J. Lightwave Technol. 27, pp.314–335, 2009.

[12] J. Capmany and D. Novak, “Microwave photonics combines two worlds”, Nat. Photonics 1, pp.319–330, 2007.

[13] A.J. Seeds and K.J.Williams, “Microwave photonics”, J. Lightwave Technol., 24, pp. 4628–4641, 2006

[14] D. R. Vizard, “Millimeter-wave applications: from satellite communications to security systems”, Microwave Journal) pp. 22-36, 2006.

[15] J. Capmany, B. Ortega, D. Pastor, and S. Sales, "Discrete-time optical processing of microwave signals", J. Lightwave Technol. 23, pp.702–723, 2005.

[16] M. Li, D. Janner, J. P. Yao, and V. Pruneri, "Arbitrary-order all-fiber temporal differentiator based on a fiber Bragg grating: design and experimental demonstration," Opt. Express 17, pp. 19798–19807, 2009.

[17] M. Ferrara, Y. Park, L. Razzari, B. E. Little, S. T. Chu, R. Morandotti, D. J. Moss, and J. Azaña, "On-chip CMOS compatible all-optical integrator," Nat. Commun. 1, pp. 1028, 2010.

[18] M. H. Asghari and J. Azaña, "All-optical Hilbert transformer based on a single phase-shifted fiber Bragg grating: design and analysis," Opt. Lett. 34, pp. 334–336, 2009.

[19] A. C. Lindsay, G. A. Knight, and S. T. Winnall, "Photonic mixers for wide bandwidth RF receiver applications," IEEE Trans. Microw. Theory Tech. 43, pp. 2311–2317, 1995.

[20] H. Shahoei and J. P. Yao, "Tunable microwave photonic phase shifter based on slow and fast light effects in a tilted fiber Bragg grating," Opt. Express 20, pp.14009–14014, 2012.

[21] J. Sancho, J. Bourderionnet, J. Lloret, S. Combrie, I. Gasulla, S. Xavier, S. Sales, P. Colman, G. Lehoucq, D. Dolfi, J. Capmany, and A. De Rossi, "Integrable microwave filter based on a photonic crystal delay line," Nat Commun., 3, pp. 1075, 2012.

[22] L. Cao, "High Efficiency Silicon Photonic Interconnects", PhD Disserataion, Rochester Institute of Technology, 3-7-2014.

[23] G. K. Celler and S. Cristoloveanu, "Frontiers of silicon-on-insulator", J. Appl. Phys., vol. 93, pp. 4955–4978, 2003.

[24] A. Liu, R. Jones, L. Liao, D. Samara-Rubio, D. Rubin, O. Cohen, R. Nicolaescu, and M. Paniccia, "A high-speed silicon optical modulator based on a metal-oxide-semiconductor capacitor," Nature, vol. 427, pp. 615–618, 2004.

[25] Q. Xu, B. Schmidt, S. Pradhan, and M. Lipson, "Micrometre-scale silicon electro-optic modulator," Nature, vol. 435, pp. 325–327, 2005.

[26] V. R. Almeida, R. R. Panepucci, and M. Lipson, "Nanotaper for compact mode conversion," Opt. Lett., vol. 28,pp. 1302–1304, Aug 2003.

[27] M. W. Geis, S. J. Spector, R. C. Williamson, and T. M. Lyszczarz, "Submicrosecond submilliwatt silicon-on-insulator thermo optic switch," IEEE Photon. Technol. Lett., vol. 16, pp. 2514–2516, 2004.

[28] M. R. Watts, D. C. Trotter, R. W. Young, and A. L. Lentine, "Ultralow power silicon microdisk modulators and switches," in 5th IEEE International Conference on Group IV Photonics, pp. 4–6, 2008.

[29] M.J. Liu, and L.C. Kimerling, “High-performance Ge-on-Si photodetectors,” Nat. Photon., vol. 4, pp. 527–534, 2010.

[30] P. R. Romeo, J. Van Campenhout, P. Regreny, A. Kazmierczak, C. Seassal, X. Letartre, G. Hollinger, D. Van Thourhout, R. Baets, J. M. 88 Fedeli, and L. Di Cioccio, “Heterogeneous integration of electrically driven microdisk based laser sources for optical interconnects and photonic ICs,” Opt. Express, vol. 14, pp. 3864–3871, 2006.

[31] A. W. Fang, H. Park, O. Cohen, R. Jones, M. J. Paniccia, and J. E. Bowers, “Electrically pumped hybrid AlGaInAs-silicon evanescent laser,” Opt. Express, vol. 14, pp. 9203–9210, 2006.

[32] L. H. Frandsen, P. I. Borel, Y. X. Zhuang, A. Harpøth, M. Thorhauge, M. Kristensen, W. Bogaerts, P. Dumon, R. Baets, V. Wiaux, J. Wouters, and S. Beckx, “Ultralow-loss 3-dB photonic crystal waveguide splitter.,” Opt. Lett., vol. 29, pp. 1623–1625, 2004.

[33] C. A. Barrios, Q. Xu, J. Shakya, C. Manolatou, and M. Lipson, “Compact silicon slot-waveguide disk resonator,” 2006 Conf. Lasers Electro-Optics 2006 Quantum Electron. Laser Sci. Conf., 2006.

[34] T. Baehr-Jones, M. Hochberg, C. Walker, and A. Scherer, “High-Q ring resonators in thin silicon-on-insulator,” Appl. Phys. Lett., vol. 85, pp. 3346, 2004.

[35] H. Subbaraman, Y. Zhang and R.T. Chen, “Recent advances in silicon-based passive and active optical interconnects”, Opt. Exp., Vol. 23, pp. 2287-2510, 2015.

[36] “Intel Milestone Confirms Light Beams Can Replace Electronic Signals for Future Computers.”http://www.intel.com/pressroom/archive/releases/2010/20100727comp_sm.htm. Accessed April 27, 2011.

[37] K.J. Preston, “Deposited Silicon Photonics: Optical Interconnect Devices in Polycrystalline Silicon,” PhD dissertation, Cornell University, 2011.

[38] A. Huang, C. Gunn, G.-L. Li, Y. Liang, S. Mirsaidi, A. Narasimha, and T. Pinguet, “A 10Gb/s photonic modulator and WDM MUX/DEMUX integrated with electronics in 0.13/spl mu/m SOI CMOS,” in Solid-State Circuits Conference, 2006. ISSCC 2006. Digest of Technical Papers. IEEE International, pp. 922 –929, 2006.

[39] S. Sridaran and S. A. Bhave, “Nanophotonic devices on thin buried oxide Silicon-On-Insulator substrates,” Opt. Express, vol. 18, pp. 3850–3857, Feb 2010.

[40] N. Sherwood-Droz, A. Gondarenko, and M. Lipson, “Oxidized Silicon-on-Insulator (OxSOI) from bulk silicon: a new photonic platform,” Opt. Express, vol. 18, pp. 5785–5790, Mar 2010.

[41] A.K.Katiyar, A.K.Sinha, S.Manna, and S.K.Ray, "Fabrication of Si/ZnS radial nanowire heterojunction arrays for white light emitting devices on Si substrates", ACS Applied Materials & Interfaces, DOI: 10.1021/am5028605, pp. 1-25, 2014.

[42] S. Kalluri, M. Ziari, A. Chen, V. Chuyanov, W. H. Steier, D. Chen, B. Jalali, H. Fetterman, and L. R. Dalton,"Monolithic integration of waveguide polymer electrooptic modulators on VLSI circuitry," IEEE Photon. Technol. Lett. 8, pp. 644-646, 1996.

[43] I. A. Young, E. Mohammed, J. T. S. Liao, A. M. Kern, S. Palermo, B. A. Block, M. R. Reshotko, and P. L. D. Chang, "Optical I/O Technology for Tera-Scale Computing," IEEE Journal of Solid-State Circuits, vol. 45, no. 1, pp. 235–248, 2010.

[44] L.C. Kimerling, "Photons to the rescue: microelectronics becomes microphotonics," Electrochem. Soc. Interface, pp. 28, Summer 2000.

[45] K. K. Lee, D. R. Lim, and L. C. Kimerling, "Fabrication of ultralow-loss Si/SiO2 waveguides by roughness reduction," Opt. Lett., vol. 26, pp. 1888, 2001

[46] K. K. Lee, "Transmission and routing of optical signals in on-chip waveguides for silicon microphotonics," Ph.D dissertation, Massachu- setts Inst. of Technology, Cambridge, 2001.

[47] B. E. Little, J. S. Foresi, G. Steinmeyer, E. R. Thoen, S. T. Chu, H.A. Haus, E. P. Ipren, L. C. Kimerling, and W. Greene, "Ultra-compact Si /SiO2 microring resonator optical channel dropping filters," IEEE. Photon. Technol. Lett., vol. 10, pp. 549–551, 1998.

[48] J. S. Foresi, P. R. Villeneuve, J. Ferrera, E. R. Thoen, G. Steinmeyer, S. Fan, J. D. Joannopoulos, L. C. Kimerling, H. I. Smith, and E. P. Ippen, "Photonic-bandgap microcavities in optical waveguides," Nature, vol. 390, pp. 143, 1997

[49] C. Angulo Barrios, V. R. Almeida, and M. Lipson, "Low-power-consumption short-length and high-modulation-depth silicon electro-optic modulator," J. Lightwave Technol., vol. 21, pp. 1089–1098, 2003.

[50] C. Z. Zhao, A. H. Chen, E. K. Liu, and G. Z. Li, "Silicon-on-insulator asymmetric optical switch based on total internal reflection," IEEE Photon. Technol. Lett., vol. 9, pp. 1113, 1997.

[51] Y. Vlasov and S. McNab, "Losses in single-mode silicon-on-insulator strip waveguides and bends", Optics Express12, pp. 1622–1631, 2004.

[52] G. Roelkens, J. Brouckaert, D. Taillaert, P. Dumon, W. Bogaerts, D. V. Thourhout, R. Baets, "Integration of InP/InGaAsP photodetectors onto silicon-on-insulator waveguide circuits", Opt. exp., vol. 13, pp. 10102-10108, 2005.

[53] K.H. Oh, “High-sweeping-speed optically synchronized dual channel terahertz-signal generator for driving a superconducting tunneling mixer and its application to active gas sensing,” Optics Express, Vol. 17, Oct. 2009.

[54] K. Ajito, “Terahertz Spectroscopy Technology for Molecular Networks,” NTT Technical Review, Vol.7, pp. 1-5, Mar. 2009.

[55] E. Pickwell and V.P. Wallace. “Biomedical applications of terahertz technology,” Journal of Physics D: Applied Physics, Vol 39, pp. R301- R310, 2006.

[56] V. P. Wallace et al., "Terahertz pulsed imaging of basal cell carcinoma ex vivo and in vivo," British Journal of Dermatology, Vol. 151, pp. 424-432, 2004.

[57] A.A. Danylov, “Coherent imaging at 2.4 THz with a CW quantum cascade laser transmitter,” Terahertz Technology and Applications III, Proceedings of SPIE Vol. 7601, Jan. 2010.

[58] J. Federici and L. Moeller,“Review of terahertz and subterahertz wireless communications,” Journal of Applied Physics, Vol.107, 2010.

[59] R. Piesiewicz, “Short-Range Ultra-Broadband Terahertz Communications: Concepts and Perspectives,” IEEE Antennas and Propagation Magazine, Vol. 49, pp. 24-39, Dec. 2007.

[60] P. H. Siegel, “Terahertz technology,” IEEE Transactions on Microwave Theory Techniques, Vol. 50, pp. 910–928, Mar. 2002.

[61] K.B. Alia, C.R. Nevea, A. Gharsallah and J.P. Raskin, “Impact of Crosstalk into High Resistivity Silicon Substrate on the RF Performance of SOI MOSFET”, J. of Tele. & Infor. Tech.Vol. 4, pp. 93–100, 2010.

[62] M. Tonouchi, “Cutting-edge terahertz technology,” Nature Photonics, Vol. 1, pp. 97-105, Feb. 2007.

[63] T. Baba, “Slow light in Photonic Crystal,” Nature Photon., vol. 2, pp. 465– 473, 2008.

[64] M. Notomi, A. Shinya, K. Nozaki, T. Tanabe, S. Matsuo, E. Kuramochi, T. Sato, H. Taniyama, and H. Sumikura, “Low-power nanophotonic devices based on photonic crystals towards dense photonic network on chip,” IET Circuits Devices Syst. 5, pp. 84–93, 2011.

[65] A. R. Knapitsch, “Photonic Crystals: Enhancing the Light Output of Scintillation Based Detectors,” PhD dissertation, Vienna University of Technology (TU Wien), 2012.

[66] B. Pesala, V. Karagodsky, and C. J. Chang-Hasnain, “Ultra-compact optical coupler and splitter using high-contrast grating hollow-core waveguide in Silicon and Nanophotonics”, OSA Technical Digest (CD) (Optical Society of America, 2010), paper IWH1.

[67] C. J. Chang-Hasnain and W. Yang, “High-contrast gratings for integrated Optoelectronics”, Advances in opt. and photon., 4,pp.379-440, 2012.

[68] M. Huang, Y. Zhou, C. Chang-Hasnain, “A surface-emitting laser incorporating a high-index-contrast subwavelength grating” Nat. Photon. 1, pp. 119-122, 2007.

[69] M. C. Y. Huang, Y. Zhou, and C. J. Chang-Hasnain, “A nano electromechanical tunable laser,” Nat. Photonics 2, pp. 180–184, 2008.

[70] P. Debernardi, J. M. Ostermann, M. Feneberg, C. Jalics, and R. Michalzik, “Reliable polarization control of VCSELs through monolithically integrated surface gratings: a comparative theoretical and experimental study,” IEEE J. Sel. Top. Quantum Electron. 11, pp. 107–116, 2005.

[71] J. M. Ostermann, P. Debernardi, C. Jalics, and R. Michalzik, “Shallow surface gratings for high-power VCSELs with one preferred polarization for all modes,” IEEE Photon. Technol. Lett. 17, pp. 1593–1595, 2005.

[72] Y. Zhou, M. Moewe, J. Kern, M. C. Y. Huang, and C. J. Chang-Hasnain, “Surface-normal emission of a high-Q resonator using a subwavelength high-contrast grating,” Opt. Express 16, pp. 17282–17287, 2008.

[73] M. G. Moharam, and T. K. Gaylord, “Rigorous coupled wave analysis of planar grating diffraction,” J. Opt. Soc. Am. 71, pp. 811-818, 1981.

[74] S. T. Peng, “Rigorous formulation of scattering and guidance by dielectric grating waveguides: general case of oblique incidence,” J. Opt. Soc. Am. A 6,pp. 1869-1883, 1989.

[75] L. Li, “A modal analysis of lamellar diffraction gratings in conical mountings,” J. Mod. Opt. 40, pp. 553–573, 1993.

[76] S. Ghosh, G.P Agarwal, B.P Pal, R.K Varshney, “Localization of light in evenscently coupled disordered waveguide lattices:Dependence on the input beam profile”, OpticsCommunication 284, pp. 201-206, 2011.

[77] D. Taillaert , F.V. Laere, M. Ayre, W.Bogaerts, D.V.Thourhout, P.Bienstman and R. Baets, “Grating Couplers for Coupling between Optical Fibers and Nanophotonic Waveguides”, Japanese Journal of Applied Physics Vol. 45, pp. 6071–6077, 2006.

[78] G.Roelkens, D. V. Thourhout and R. Baets, “High efficiency Silicon-on-Insulator grating coupler based on a poly-Silicon overlay”, Optics Express, Vol. 14, pp.11622,27 November 2006.

[79] O. Mitomi, K. Kasaya and H. Niyazawa, “Design of a single-mode tapered waveguide for low-loss chip-to-fiber coupling”, IEEE J. of Q. Elec., 30, pp. 1787-1793, 1994.

[80] S. H. Tao, J. Song, Q. Fang, M. B. Yu, G. Q. Lo and D. L. Kwong, "Improving coupling efficiency of fiber-waveguide coupling with a double-tip coupler", Opt. Exp., 25, pp.20803-20808, 2008.

[81] S. Galoda and G. Singh, "Fighting terrorism with terahertz", IEEE Potential Magazine, 26 pp. 24–29, 2007.

[82] J. Grade, P. Haydon, and D. V. Weide, "Electronic terahertz antennas and probes forspectroscopic detection and diagnostics", Proc. IEEE, 95 pp. 1583–1591, 2007.

[83] S. J. BenYoo, Ryan P.Scott, David J.Geisler, Nicolas K. Fontaine and Francisco M.Soares,"Terahertz Information and Signal Processing by RF-Photonics", IEEE Transactions on terahertz science and technology,2,pp. 167-176, 2012.

[84] R. Honnungar, T. Srinivas, "Design and Simulation of an Optical Integrated Passive S-bend Waveguide Delay Line Phase Shifter", Proc. IEEE, DOI 10.1109/CICSyN.2012, 32, pp. 125-128, 2012.

[85] B.M.A. Rahman, M. Uthman, A. Quadir, K. T. V. Grattan, C. Markides and C. Themistos, "Emergence of THz Technologies and Design and Optimisation Low-loss Waveguides and Devices", Proc. IEEE, Vol. 14, pp. 389-393, 2014.

[86] A. Agrawal, N. Kejalakshmy, M. Uthman, B. M. A. Rahman, A. Kumar, and K. T. V. Grattan, "Ultra low bending loss equiangular spiral photonic crystal fibers in the terahertz regime", AIP Advances, http://dx.doi.org/10.1063/1.4726055, Volume 2, pp. 022140-1-5, 2012.

[87] J. K.Thind, M.Kumar, and B.K.Kaushik, "Electrical Tuning of Optical Delay in Graphene based Photonic Crystal Waveguide", IEEE Journal of Quantum Electronics, DOI 10.1109/JQE.2015.2476353, p 0018-9197 (c), 2015.

[88] K. Nozaki, S.Matsuo, K. Takeda, T. Sato, E. Kuramochi and M. Notomi, "InGaAs nano-photodetectors based on photonic crystal waveguide including ultracompact buried heterostructure", Optics Express, Vol.21, DOI:10.1364/OE.21.019022, pp. 1-7, August 2013.

[89] C. J. Chang-Hasnain, Y. Zhou, M. C. Y. Huang, and C. Chase, "High-Contrast Grating VCSELs," IEEE J. Sel. Top. Quantum Electron. 15, pp. 869, 2009.

[90] Y. Zhou, V. Karagodsky, B.Pesala, F.G Sedgwick, C.J Chang-Hasnain., "A novel ultra-low loss hollow-core waveguide using subwavelength high-contrast gratings", Opt. Exp, 17 pp. 1508 – 1517, 2009.

[91] W.Yang, J. Ferrara, K. Grutter, A. Yeh, C. Chase, Y. Yue, A.E. Willner, M.C. Wu and C. J. Chang-Hasnain, “Low loss hollow-core waveguide on a silicon substrate”, Nanophotonic, 1, 23-29, 2012 .

[92] P. Dong and A. G. Kirk., “Compact double-grating coupler between vertically stacked silicon-on-insulator waveguides”, Appl. Opt., 44, pp. 7540-7547, 2005.

[93] N. Krishnaswamy, T. Srinivas, G.M. Rao and M.M. Varma, “Analysis of Integrated Optofluidic Lab-on-a-Chip Sensor Based on Refractive Index and Absorbance Sensing”, IEEE Sensors J., 13, pp. 1730-1741, 2013,.

[94] J.B. Lask, “Wafer bonding for silicon-on-insulator technologies", Applied Physics Letter48, pp. 78-80, 1986.

[95] D. Feng, S. Liao, P. Dong, N.-N. Feng, H. Liang, D. Zheng, C.-C. Kung, J. Fong,R.Shafiiha, J. Cunningham, A. V. Krishnamoorthy, and M. Asghari, “High-speed Ge photodetector monolithically integrated with large cross-section silicon-on-insulatorwaveguide”, Applied Physics Letter 95, pp. 261105(1-3), 2009.

[96] D. Ahn, C. Hong, J. Michel, “High performance, waveguide integrated Ge photodetectors", Opt. Exp., 15, pp. 3916-3921, 2007.

[97] F. Horst, William M. J. Green, B. Jan Offrein and Y. A. Vlasov, “Silicon-on-Insulator Echelle Grating WDM Demultiplexers with Two Stigmatic Points”, IEEE PhotonicsTechnology Letters21,pp. 1743-1745, 2009.

[98] T. Spuesens, F. Mandorlo, P. Rojo-Romeo, P. Regreny, Nicolas Olivier, Jean-Marc Fedeli and D. Van Thourhout, “Compact Integration of Optical Sources and Detectors on SOI for Optical Interconnects Fabricated in a 200 mm CMOS Pilot Line”, Journal of lightwave Technology 30,pp. 1764-1770, 2012.

[99] V.R. Kumar, B.K. Kaushik, A. Patnaik, “An accurate model for dynamic crosstalk analysis of CMOS gate driven on-chip interconnects using FDTD method”, Microelectronics Journal, Vol. 45, pp. 441-448, 2014.

[100] M.L.Vanblaricum, “Photonic systems for antenna applications”, IEEE Antennaspropagation Magazine36, pp. 30-38, 1994.

[101] G. Tzeremes, H. Tanner, T. Liao, and C. Christodoulou, “Wireless communication withsmart photonic antennas using transmission power control”, IEEE Antennas and WirelessPropagation Letter3 (2004) 232–235.

[102] O. Graydon, C. Gilloch and T. Wilson, “Wireless future drives microwave photonics”, Nature Photonics5, pp.723-736, 2011.

[103] B.Canon, “Microwave Photonic Mixing”, Shrif University of Technology17,pp. 149-162, 2010.

[104] J. Marti and J. Capmany, “Microwave photonics and radio-over- fiber research”, IEEE Microwave Magazine10, pp. 96-105, 2009.

[105] J.C. Wirth, “Silicon Grating Couplers for Low Loss Coupling between Optical Fiber and Silicon Nanowires,” PhD dissertation, Purdue University, 2011.

[106] I. Moerman, P. P Van Daele, and P.M. Demeester, “A review on fabrication technologies for the monolithic integration of tapers with III-V semiconductor devices,” IEEE J. Quantum Electron., Vol. 3, pp. 1308-1320, 1997.

[107] P.V. Studenkov, M.R. Gokhale, and S.R. Forrest, “Efficient coupling in integrated Twin-waveguide lasers using waveguide tapers,” IEEE Photon. Technol. Lett., Vol. 11, pp. 1096-1098, 1999.

[108] R. Waldhaus, B. Schnabel and W. Karthe, “Efficient coupling into polymer waveguides by gratings”, Appl. Opt., 36, pp. 9383-9390, 1997.

[109] A. Narasimha and E. Yablonovitch, “Efficient optical coupling into single mode Silicon-on-Insulator thin films using a planar grating coupler embedded in a high index contrast dielectric stack”, Optical Society of America, 2002.

[110] D.Taillaert, “Grating couplers as Interface between Optical Fibres and Nanophotonic Waveguides”, Ghent University, PhD Thesis, June 2004.

[111] F.Van Laere, M.V. Kotlyar, D.Taillaert, D.Van Thourhout, T.F. Krauss, and R.Baets, “Compact Slanted Grating Couplers Between Optical Fibre and InP–InGaAsP Waveguides”, IEEE Photonics Technology Letters, Vol. 19, no. 6, pp.396-398, March 2007.

[112] F.V. Laere, G. Roelkens, M. Ayre, J. Schrauwen, , D. Taillaert, D.V. Thourhout, T.F. Krauss and R. Baets, “Compact and Highly Efficient Grating Couplers Between Optical Fiber and Nanophotonic Waveguides”, Journal of Lightwave Technology, 25, no. 1, pp.151-156, Jan. 2007.

[113] S.Scheerlinck, J.Schrauwen, F.Van Laere, D.Taillaert, D.Van Thourhout and R.Baets, “Efficient, broadband and compact metal grating couplers for silicon-on-insulator waveguides”, Optical Society of America, 2007.

[114] X. Chen, C. Li and H. K. Tsang, “Characterization of Silicon-on-Insulator Waveguide Chirped Grating for Coupling to a Vertical Optical Fibre”, IEEE 978-1-4244-1918-0/08, 2008.

[115] J. V. Galan, P. Sanchis, J. Blasco, and J. Marti, “Study of High Efficiency Grating Couplers for Silicon-Based Horizontal Slot Waveguides”, IEEE Photonics Technology Letters, Vol. 20, no. 12, pp.985-987, June 2008.

[116] F.Van Laere, T.Stomeo, D.Taillaert, G.Roelkens, D.Van Thourhout, T.F. Krauss, and R.Baets, “Efficient Polarisation Diversity Grating Couplers in Bonded InP-Membrane”, IEEE Photonics Technology Letters, Vol. 20, no. 4, pp. 318-320, February 2008.

[117] F.Van Laere, W.Bogaerts, P.Dumon, G.Roelkens, D.Van Thourhout and R.Baets, “Focusing Polarisation Diversity Grating Couplers in Silicon-on-Insulator”, Journal Of Lightwave Technology, Vol. 27, no. 5, pp. 612-618, March 2009.

[118] X. Chen, C. Li, C.K.Y. Fung and H.K. Tsang, “Apodized Waveguide Grating Couplers for Efficient Coupling to Optical Fibers,” IEEE PTL., 22, pp. 1156–1158, 2010.

[119] J. Covey and R.T. Chen, “Efficient perfectly vertical fiber-to-chip grating coupler for silicon horizontal multiple slot waveguides”, Opt. Exp., pp.10886-10896, 2013.

[120] Y. Ding, C. Peucheret, H. Ou and K. Yvind, “Fully etched apodized grating coupler on the SOI platform with −0.58 dB coupling efficiency,” opt. lett., 39, pp. 5348–5350, 2014.

[121] A. Andryieuski, and A.V. Lavrinenko, "Nanocouplers for infrared and visible light", Advances in Opto Electronics, Vol. 2012, pp. 1-17, 2012.

[122] W.P. Huang, “Coupled mode theory for optical waveguides: an overview”, J. Opt. Soc. Am.A, 11, no.3, pp. 963-983, 1994.

[123] D. F. G. Gallagher and T. P. Felici, “Eigenmode expansion methods for simulation of optical propagation in photonics - Pros and cons”, in Conference on Integrated Optics - Device, Materials and Technologies VII, San Jose, CA, 67, pp. 69-82, 2003.

[124] E.G. Neumann, “Single-mode fibers – fundamentals”, Springer-Verlag, Berlin, 1988.

[125] V. A. Sychugov, “Optimization and control of grating coupling to or from a silicon-based optical waveguide”, Optical Engineering, 35, no. 11, pp. 3092- 3100, Nov 1996.

[126] C. Kopp, E. Augendre, R. Orobtchouk, O. Lemonnier and J.M. Fedeli, “Enhanced Fiber Grating Coupler Integrated by Wafer-to-Wafer Bonding”, J. Of Lightw. Tech., 29, pp.1847-1851, 2011.

[127] D. Taillaert, P. Bienstman, and R. Baets, “Compact efficient broadband grating coupler for silicon-on-insulator waveguides”, Optics Letters, 29, no. 23, pp. 2749-2751, 1 Dec. 2004.

[128] R. Waldhausl, “Efficient coupling into polymer waveguides by gratings”, Applied Optics, 36, no. 36, pp. 9383-9390, Dec 1997.

[129] A. Umbach, “High-speed integrated photodetectors for 40 Gb/s applications”, Proc. SPIE, 5246, pp. 434–442, 2004.

[130] V.R.Kumar, M.K. Majumder, and B. K. Kaushik, “Graphene- Based On-Chip Interconnects and TSVs”, IEEE nanotechnology magazine, 14, pp. 14-20, 2014.

[131] M. Notomi, A. Shinya, K. Nozaki, T. Tanabe, S. Matsuo, E. Kuramochi, T. Sato, H. Taniyama, and H.Sumikura, “Low-power nanophotonic devices based on photonic crystals towards dense photonic network on chip”, IET Circuits Devices Syst., 5,pp. 84–93, 2011.

[132] C. T. DeRose, D. C. Trotter, W. A. Zortman, A. L. Starbuck, M. Fisher, M. R. Watts, and P. S. Davids, “Ultracompact 45 GHz CMOS compatible Germanium waveguide photodiode with low dark current”, Opt. Exp., 19, pp. 24897–24904, 2011.

[133] K. Das, S. Mukherjee, S. Manna, S. K. Ray and A .K .Raychaudhuri, “Single Si nanowire (diameter ≤ 100nm) based polarization sensitive near-infrared photodetector with ultra-high responsivity”, Nanoscale, DOI: 10.1039/C4NR03170A, pp. 1-10, 2012.

[134] L. Chen, P. Dong, and M. Lipson, “High performance germanium photodetectors integrated on submicron silicon waveguides by low temperature wafer bonding”, Opt. Exp., 16,pp. 11513-11518, 2008.

[135] M. Kumar, “Narrow bandwidth and polarization independent design of hollow waveguide in-plane mirror with ultrawide tuning-range”, Appl. Opt., 53, pp. 1847-51, 2014.

[136] M. Kumar, C. Chase, V. Karagodsky, T. Sakaguchi, F. Koyama, and C. J. Chang-Hasnain, “Low birefringence and 2-D optical confinement of Hollow waveguide with distributed Bragg reflector and high index contrast grating”, IEEE Photon. J., 1,pp. 135–143, 2009.

[137] Miura T, Koyama F. Low-loss and polarization-insensitive semiconductor hollow waveguide with GaAs/AlAs multi-layermirrors. Jpn J Appl Phys 2004;43(1A/B):L21 – 3.

[138] C. Yadav, A. Dutta, S. Sirohi, T. Ethirajan, and Y.S. Chauhan, “Unified Model for Sub-Bandgap and Conventional Impact Ionization in RF SOI MOSFETs with Improved Simulator Convergence”, Proc IEEE, DOI 10.1109/VLSID.2016.85, Vol. 1,pp. 328-333, 2016.

[139] M. Mutlu, A. E. Akosman, G.Kurt, M. Gokkavas and E. Ozbay, “Experimental realization of a high-contrast grating based broadband quarter-wave plate”, Opt. Exp., 20, pp. 27966-27973, 2012.

[140] E.N. Glytsis, N.M. Jokerst, R.A. Villalaz and S.Y. Cho, "Substrate-Embedded and Flip-Chip-Bonded Photodetector Polymer-Based Optical Interconnects: Analysis, Design, and Performance", J. ofLightwave Tech., 21,pp. 2382-2394, 2003.

[141] S.Q. Feng, Y.Geng, K.M.Lau, A.W. Poon, "Epitaxial III-V-on-silicon waveguide butt-coupled photodetectors", Opt. Lett., 37, pp. 4035-4037, 2002.

[142] K.W.Ang, S.Y.Zhu, J.Wang, K.T.Chua, M.B.Yu, G.Q.Lo and D.L.Kwong, "Novel Silicon-Carbon (Si:C) Schottky barrier enhancement layer for dark-current suppression in Ge-on-SOI MSM photodetectors", IEEE Electron Dev. Lett., 7, pp. 704-707, 2008.

[143] I.G.Kim, K.S.Jang, J.Joo, S.H.Kim, S.G.Kim, K.W.Choi, J.H.Oh, S.A.Kim and G.G.Lim, "High-performance photoreceivers based on vertical-illumination type Ge-on-Si photodetectors operating up to 43 Gb/s at λ ~1550 nm", opt. exp., 21, pp. 30716-30723, 2013.

[144] M.W.Geis, S.J.Spector, M.E.Grein, J.U.Yoon, D.M.Lennon and T.M.Lyszczarz, "Silicon waveguide infrared photodiodes with > 35 GHz bandwidth and phototransistors with 50 A/W-1 response", opt. exp., 17, pp. 5193-5204, 2009.

[145] S.Zhu, G.Q.Lo and D.L.Kwong, "Low-cost and high gain silicide Schottky-barrier collector phototransistor integrated on Si waveguide for infrared detection", Appl. Phys. Lett., 93, pp. 071108, 2008.

[146] F. Miyamaru, M. Saito andW. Takeda, "Emission of terahertz radiations from fractal antennas", Appl. Phys. Lett., 95, pp. 221111, 2009.

[147] H. Amarloo, M. Neshat, S. Safavi-Naeini, "Terahertz plasmonic-like waveguide for integrated sensing applications", IEEE Electr. Lett., 49, pp. 836–838, 2013.

[148] S. Nakajima, H. Hoshina, M. Yamashita, C. Otani,N. Miyoshi, "Terahertz imaging diagnostics of cancer tissues with a chemometrics techniques", Appl. Phys. Lett., 90, pp. 041102 2007.

[149] N. Karpowicz, H. Zhong, C. Zhang, "Compact continuous-wave subterahertz system for inspection applications", Appl. Phys. Lett., 86, pp. 054105, 2005.

[150] H. T. Chen, W. J. Padilla, J. M. O. Zide, "Active terahertz metamaterial devices", Nature, 444, pp. 597–600, 2006.

[151] M. Tamagnone,J. Gomez-Diaz,J. Mosig,J. Perruisseau-Carrier, "Analysis and design of terahertz antennas based on plasmonic resonant graphene sheets", J. Appl. Phys., 112, pp. 114915, 2012.

[152] P.Muhlschlegel, H. J. Eisler, O. J. F. Martin, B. Hecht,D. W. Pohl, "Resonant optical antennas", Science, 308, pp. 1607–1609, 2005.

[153] L. K. Oxenlowe, H. Galili and M. Ji, “Silicon photonics for signal processing of Tbit/s serial data signals”, IEEE J. Sel. Top. Quantum Electron., 18, pp. 996–1005, 2012.

[154] T. Spuesens, F. Mandorlo, P. Rojo-Romeo, “Compact integration of optical sources and detectors on SOI for optical interconnects fabricated in a 200 mm CMOS pilot line”, J. Lightwave Technol., 30, pp. 1764–1770, 2012.

[155] R. Kakimi, M. Fujita, M. Nagai, “Capture of a terahertz wave in a photonic-crystal slab”, Nature Photon., 8, pp. 657–663, 2014.

[156] E.R. Brown, O.B. McMahon, C.D. Parker, “Photonics-crystal antenna substrates”, Lincoln Lab. J., 11, pp. 159–174, 1998.

[157] M.L. Vanblaricum, “Photonic systems for antenna applications”, IEEE Antenna Propag. Mag., 36, pp. 30–38, 1994.

[158] Zhang, X., Subbaraman, H., Hosseini, A.: “Highly efficient mode converter for coupling light into wide slot photonic crystal waveguide”, Opt. Express, 22, pp. 20678–20690, 2014.

[159] S. Luo, Y. Wang, X. Tong and Z. Wang, “Graphene-based optical modulators”,Nanoscale R. Lett., 110, pp. 1-11, 2015.

[160] C. Yeh, F. Shimabukuro, P. Siegel, “Low-loss terahertz ribbon waveguides”, Appl. Opt., 44, pp. 5937–5946, 2005.

[161] H.J. Chang, S.H. Kim, Y.H. Lee, E.P. Kartalov, A. Scherer, “A photonic-crystal optical antenna for extremely large local-field enhancement”, Opt. Express, 18, pp. 24163–24177, 2010.

[162] R. Gonzalo, I. Ederra, C.M. Mann, P.De Maagt,. “Radiation properties of terahertz dipole antenna mounted on photonic crystal”, Electr. Lett., 37, pp. 613–614, 2001.

[163] E.R. Brown,C.D. Parker, E. Yablonovitch, “Radiation properties of a planar antenna on a photonic-crystal substrate”, J. Opt. Soc. Am. B, 10, pp. 404–407, 1993.

[164] A.K. Jha, T. Sreenivasulu, S.A. Samad, T. Srinivas, “Variation of Single waveguide modes with dielectric constant of line defect in 2D Photonic Crystals of dielectric rods in air: A Simulation based analysis”, Int. J. of Engineering Research & Technology, 1,pp. 1-10, 2012.

[165] H. Ammari, N. Bereux and E. Bonnetier, “Analysis of the radiation properties of a planar antenna on a photonic crystal substrate”,Math. Meth. Appl. Sc, 24, pp. 1021–1042, 2001.

[166] R.N. Tiwari, P. Kumar, N. Bisht, Rectangular microstrip patchantenna with photonic band gap crystal for 60 GHz communica-tions, in: Prog. Electromagn. Res. Symp. Proc., Suzhou, China,2011, pp. 256–259.

[167] M. El-Nawawy, A.M.M.A. Allam, D. Korzec, The design of a0.35 THz microstrip patch antenna on LTCC substrate, J. Electr.Electron. Eng. 1 (2011) 1–4.

[168] A. Sharma, V.K. Dwivedi, G. Singh, THz rectangular patchmicrostrip antenna design using photonic crystal as substrate, in:Progress in Electromagnetics Research Symposium, Cambridge,USA, 2008, pp. 161–165.

[169] A. Sharma, G. Singh, Rectangular microstirp patch antennadesign at THz frequency for short distance wireless communi-cation systems, J. Infrared Millim. Terahertz Waves 30 (2009)1–7.

[170] Z. Wu, A. Young, M. Gehm, "Investigation of several terahertz electromagnetic band gap structures", Micro. Opt. Tech. Lett., 52, pp. 678–686, 2010.

[171] R.C. Diaz, S.V. Hoeye, C.Vazquez, "Sub-millimeter wave frequency scanning 8 × 1 antenna array", Prog. Electromagn. Res., 132, pp. 215–232, 2012

[172] A. Donghwan, L.C. Kimerling, J. Michel, "Evanescent Coupling Device Design for Waveguide-Integrated Group IV Photodetectors", J. Lightwave Technol. 2, pp. 3387–3394, 2010.

[173] R. B. Waterhouse, "Stacked patches using high and low dielectric constant material combination," IEEE Trans. Antennas Propagat., 47, pp. 1767–1771, 1999.

[174] W. S. T. Rowe and R. B. Waterhouse, "Efficient wideband printed antennas on lithium niobate for OEICs," IEEE Trans. Antennas Propagat., 51, pp. 1413–1415, 2003.